Nansen Environmental and Remote Sensing Center

A non-profit
Research institute affiliated
With the University of
Bergen

NERSC

Thormøhlensgate 47
N-5006 Bergen,
Norway
http://www.nersc.no

NERSC Technical Report no. 282

Satellite data acquisition for iceberg monitoring in the Svalbard area

Grounded iceberg observed north of Svalbard during the Lance cruise in April 2007

Project for Statoil ASA 2007

Statoil Order no. 4501294663

Authors:
Stein Sandven, Kjell Kloster and Mohamed Babiker

August 2007

Nansen Environmental and Remote Sensing Center (NERSC)

Thormøhlensgate 47
N-5006 Bergen, Norway
Phone: + 47 55 20 58 00
Fax: + 47 55 20 58 01
E-Mail: Stein.Sandven@nersc.no
http://www.nersc.no

TITLE: **Satellite data acquisition for iceberg detection in the Svalbard area**	**REPORT IDENTIFICATION** **NERSC Technical report no. 282**
CLIENT STATOIL ASA	**CONTRACT** Order no. 4501294663
CLIENT REFERENCE Einar Nygaard	**AVAILABILITY** Customer report
INVESTIGATORS Stein Sandven, Kjell Kloster, and Mohamed Babiker	**AUTHORISATION** Bergen, 21 August 2007 Stein Sandven

Contents

Executive Summary

Observation and forecasting of icebergs is an important task for offshore oil and gas development in Arctic regions. For many decades the Russian conducted regular aircraft monitoring of icebergs in Arctic seas, but in the last 15 years only occasional expeditions with icebreakers and aircraft have collected iceberg data in the Barents Sea. Monitoring of icebergs from satellites has been studied in research projects since the early 1990s, but has not yet been implemented as an operational service. New satellite systems are under development that can improve iceberg detection in the coming years.

This report presents a set of high-resolution satellite images collected in the Svalbard area for iceberg detection in April-May 2007. Several images were taken during the field expedition with Lance north of Svalbard. During the Lance expedition, ICEX buoys with ARGOS transmitters provided by CMR were deployed on four different icebergs. The ARGOS data were used during April and May to follow the four icebergs. Two of the icebergs continued to send ARGOS positions from June to August.

Two types of high-resolution satellite images were used: optical images from SPOT, Landsat and Terra ASTER, and Synthetic Aperture Radar (SAR) images form ENVISAT and Radarsat. The optical satellite data are limited by cloud cover. This means that good-quality images can be produced only on days with little clouds. SAR data gives good quality radar images independent of clouds and daylight, but the SAR images have speckle noise which disturbs the detection of icebergs. For optimal observation of icebergs it is necessary to use both optical and SAR images of resolution 10 m or better. Most of the images are presented in quicklook format, which is useful for an overview and planning the analysis of full-resolution images. In this study, a few examples of full-resolution images are presented. One RADARSAT SAR and one SPOT image covering the positions of the tagged icebergs were analysed in detail. In some cases potential icebergs were found in the images, but in other cases there was no iceberg signal even if iceberg positions wre documented by ARGOS data. The size of the tagged icebergs were around 50 m, which is rather small size for detection in the present images. The possibility to detect the known icebergs in the satellite images depends on several factors such as the ice conditions around the icebergs, the size and shape of the icebergs and resolution of the satellite images.

This study has demonstrated how satellite data collection for iceberg monitoring can be done for the Svalbard area. More information about icebergs in this area can be obtained if the images are analysed in full-resolution. In particular several of the 35 SPOT images are expected to give more data on icebergs in the Hopen and Kong Karls Land area. This area was also covered by high-resolution SAR images in alternating polarization images. Also the area around Nordaustlandet have icebergs that potentially can be detected in the images. Future schemes for iceberg monitoring should include use of new high resolution SAR images with full polarization, optical images, airborne surveys with fixed-wing aircraft or helicopters, and deployment of Argos buoys on selected icebergs.

1. Introduction

Drifting icebergs are a challenge for oil and gas developments in the Barents Sea region. Reliable statistics regarding iceberg occurrence and size distribution will be required in order to establish design criteria for iceberg for offshore fields and pipelines. In order to operate in the Barents Sea an iceberg management system must be implemented. Reliable forecasts for icebergs drift will be required as part of such a system.

The size and shape distribution of the icebergs is such that the vast majority is of small scale, less than 20 m (bergy bits and growlers), while tabular icebergs, glacier bergs and other types at scales of 100 m or more represent a minority. This is a real challenge for implementation of monitoring systems. In the Soviet Union, aircraft surveys operated by Arctic and Antarctic Research Institute was the main monitoring method for several decades, but during the 1990s this survey has declined. In the last 15 years, there has been practically no iceberg monitoring by aircraft in the Barents Sea. Other observation methods include ship and polar station observations, but these have also declined in the last decade. Satellite observations have not been used regularly, but several research projects have demonstrated the possibilities to observe icebergs from satellite images in the Barents Sea region (e.g. Kloster and Spring, 1993; Sandven et al., 1991, 2007).

In March-April 2007 several research cruises in the Svalbard area with the vessels KV Svalbard and RV Lance were conducted. Personnel from the Nansen Center participated in two of the expeditions. The expedition with KV Svalbard took place in the Storfjorden area, but no icebergs were observed in this area During the Lance cruises north of Svalbard several icebergs were observed and ICEX buoys were deployed on some of them to monitor the drift of icebergs. Positions data for four icebergs were collected in the period April – May as support to satellite images obtained in the Svalbard region. The buoy positions provide validation data for iceberg observations in the satellite images. This report describes a set of high-resolution satellite images collected in the Svalbard area for the purpose of detecting icebergs.

The winter of 2007 was the third year in row with minimum sea ice extent in the Barents Sea. The ice edge in April was located between Hopen and 78° latitude in the northeastern Barents Sea (Fig. 1). The eastern Barents Sea south of 78°N was practically ice-free the whole winter, similar to the winters of 2005 and 2006. The total ice area for the Arctic has been monitored by passive microwave satellite data since 1979. For the Barents Sea the variability and trend in ice area from 1978 to 2006 is presented in Fig. 2.

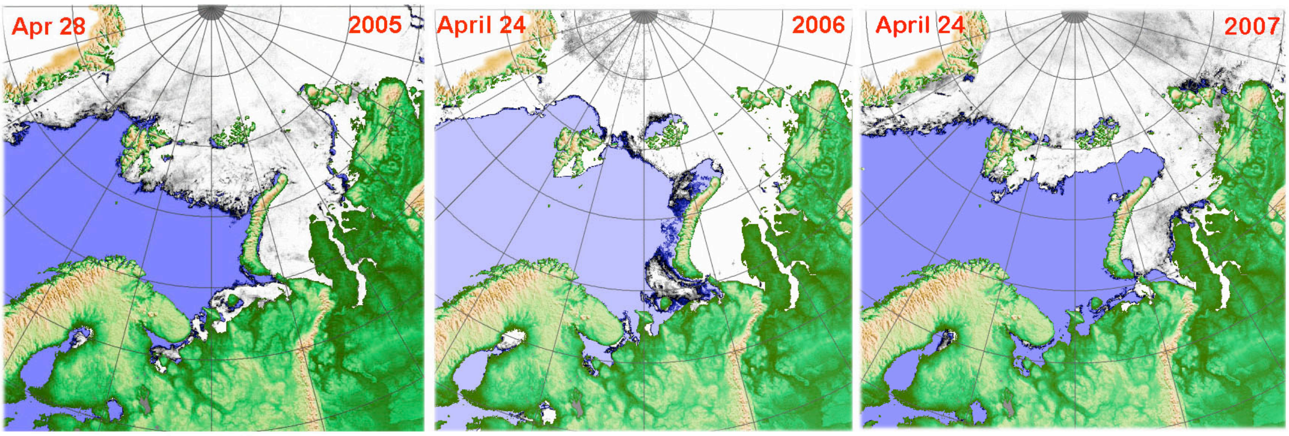

Figure 1. Ice maps from passive microwave data (AMSRE data) in the Barents Sea for April 2005, 2006 and 2007. The maps show ice concentration in greyscale and open water as blue. The maps are produced by Institute of Environmental Physics, University of Bremen.

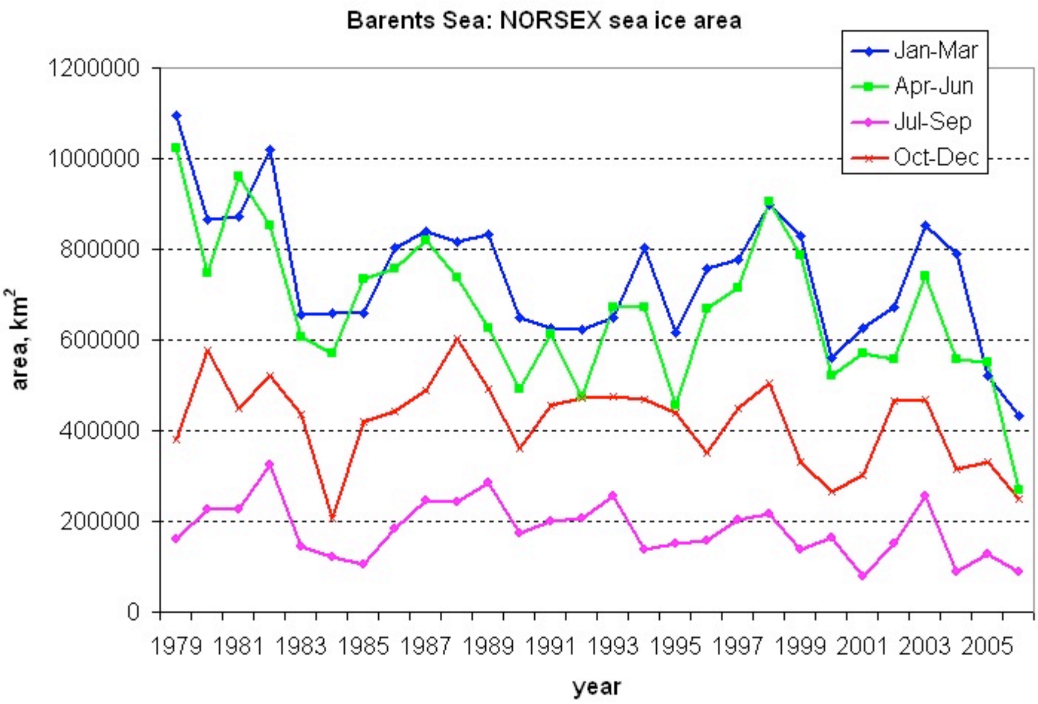

Figure 2. Three-monthly mean ice area for the Barents Sea sector of the Arctic from 1979 to 2006.

The three last years show strong decline in ice area for the winter and spring months. The year 2006 showed minimum ice area for all periods of the year. Data for 2007, which are not included in Figure 2, shows similar ice areas as 2005 and 2006.

Two types of satellite data can be used for iceberg detection: high-resolution optical images and high-resolution SAR images. These have complementary properties and have capability to detect icebergs in three different situations:

(1) Icebergs in open water: icebergs will show bright spots against dark background for both optical and SAR. For SAR higher wind reduces the contrast between open water and icebergs, making iceberg detection more difficult. The best condition is little or no wind, producing low backscatter in the SAR image and consequently good contrast between iceberg signature and open water.
(2) Icebergs in drifting ice: iceberg can create tracks in high concentration drifting ice or in are large floes of consolidated ice since icebergs and sea ice have different drift velocity. Grounded icebergs will create tracks with tidal ellipses. It is difficult to distinguish icebergs from background both for optical and SAR if only backscatter information is available. This is the most difficult situation for iceberg detection.
(3) Icebergs in fastice near calving areas: optical images shows icebergs and their shadows against background. Stationary ice means possible to identify icebergs over longer time periods, which is necessary for obtaining images with little clouds. Optical images provide reliable detection if there is a sufficient time interval, say 1 – 2 months. SAR can also be used to detect icebergs, but there are also ambiguous signals in the SAR due to inherent speckle noise in radar images.

The report will present an overview of the data collected and preliminary results of iceberg observations done in April – May 2007.

2. ARGOS buoy deployment on icebergs

During two Lance cruises north of Svalbard in April 2007, CMR ICEX buoys with temperature sensors and ARGOS system were deployed on four icebergs with the primary objective to track the drift and provide data on drift velocity. The ICEX buoys were dug into the snow cover on top of the icebergs (Fig. 3a). In the first cruise, led by the Norwegian Polar Institute, two buoys were deployed. Buoy no. 26911 was deployed on Norskebanken north of Svalbard on 10 April and buoy no. 26914 was deployed near Sjuøyane on 13 April. The trajectories for the first few days are shown in Fig. 3b. Buoy trajectories for a longer period (April and May) are presented in Figs. 4 and 5.

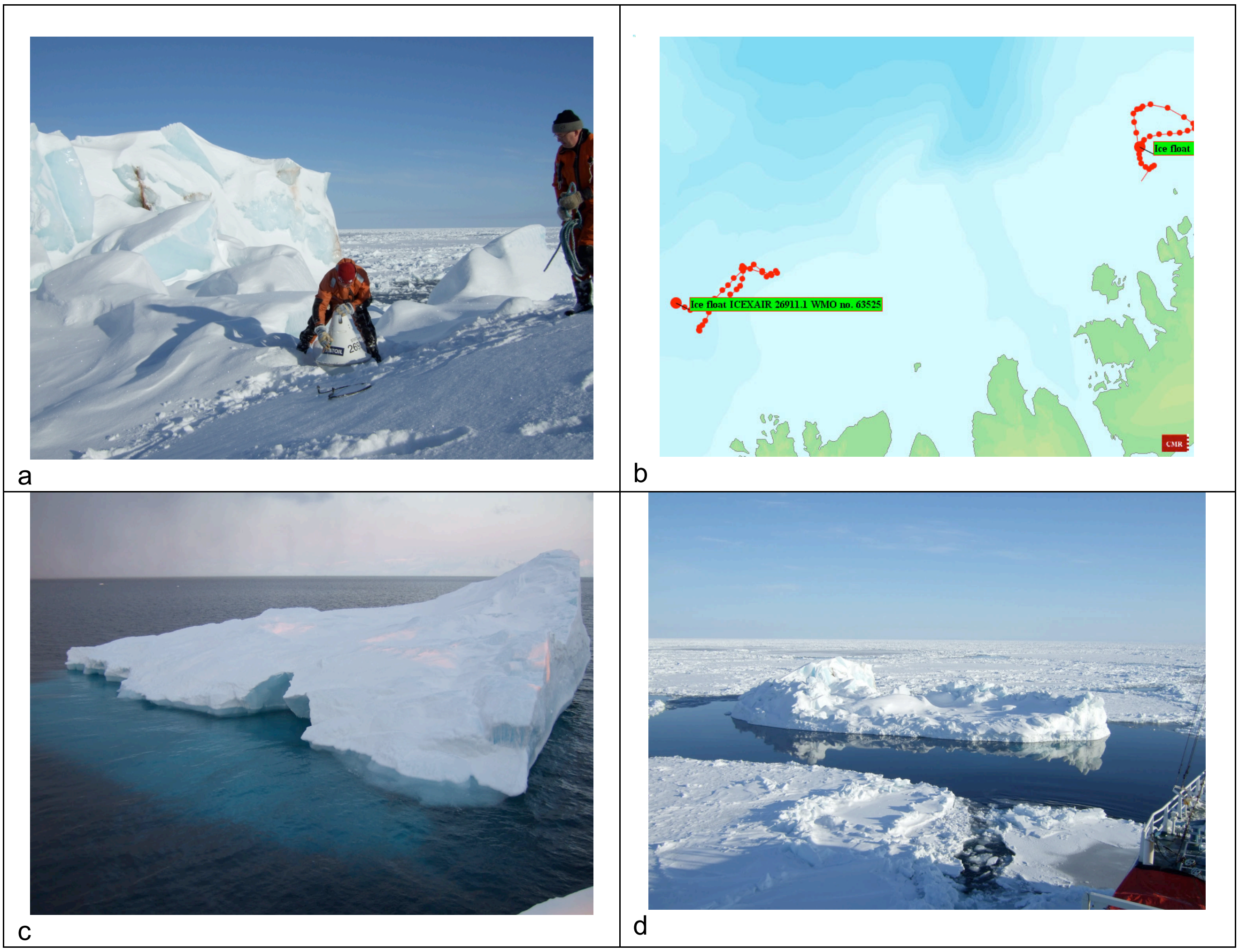

Figure 3. (a) Deployment of CMR buoy on a pinackle iceberg north of Svalbard on 23 April 2007, (b) trajectories of two icebergs until 16 April deployed in the beginning of the month by Lance.

During the second Lance cruise, led by UNIS and with participation of personnel from Statoil and NERSC, two more buoys were deployed. No 26939 was deployed on 17 April north of Spitzbergen, just west of Moffen, on an iceberg with triangular shape and horizontal dimension of about 50 by 50 m (Fig. 3c). The last buoy, no. 26931, was deployed north of Hinlopen on 23 April. This was a pinackle-shaped iceberg 70 m long and 30 m wide (Fig. 3d). Maximum height of the iceberg was about 10 m (Fig. 3a) and the depth was observed by ROV to be 23 m. After a few days with ARGOS position data, it was seen that buoy 26939 did not move because the iceberg was grounded. Therefore this buoy was recovered and redeployed on another iceberg further northwest on 26 April. The ARGOS position data were used to monitor the drift of the four icebergs during April and May. The drift pattern of the buoys are presented in Figs. 4 and 5.

Buoy 26911 drifted westwards after a few days and moved into the central Fram Strait where it continued southwards with the Eastgreenland Current. At the end of May it was located near 77°N 2°W (Fig. 5 lower map). Buoy 26914 stayed in the shallow area northwest of Sjuøyane to the end of May. Buoy 26939 was first stuck on a grounded iceberg, and after a few days relocated on a new iceberg further northeast (80°11'N, 11°43'E). This iceberg drifted on Norskebanken north of Spitzbergen for a week or so before it moved westwards into the Fram Strait. By the end of May it was located at about 80° N 2° E. Buoy 26931 was deployed in Hinlopenrenna north of Hinlopen Strait were it drifted in southeasterly direction in the first week. During May it drifted westwards and stayed on Norskebanken to the end of the month.

The ICEX buoys also measured temperature in the air and at bottom, indicating when the buoy goes from ice into water. For iceberg detection in satellite images, the position data offer a unique opportunity to check if any of the four icebergs equipped with buoys are recognized in the satellite images. This requires that the satellite images cover the same area as the buoy positions for the same period. In the next chapters, we provide an overview of the satellite data collected for iceberg detection with extraction of the images that coincide with the ARGOS positions.

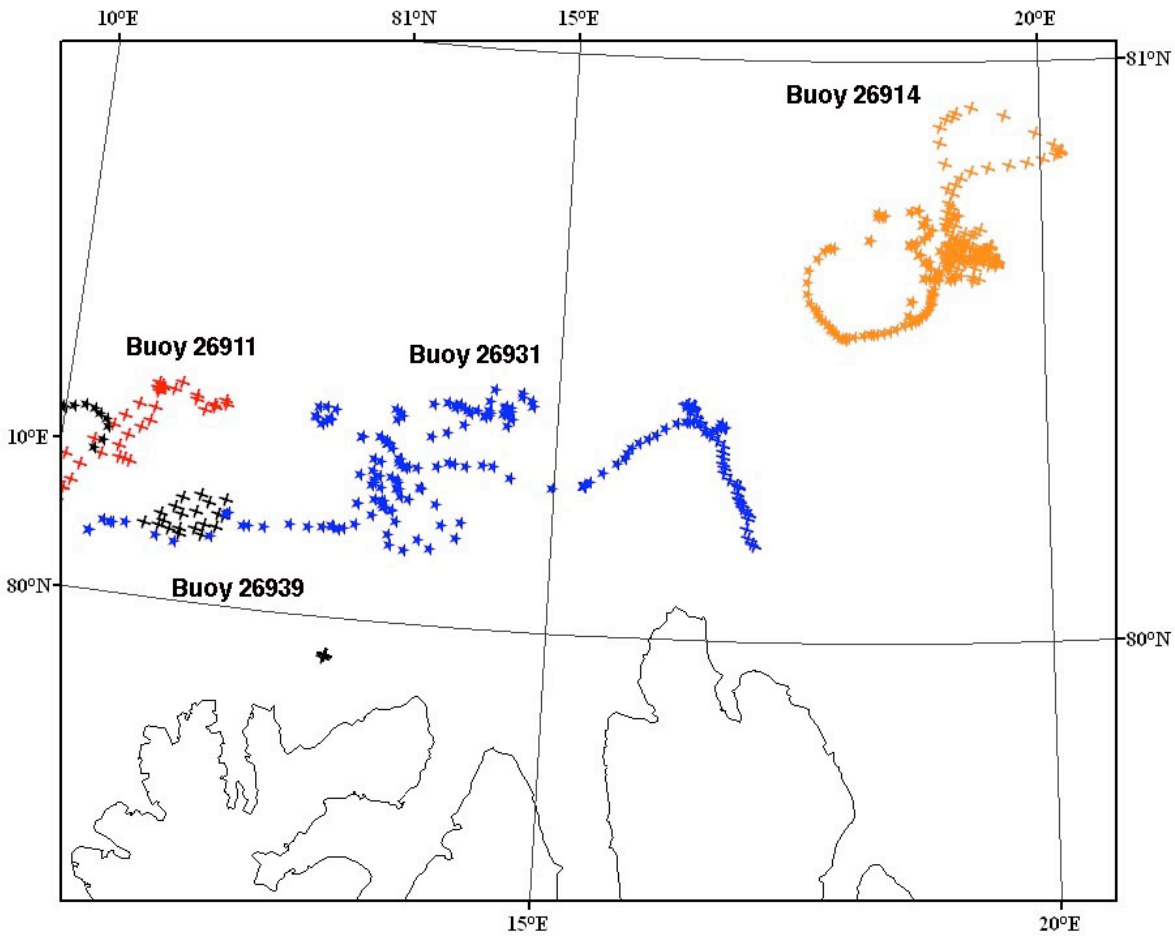

Figure 4. Trajectories of the four icebergs north of Svalbard in April ("x") and May ("").*

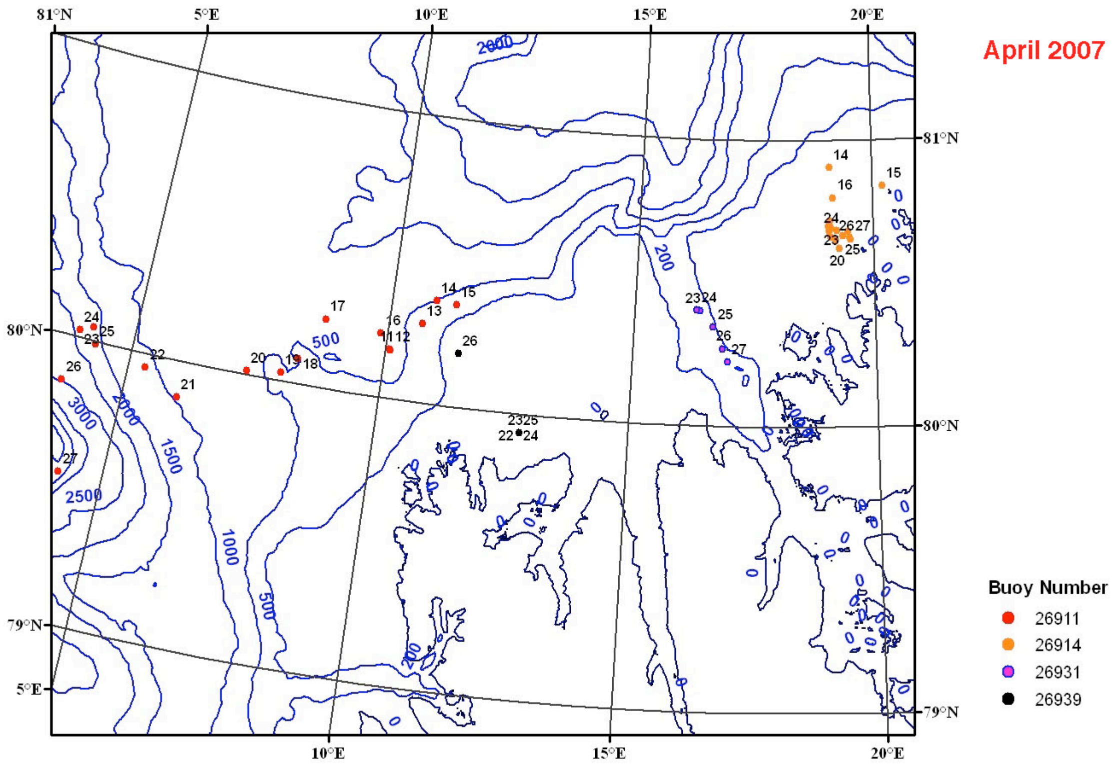

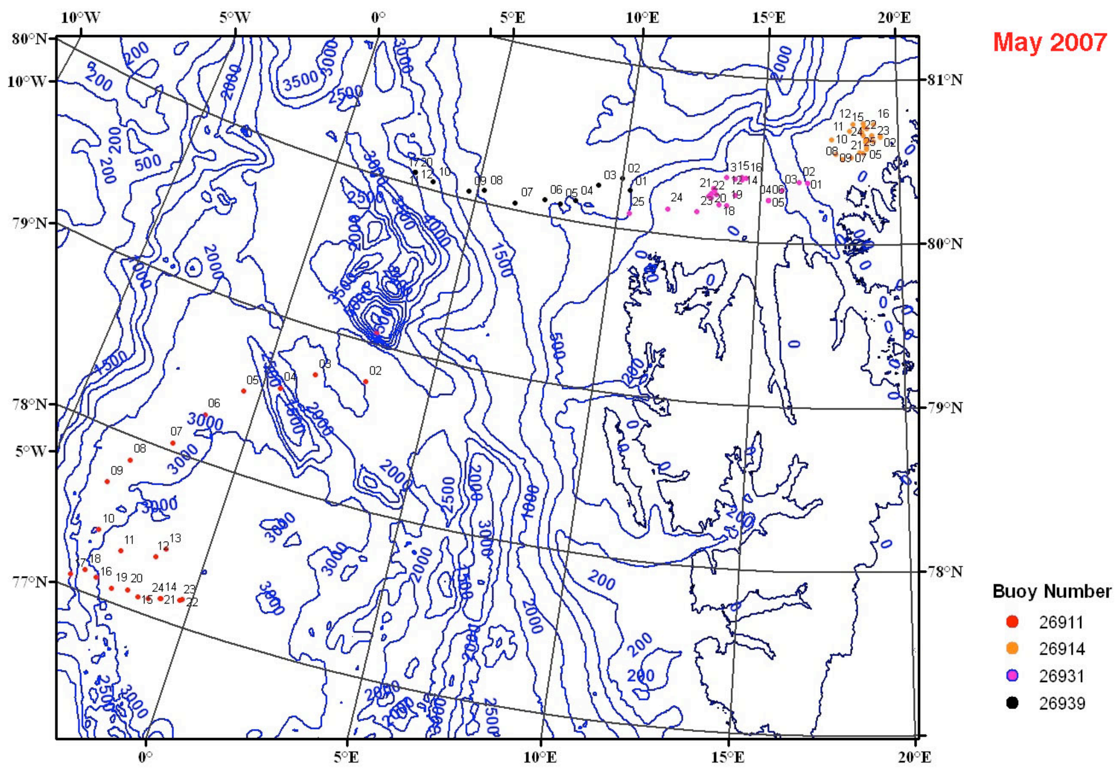

Figure 5. Daily positions of four icebergs with ARGOS buoys superimposed on bathymetric charts. The upper map is for April and the lower map is for May 2007.

3. Satellite data

Two main types of satellite images are useful for iceberg detection: high-resolution optical images from Landsat, SPOT and Terra ASTER, and high-resolution SAR images from RADARSAT and ENVISAT. A selection of these data were collected for the Svalbard area and are presented in this report.

3.1 Optical images

Landsat ETM+ images

Images form Landsat ETM+ cover 180 x 180 km (Fig. 6) with resolution of 15 m in panchromatic channel and 30 m in the optical channels. Pixel size of the images are 12.5m and 25m, respectively. Data acquisition was ordered for the Svalbard area from 25 March to the end of April, giving the possibility to view quicklooks and order full resolution images if they had little clouds and covered the right areas. A coverage map for the Svalbard area is shown in Fig. 6, and the acquisition schedule for the paths and rows over Svalbard is presented in Table 1.

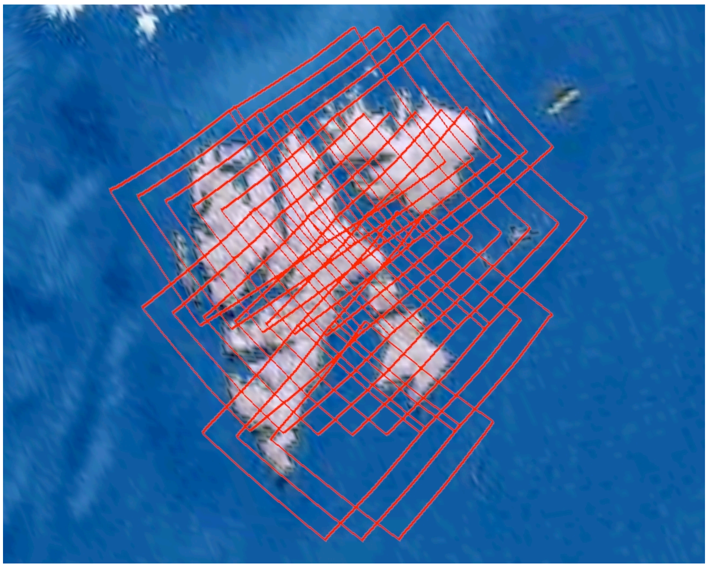

Figure 6. Landsat scenes covering Svalbard for April. Each scene, marked by the boxes, is defined by a row and a path number (Table 1). The coverage pattern is repeated every 16 days.

Table 1. Dates for Landsat image acquisition over Svalbard for March – June 2007

Scenes	Months 2007			
Paths /Rows	March	April	May	June
207 / 4,5	29	14, 30	16	1
208 / 4,5	20	5, 21	7, 23	8
209 / 4,5	27	12, 28	14, 30	15
210 / 3,4	18	3, 19	5, 21	6
211 / 3,4	25	10, 26	12, 28	13
212 / 3,4	16	1, 17	3, 19	4
213 / 3,4	23	8, 24	10, 26	11
214 / 2,3	14, 30	15	1, 17	2
215 / 2,3	21	6, 22	8, 24	9
216 / 2,3	28	13, 29	15, 31	16
217 / 2,3	19	4, 20	6, 22	7
218 / 2,3	26	11, 27	13, 29	14
219 / 2,3	17	2, 18	4, 20	5

When Landsat images have been acquired, a quicklook version can be browsed and downloaded to check if the quality is OK before full-resolution image can be ordered. An example of a quicklook Landsat image is shown in Fig. 7, covering the Storfjorden area on 19 April 2007. The quicklook image shows the refreezing of the polynya in Storfjorden, leads, ice floes, and the border between landfast ice and drifting ice. More Landsat quicklook images from are presented in Appendix C.

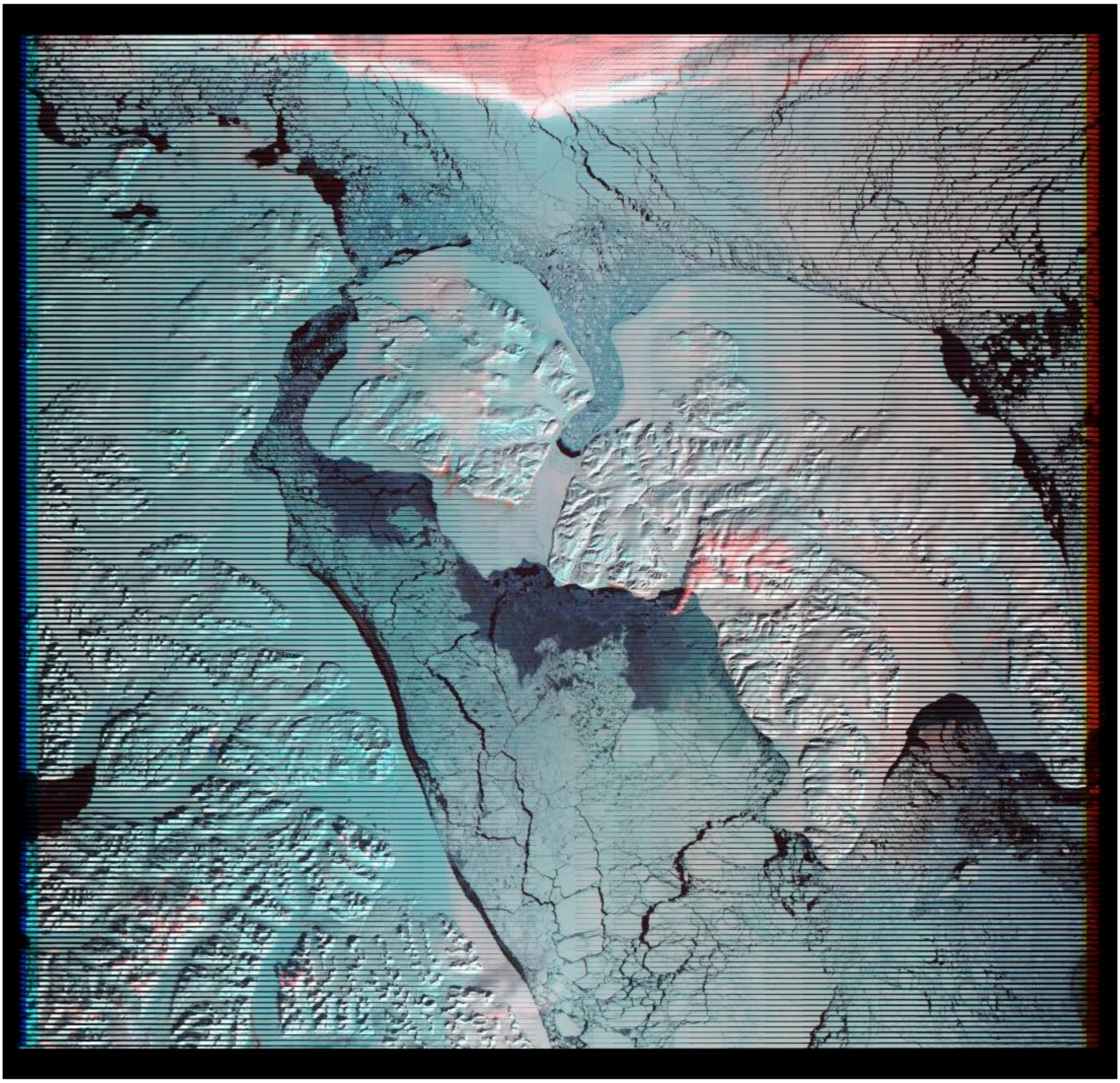

Figure 7. Landsat ETM+ quicklook image from 19 April 2007.

Terra ASTER

Terra ASTER images cover 60 by 60 km, with resolution & pixelsize of 15 m for both panchromatic and optical channel images. This is opportunity data taken occasionally over the Svalbard area. Quicklook images can be browsed and downloaded. Good quality images can be ordered in full resolution if they cover relevant areas. Example of coverage map and quicklook images are presented in Fig. 8.

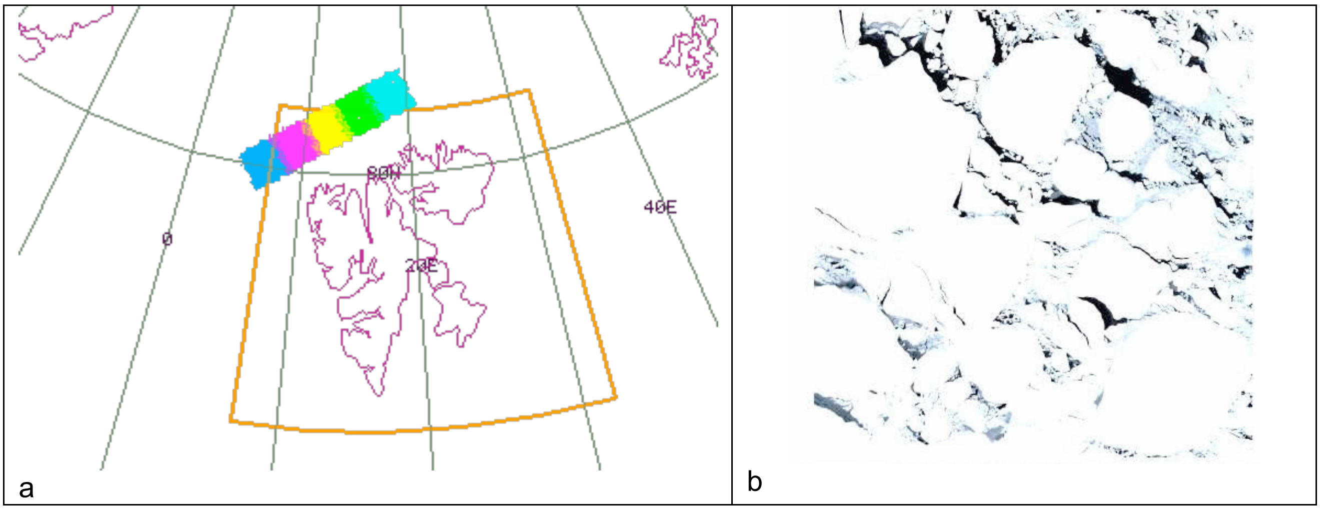

Figure 8. (a) Coverage map showing ASTER images acquired in sea ice north of Svalbard on 28 April 2007. Each image is indicated by a coloured rectangle; (b) quicklook image for the easternmost rectangle. More examples of ASTER quicklooks are presented in Appendix B.

SPOT

SPOT can offer the best quality and coverage of high-resolution optical images in any areas of the world. Resolution can be provided in 5 m for panchromatic images and 10 m for multichannel images. Swath width is 60 x 60 km and up to three satellites are in operation with steerable antennas to map areas on request from customers. This makes it possible to have more frequent coverage of a given area compared to Landsat and ASTER. There is ordering, acquisition and distribution services to users. In this project we ordered image acquisition over Svalbard for the month of April. SPOT has a quicklook service where low resolution images can be browsed before full resolution images are ordered. Example of coverage map and quicklook from SPOT is shown in Fig. 9. About 35 quicklook images were obtained in the Svalbard area during April. These are presented in Appendix A.

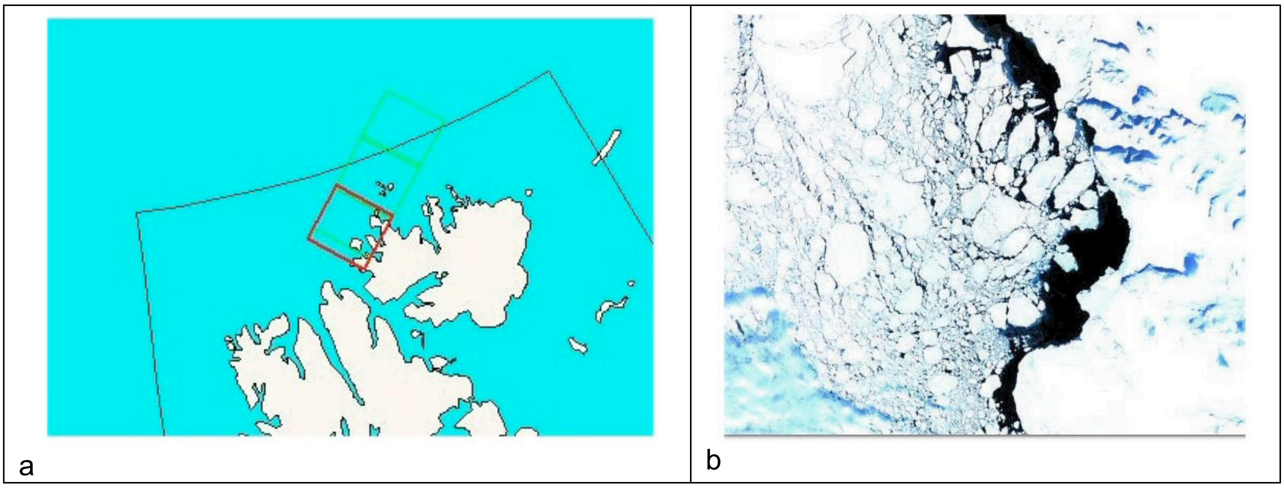

Figure 9. (a) Coverage map for SPOT images in the Svalbard area on 22 April 2007, (b) quicklook from SPOT on the northern side of Nordaustlandet, as shown by the red rectangle in (a).

3.2 SAR images

ENVISAT ASAR

ENVISAT produces wideswath SAR images for the Svalbard area almost every day, both in decending and ascending orbits (Fig. 10a). The images have 75 m pixels and cover about 400 km wide swaths. They are provided from the ESA rolling archive in long stripes as show in Fig. 10b. These images provide detailed information about the sea ice cover, but the resolution is not sufficient for iceberg detection. ENVISAT also provides higher resolution images with 12.5 m pixels in so-called Image Mode (IM) and Alternating Polarisation (AP) Mode. These images covers 100 km swath and are only produced on request from users. Use of AP images, which are produced in both VV- and HH- polarization, have been investigated for iceberg detection in the Franz Josef Land in a previous study by Sandven et al., (2007). The study showed that the AP images have good capability to detect icebergs, but there is ambiguities in the detection of icebergs because of speckle noise. In March 2007 a set of AP images were collected in the area around Kong Karls Land. One of them showed iceberg tracks in the drifting ice, as described in section 3.3.

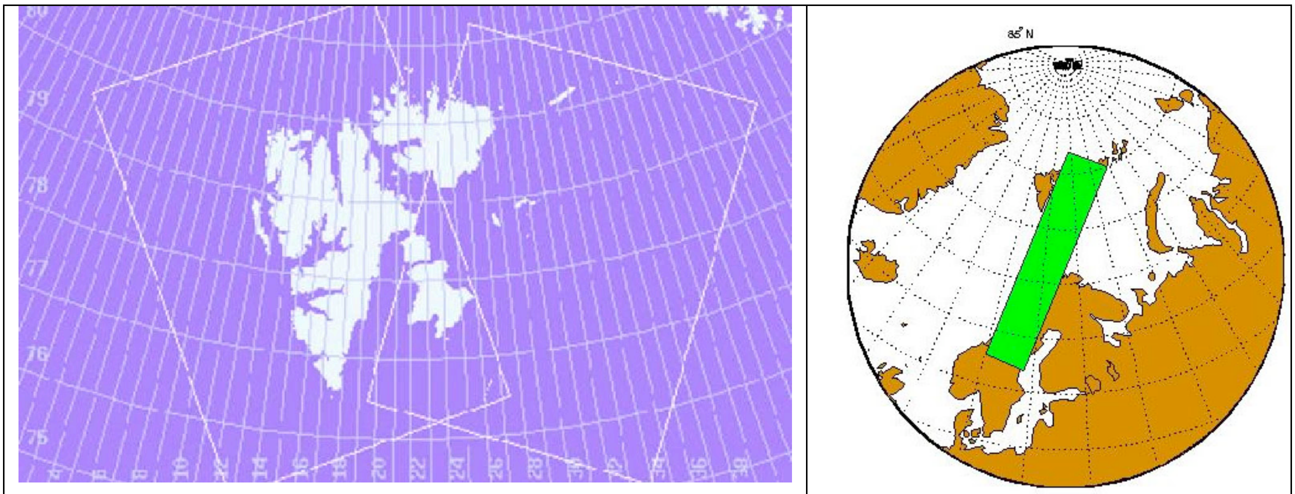

a b

Figure 10. (a) Map showing example of how descending orbits of ENVISAT (morning passes over the eastern part) and ascending orbits (evening passes over the western part) provide SAR wideswath coverage in the Svalbard region; (b) example of a long SAR wideswath stripe from a descending orbit over the western Barents Sea. The coverage from RADARSAT is similar to ENVISAT ASAR.

RADARSAT

SAR images from RADARSAT are produced in several modes on request from users. Most of the images over sea ice areas are ScanSAR images, with 300 or 500 km swath width, similar to ENVISAT wideswath images. RADARSAT can also produce images in several other modes with higher resolution. For iceberg detection it is appropriate to use ScanSAR Narrow images 25 m pixels and 300 km swath width. These images offer a good compromise between coverage and resolution. For iceberg detection 25 m pixel size is not sufficient for reliable detection, and SAR images with this resolution give ambiguous identification of icebergs. Examples of these are presented in chapter 4. For more reliable iceberg detection, the pixel size should be 10 m or better. This can be obtained from RADARSAT Fine Resolution mode with 40 km swath. In this project we acquired RADARSAT images over the northern part of the Svalbard to coincide with the

Lance cruise on the following dates: 14, 16 and 22 April. The image on 22 April is presented in Figure 11 together with a Landsat and a SPOT image.

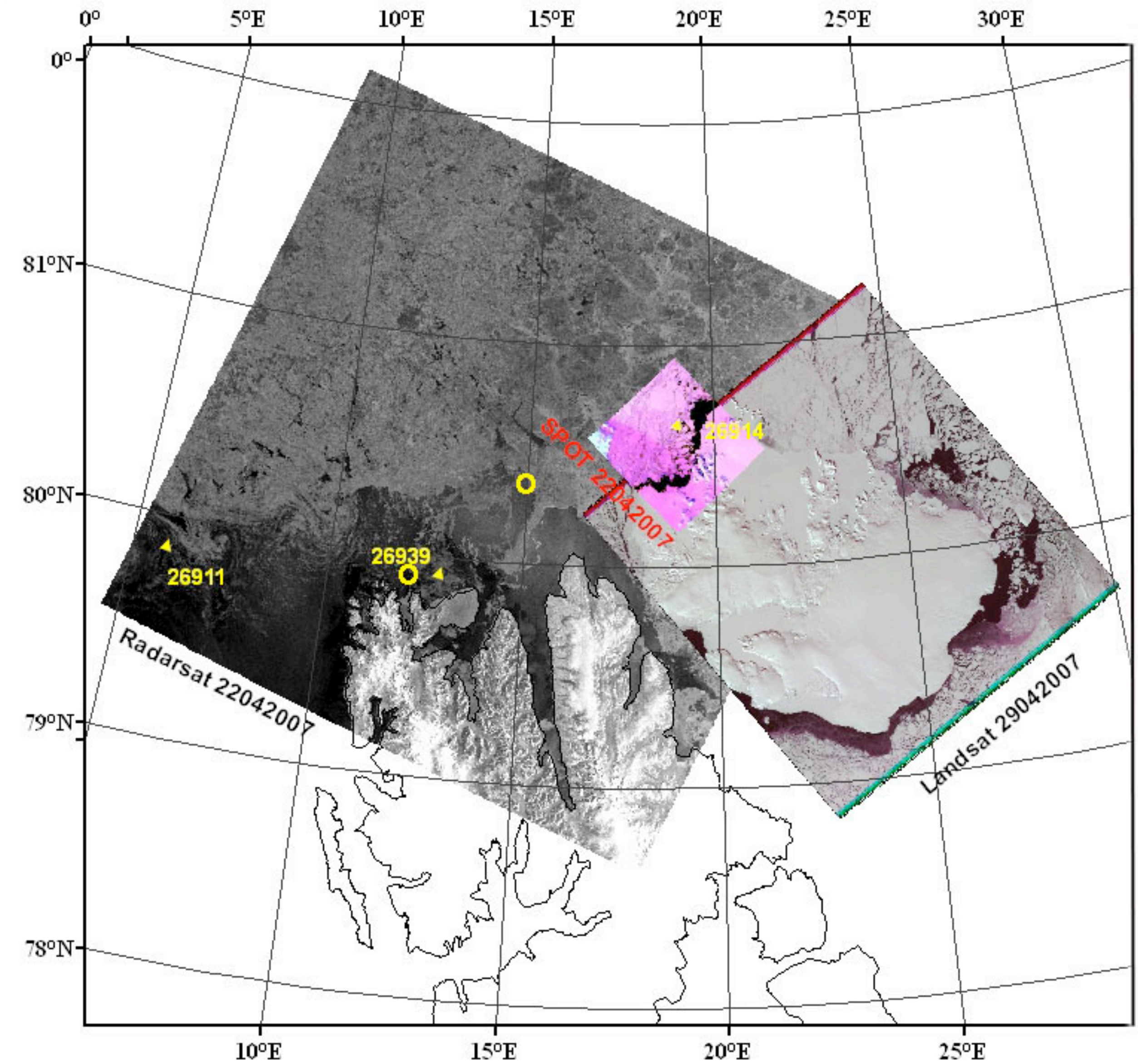

Figure 11. Composite map with a RADARSAT ScanSAR image (300 by 300 km), a Landsat image (180 by 180 km) and a SPOT image (60 by 60 km). Three positions of icebergs with ARGOS buoys are indicated by the triangles. Two icebergs located by Lance are indicated by the circles. Zoomed sub-images for each of the five iceberg locations are presented in Figs. 14 – 19.

3.3 Iceberg locations in the images

With four drifting icebergs marked with ARGOS transponders it is possible to search for these icebergs in the satellite images that cover the iceberg locations. This is illustrated in Fig. 11 where three ARGOS positions are marked. Three of them are located inside the SAR image and one is also located inside the SPOT image. In addition, one grounded iceberg documented by the Lance expedition, located at 80° 21.3N 15° 01.2E, could be used to verify observations in the images. This iceberg was about 80 by 60 m in horizontal extent and the height above sea surface was 12 – 15 m. This was the largest iceberg observed during the Lance expedition.

In addition to the icebergs observed north of Svalbard during the Lance cruise, satellite images were collected in the area between Hopen and Kong Karls Land. In this area icebergs originating in Franz Josef Land and Nordaustlandet are traditionally found to be drifting in a southwesterly direction. In the period from 12 to 24 March 2007 a set of ASAR AP images were collected in the area from Storforden, Edgeøya and Kong Karls Land (Fig. 12 a). Some of these images show tracks of iceberg in the drifting packice. Example of SAR signatures of these tracks are found in the image from 19 March (Fig. 12 b) where the bright line features against a darker background represent the iceberg tracks.

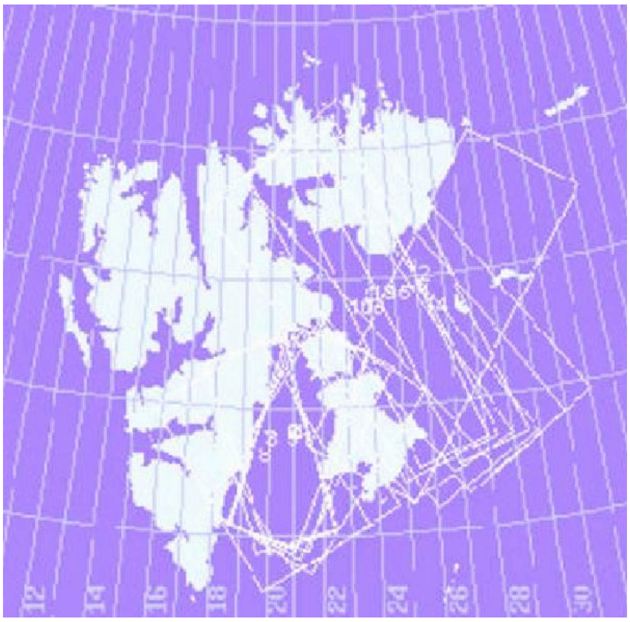

a

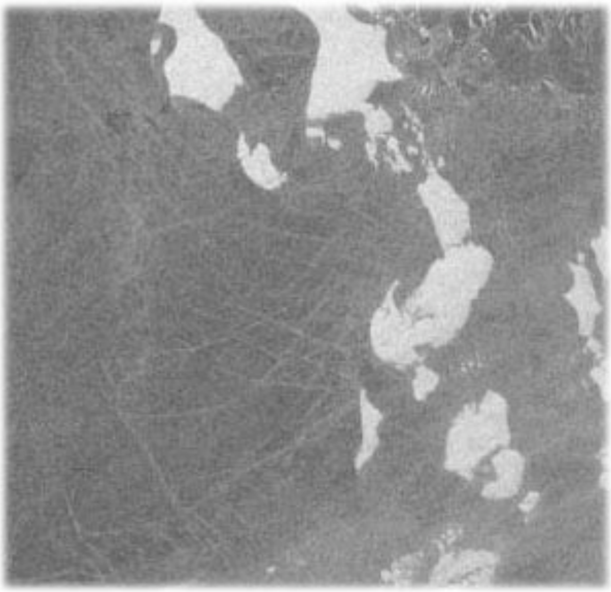

b

Figure 12. (a) Map of ASAR AP coverage in the eastern part of Svalbard during the period 12 – 24 march 2007. (b) Sub-image of the SAR AP image obtained on 19 March 2007 in the area between Edgeøya and Kong Karls Land. The bright lines show the tracks made by icebergs in the drifting sea ice. The bright areas in the image are open water. The size of the sub-image is 30 by 30 km.

Iceberg tracks in drifting ice can be identified also in high-resolution optical images. The SPOT quicklook images obtained in the same area in April 2007 showed similar line features. Two examples are presented in Figure 13 where image (a) is south of Kong Karls Land (same area as the SAR images in Fig. 12) and (b) is north of Hopen island. Both images show characteristic curved lines cutting through the sea ice floes. When icebergs are grounded on shallow banks, or they move with different velocity compared to the sea ice, they cut through the sea ice and leaves a track behind which can be recognised in the satellite images. These tracks can be different from the leads as shown in Figs 12 and 13, both in shape and greyscale. The iceberg tracks in the SAR image (Fig. 12b) have a greyish signature due to a mixture of broken floes, brash ice and open water. The same phenomenon was previously found by Sandven et al. (1991) in SAR images on Spitzbergenbanken. The optical image from the Hopen area (Fig. 13 b) shows a dense pattern of line features around the northeastern tip of the island, indicating that there must be a large number of icebergs in this area. The quicklook images are difficult to use for detection of individual icebergs, but the full resolution SPOT images are available and can be used for detailed studies of the icebergs. Iceberg tracks in the drifting sea ice has previously been investigated during the MIZEX and SIZEX projects and during IDAP.

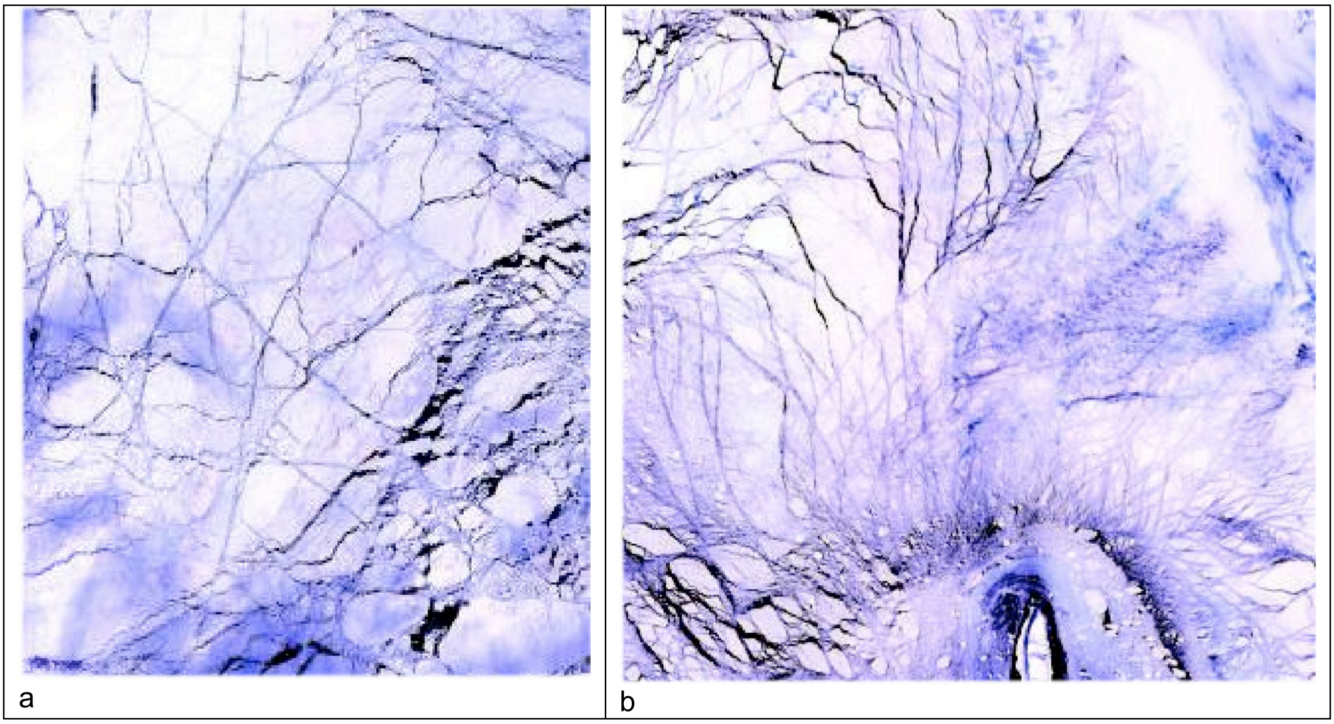

Figure 13. Sub-images of about 30 by 30 km from SPOT quicklook images showing example of tracks in the sea ice produced by icebergs. (a) is from the area south of Kong Karls Land on 18 April 2007, and (b) is from Hopen area on 21 April 2007. SPOT full-resolution images (10 m pixels) will provide much more detailed information and should be used to identify individual icebergs.

A few SPOT images were obtained north of Svalbard, in the area of the Lance expedition. One SPOT image coincided with the location of one of the icebergs with ARGOS buoy, as shown in Fig. 11. This image was ordered in full resolution (10 m pixels) and analyzed in order to identify the iceberg with ARGOS buoy. The position of the buoy approximately at the time when the SPOT image was obtained is marked in the image shown in Fig. 14. The iceberg must be located inside the red circle indicating the area around the buoy position, marked by the yellow triangle. The position is superimposed on a subset of the full resolution image, but the position of the buoy has some uncertainty due to (a) time of satellite data is a few hours different from the ARGOS position, and (b) ARGOS position error, and (c) geolocation of the image has some inaccuracy. The geolocation error is small, so the iceberg is expected to be within a few hundred meters from the triangle. The size of the area covered by the sub-image is about 10 by 10 km.

In spite of the high-resolution image and ARGOS tracking of the iceberg, it is not possible to identify the iceberg in the image. The size of the iceberg, reported by the personnel who deployed the ARGOS buoy on 13 April is about 50 by 50 m. With 10 m pixel size, the size of the iceberg is large enough to be detected in the image, provided that the iceberg pixels can be discriminated from the background. This is not the case since the sea ice conditions surrounding the iceberg consist of many small floes, open water between the floes, and weak ice drift. The drift of the iceberg is very small, as can be derived from the ARGOS positions. Therefore, no tracks from the iceberg are expected to appear in the sea ice, as was observed in the Hopen area. In conclusion, the iceberg could not be identified in the SPOT due to the characteristics of the surrounding sea ice.

To compare SPOT quicklook and full resolution images, the quicklook version of the sub-image in (a) is shown in (b). The full resolution image has pixels size of 10 m, while the quicklook image has pixels size of about 100 m. The quicklook image shows the same picture as the full-resolution image, except that the small objects, less than a few hundred meters are blurred. Small floes and narrow leads are therefore not observable in the quicklook image. To identify objects of order 100 m requires full resolution images are needed.

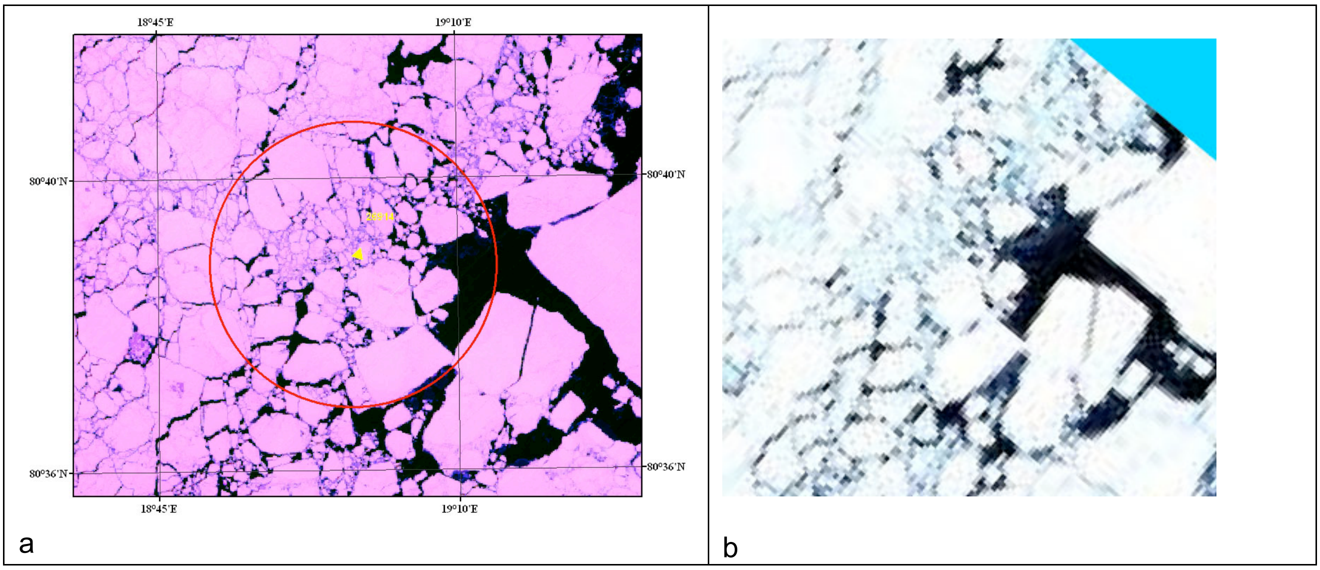

Figure 14. (a) Subset of the full-resolution SPOT image with geolocation obtained north of Svalbard on 22 April in the same area where one of the ARGO-tracked icebergs was located (no. 26914). The position of the iceberg is marked by the yellow triangle. The red circle is about 7 km in diameter. (b) quicklook version of the same image as in (a).

Some examples of zoomed subimages of the RADARSAT ScanSAR image of 22 April are presented in Figs. 15 – 19. The subimages cover the area around known positions of icebergs using the ARGOS data and directly observed icebergs from Lance. The first image (Fig. 15) covers an area on Norskebanken north of Svalbard where several icebergs where observed when Lance sailed through the area. One iceberg with horizontal size 80 by 60 m and height above surface of 12 – 15 m was documented to be grounded at a depth of 65m using an ROV. The position of the iceberg was 80° 21.3N 15° 01.2 E, which is inside the circle marked in the SAR image in Fig. 15. The circle has a diameter of 7 km, indicating uncertainty in the geolocation of the image. There are several bright spots inside the circle, but the largest bright spot inside the circle, marked by the arrow, is most probably the specific iceberg.

Figure 16 is a SAR subimage northwest of Svalbard where the iceberg with buoy 26911 drifted in a westerly direction, as shown in Fig. 5. The image has a well-defined bright spot near the centre of the red circle, marked by the arrow. There are many bright spots in the image, so it would be difficult to find a specific iceberg without a priori information about position.

Figure 17 is a SAR subimage west of Sjuøyane, showing the location of an iceberg with Argos buoy no. 26914. The ice consists of many small floes of high concentration, as shown more clearly in the SPOT image in Fig. 14. Under such ice conditions it is not possible to identify icebergs in satellite images, even when Argos position data are available.

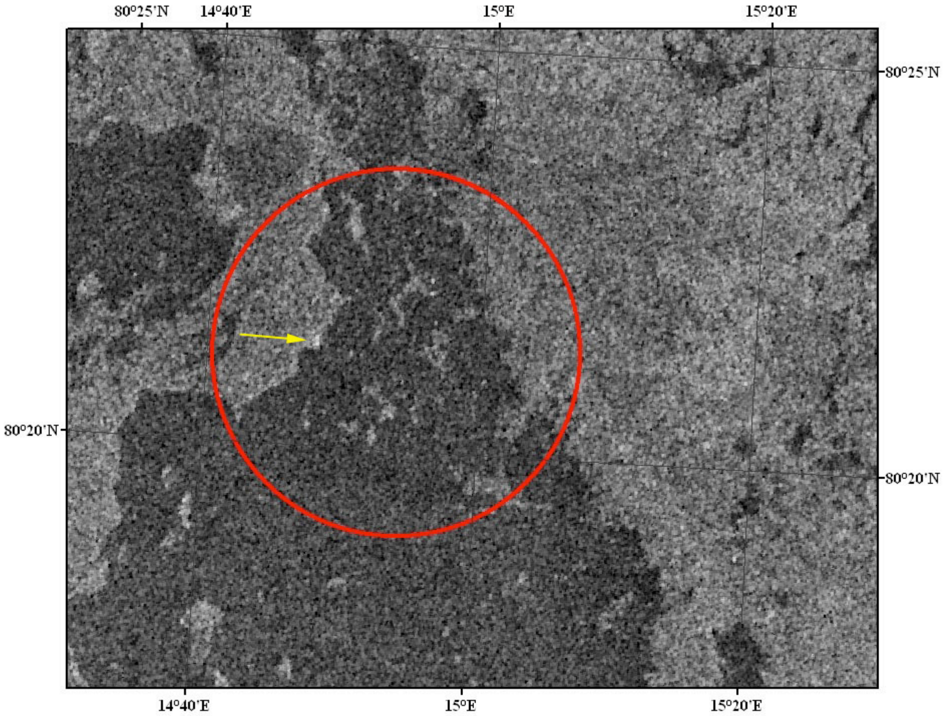

Figure 15. SAR sub-image of the area of a grounded iceberg at 80°21.3'N 15°01.21E

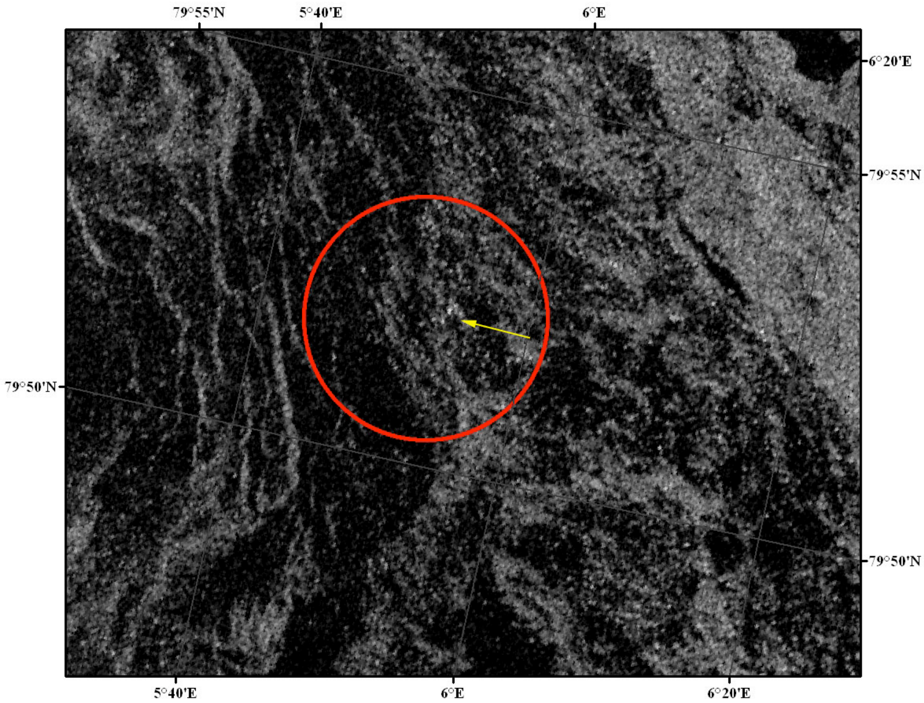

Figure 16. SAR sub-image of the area of a drifting iceberg northwest of Svalbard, marked with Argos no. 26911.

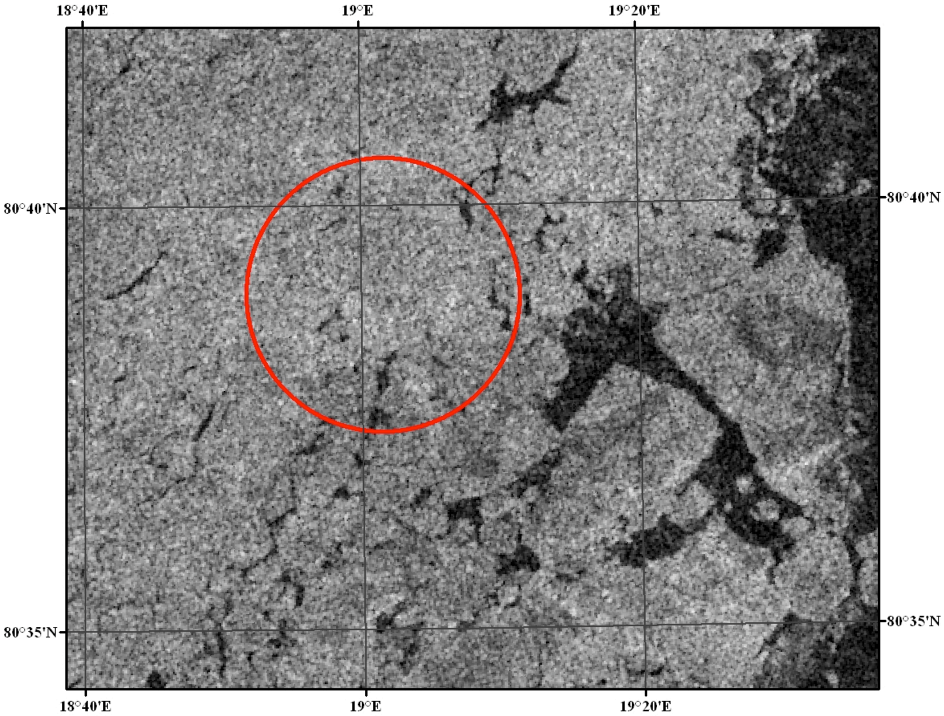

Figure 17. SAR sub-image of the area of the drifting iceberg near Sjuøyane, with ARGOS no. 26914 (the same area as shown in the SPOT image Fig. 14).

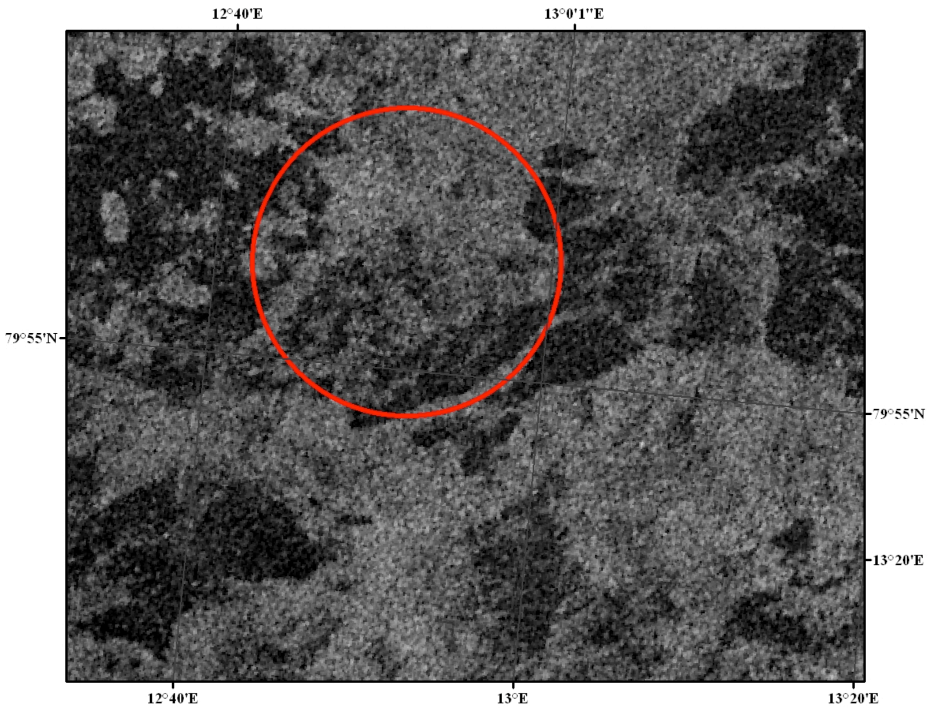

Figure 18. SAR sub-image of the area of a grounded iceberg on Norskebanken marked with Argos no. 26939.

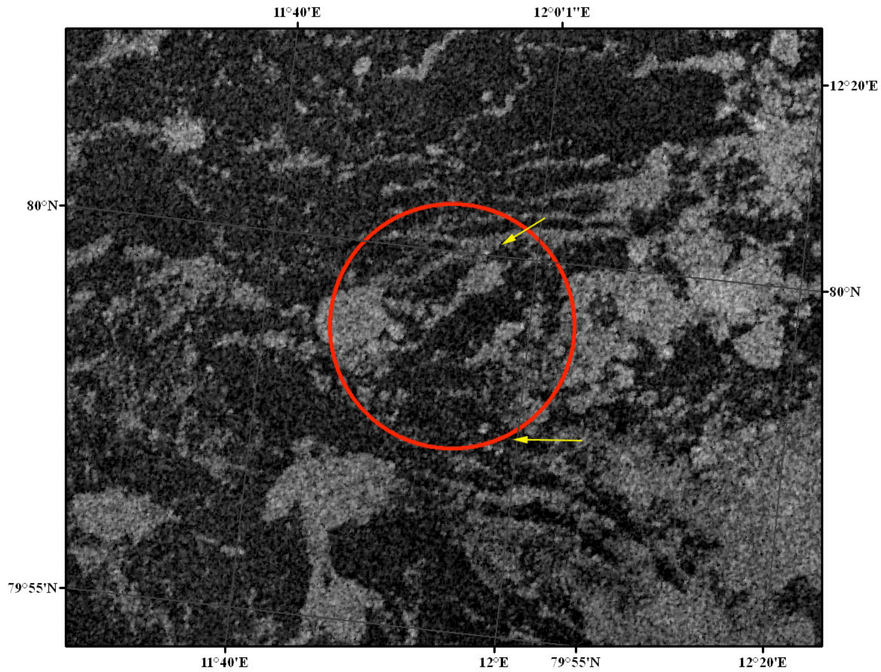

Figure 19. SAR sub-image of the area of a tabular iceberg north of Svalbard, observed by Lance on 25 April.

Figure 20. Photo of the tabular iceberg observed at 79°59'N 11°54'E on 25 April.

Figure 18 is a SAR subimage of the area where an ARGOS-marked iceberg grounded on Norskebanken was located. The size of the iceberg was about 50 by 50 m, surrounded by many small floes and scattered ice. It is not possible to identify any iceberg in this image.

Figure 19 is a SAR subimage in an area north of Svalbard where a tabular iceberg of size 120 by 30 m was observed by Lance. A photograph of the tabular uceberg is shown in Fig. 20. Freeboard height was 4 – 5 m and water depth was about 40 m. It was not clear if the iceberg was grounded or drifting. The image shows several bright spots which can be the tabular iceberg. Other iceberg were also observed by Lance in this area.

4. Discussion and conclusion

This study has focused on acquisition of high-resolution satellite images for iceberg detection in the Svalbard area in April – May 2007. The data acquisition has been coordinated with the Lance cruises north of Svalbard where Argos buoys were deployed on four icebergs. Optical images were ordered from SPOT, Landsat and Terra ASTER, and quicklook version of each image are presented in this report. The purpose of the quicklook images is to assess the cloud cover and the location, and use this information to select which images are suitable for ordering in full resolution. Iceberg detection is only feasible with full resolution images (10 m pixels), and these can be ordered from the data providers at a later stage as needed. A full-resolution image from SPOT was obtained in one case to check if an iceberg with known position and size could be identified. This was an area of high ice concentration with many small floes, so the ARGOS tagged iceberg could not be discriminated from the sea ice floes. Previous studies have shown that high-resolution optical images can be used successfully to detect icebergs of size 50 m or more when they are embedded in fastice or drifting in open water. If they are located in drifting ice, detection is more difficult, depending on the characteristics of the sea cover. In areas with significant ice drift, icebergs can generate tracks in the sea ice cover because they have different drift velocity compared to the sea ice or when they are grounded. In the area north of Hopen, many iceberg tracks could be identified even in the quicklook version of the SPOT images. The main limitation of the optical images is the cloud cover. During the month of April 2007, which was characterized by many days with good weather, we obtained 35 SPOT quicklook images with less than 10 % cloud cover on 9 different days. On some of the days we also got a few Landsat and ASTER images.

Since the optical images are limited by cloud cover and darkness, it is important to use SAR images which can be obtained much more frequently and with good quality independent of cloud and darkness. SAR images have other limitations, primarily speckle noise. SAR images were collected from two satellites: Radarsat and ENVISAT. Both produce SAR data in C-band with HH-polarisation. From Radarsat, ScanSAR Narrow Far mode with 300 km width were used. The images have incidence angle from 31° - 46° and 25 m pixel size. The speckle noise at 4 looks is ±1.8dB, which corresponds to 70 m resolution. Envisat ASAR Wide mode images with 420 km width and 18° - 43° incidence angle were obtained almost every day in the Svalbard area. They have 75 m pixels and a speckle noise of 1.2dB at 12 looks, which corresponds to about 150 m resolution. Resolution is the smallest distance in an image allowing two adjacent objects to be distinguished. Therefore, resolution is the most critical parameter for iceberg detection. The Radarsat ScanSar Narrow Far mode is more suitable for iceberg detection than the ENVISAT Wideswath images. Examples of iceberg detection in Radarsat are shown in Figs. 15 and 16. SAR images with higher resolution (Alternating Polarisation images with 100 km swath and 12.5 m pixel size) were provided by ENVISAT in the southeastern part of Svalbard during March. Detailed analysis of these images were not done, but quicklook images showed example of iceberg tracks in the drifting ice south of Kong Karls Land (Fig. 12).

Previous studies of SAR imagery for iceberg detection have been done in the Franz Josef Land area using ERS SAR data in combination with field observations from ship and aircraft (Wahl, 1993). This study showed that the detection capability is strongly dependent on iceberg size and also on wind speed and surface temperature. At size above 200m most of the icebergs could be detected in the SAR images, but in the range 100 – 200 m many icebergs could not be detected. In some cases icebergs less than 100 m could be detected. The study compared the highest resolution images (FRI) of 30 m pixels and 3 looks noise at ±2dB with noise-filtered images (LRI) of about 150m resolution and 50 looks noise at ±0.6dB. The detection capability was similar for the two types of images, showing the noise level is as important as resolution for detection of icebergs. Even with a low noise level of ±0.6dB the SAR images are considerably more “grainy” than optical images, illustrating that optical images are very important to use as a supplement to SAR images for iceberg detection.

The main backscattering effect from icebergs of this size is generally the “corner-reflection”. This gives a large enhancement of the signal from two plane surfaces that forms a 90 degree angle with each other and has the intersecting line perpendicular to the satellite direction. The right angle requirement is often fulfilled for the vertical sides of a tabular berg and the sea surface, but the last requirement requires an optimal angle to the satellite that may seldom occur. For more irregular shaped icebergs, no useful backscatter characteristics are generally known or predictable. The other enhancement effects for the backscatter are weaker and also very variable. They include the possible higher backscatter from the upper surface(s) of the iceberg relative to surrounding surface (again a tabular berg here gives the simplest example). The presence of small very dark area adjacent to the bright pixel(s) will add confidence to it as a possible iceberg signature. Such dark areas can be caused by the presence of a radar-shadow (shadow length is 2 -3 times a tabular berg freeboard, depending on incidence angle), or a change in the water close to the berg (e.g. damping of capillary waves caused by meltwater or lee effect).

Snow-covered icebergs have backscatter depending on temperature (low signal with near-melting conditions) that may well be quite similar to the surrounding area. Backscatter from this surrounding area may also be highly variable: Open water signal is wind speed dependent, backscatter from drifting sea is generally very variable. Also fast ice changes backscatter as function of temperature and ice composition. High incidence angle for the SAR is preferred since this will increase the corner-effect. Use of HH-polarization is better than VV-polarization because HH will decrease the signal from the surrounding areas compared the iceberg with more vertical structures. For iceberg detection a bright pixel (or a few connected pixels) surrounded by a reasonably smooth area of darker pixels should be sought in the area where there is a priori information about icebergs or where icebergs are expected to occur. If we find spots with 3dB higher signal (at >10 looks) than the background, they can be potential icebergs. However, many other sea ice features can produce the same kind of bright spots, for example small ice floes, ridges and irregularities at the edges of larger floes.

The use of ARGOS buoys deployed on four icebergs and direct observation of icebergs from the Lance are very important components of the iceberg studies using satellite data. First of all, field observations from ship or aircraft is the best method to document the location of icebergs in drifting sea ice and to obtain estimates of size and shape of the icebergs. In specific cases, such as grounded icebergs creating tracks in the drifting ice and stationary icebergs in fastice, satellite images can document the existence of icebergs without direct in situ observations. Secondly, ARGOS drifters on icebergs the areas where the icebergs are drifting, allowing new satellite images to be acquired in the right areas. This makes it possible to confirm if potential icebergs detected in the satellite images are real icebergs. Thirdly, iceberg drift data from the ARGOS positions are very important for validation of iceberg drift models. The Lance expedition did not use helicopter for iceberg reconnaissance, although a helicopter was part of the first cruise north of Svalbard. Airborne surveys by helicopter using video with GPS is the best method to map icebergs within an area of 50 – 100 km around the ship. Helicopter observations can document the amount, size and distribution of icebergs in a given area. These data can furthermore be used for more extensive validation of iceberg detection in satellite images.

The possibility to detect icebergs from satellites will improve significantly in the next few years. New SAR (RADARSAT-2, TerraSAR-X, and Sentinel-1), will have several modes allowing users to select scan width, resolution and polarisation. For iceberg monitoring, the most important new capability is higher resolution and full polarization. RADARSAT-2 and TerraSAR-X SAR images can deliver images with pixel size down to 2 – 3 m, which will increase the detection capability significantly. The usefulness of cross- (VH, HV) and co-polarisation (HH, VV) images in iceberg detection need to be investigated when data from TerraSAR-X (launched in 2007) and RADARSAT-2 becomes available. In parallel with use of SAR images, optical images from

ASTER, LANDSAT and SPOT should continue be used to supplement and validate the SAR observations. SPOT and ASTER can provide stereo photographs to study iceberg height and geometry, but this capability has not been investigated yet. The data presented in this report offer a good opportunity to extend the iceberg detection by analyzing full-resolution images.

5. References

Kloster, K. and W. Spring, Iceberg and glacier mapping using satellite optical imagery during the sea ice data acquisition programme (IDAP). Proceedings of POAC 1993, pp. 413 – 424.

Sandven, S, K. Kloster and O. M. Johannessen. Remote sensing of icebergs in the Barents Sea during SIZEX89. Presented at First International Offshore and Polar Engineering Conference, Edinburgh, 1991.

Sandven, S., M. Babiker, and K. Kloster. Analysis of high-resolution satellite images for iceberg detection in the Barents Sea. Project for Hydro Oil and Energy 2006. NERSC Technical Report no 275, February 2007, 42 pp.

Wahl, T. ERS-1 SAR iceberg detection experiment. Norwegian Defense Research Establishment, Final Report under contract with OKN, April 1993, 70 pp.

Appendices: Presentation of quicklook images

Appendix A: SPOT quicklook images

Satellite	GRS reference		Acquisition date	Instrument	SAT
4	*153*	*141*	*04/04/2007 11:24:02*	*1*	*0*

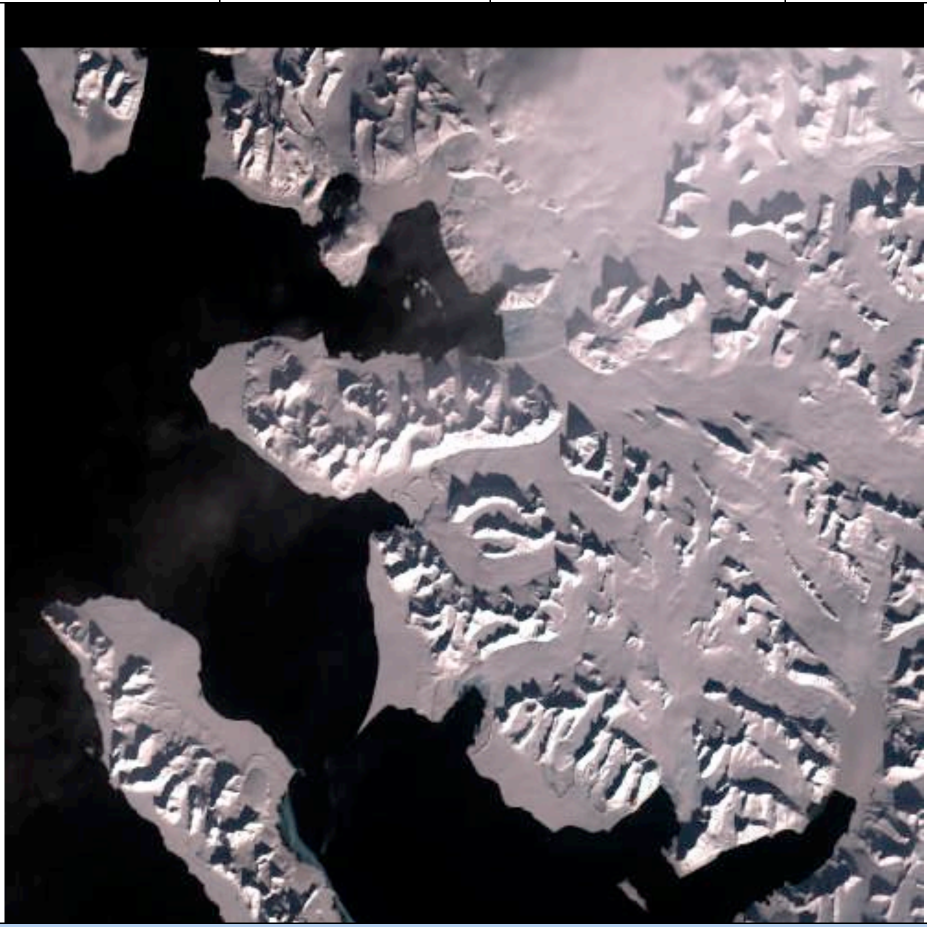

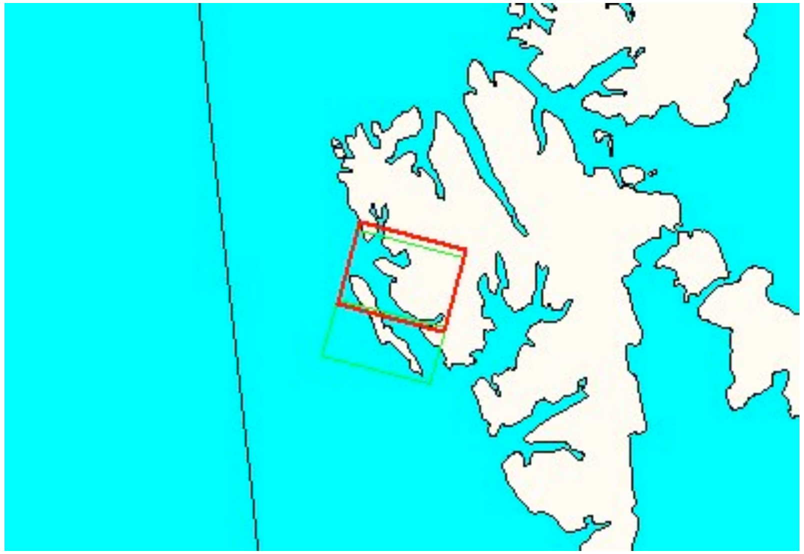

Technical information			
Spectral Mode	[I] 20 m C	Scene Orientation	026.7
Cloud cover (avg.)	AAAAAAAA (A)	Technical quality	Excellent
Snow cover (avg.)	11111111 ()	Incidence angle	-29.6
Sun azimut	182.5	Gains	3246
Sun elevation	+16.4		

Geographic location		
NW Corner		NE Corner
11°07' E / 79°14' N	Center	14°25' E / 78°54' N
SW Corner	12°08' E / 78°50' N	SE Corner
9°54' E / 78°45' N		13°06' E / 78°26' N

Satellite	GRS reference		Acquisition date	Instrument	SAT
4	154	143	04/04/2007 11:24:10	1	0

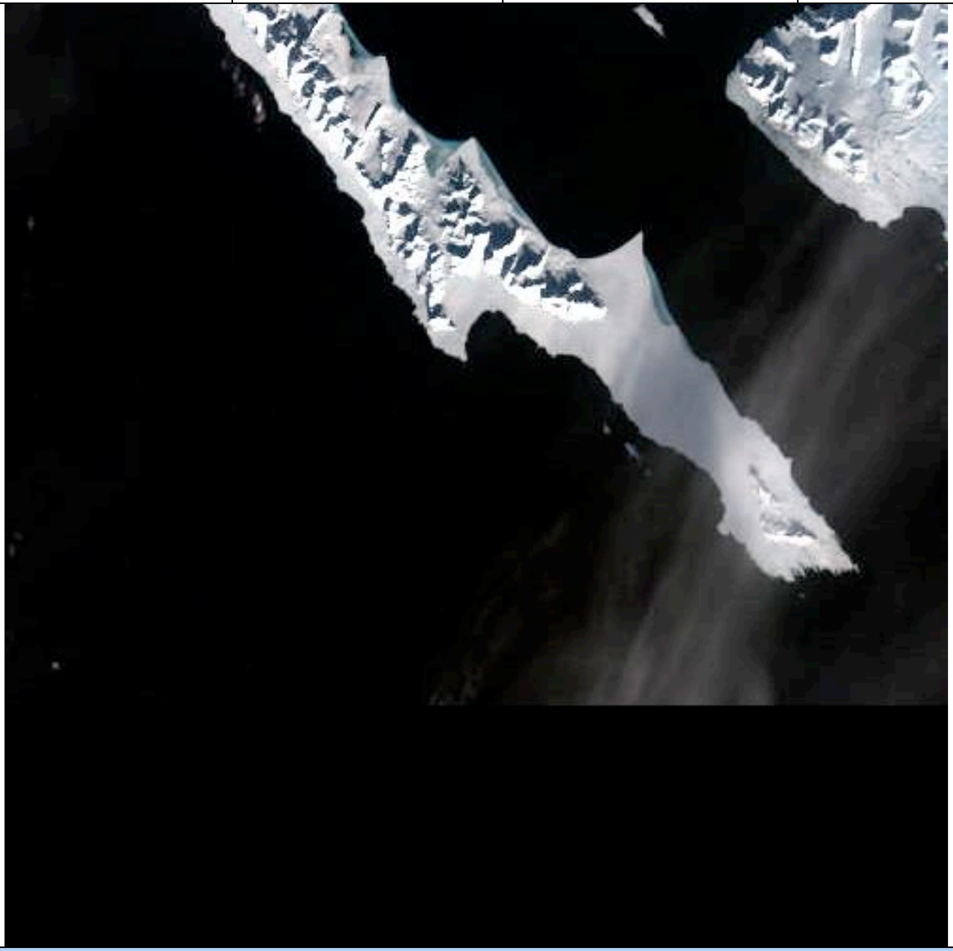

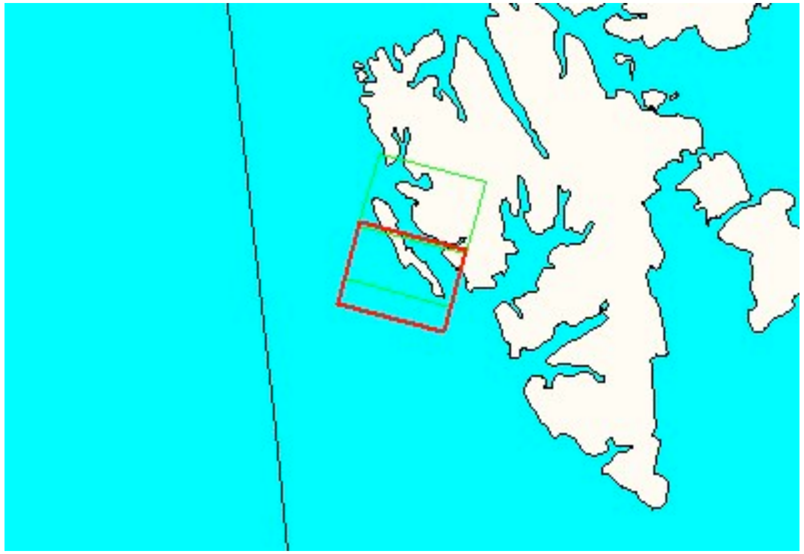

Technical information			
Spectral Mode	[I] 20 m C	Scene Orientation	026.0
Cloud cover (avg.)	AAAAAA** (A)	Technical quality	Excellent
Snow cover (avg.)	111111** ()	Incidence angle	-29.6
Sun azimut	181.3	Gains	3246
Sun elevation	+16.9		

Geographic location		
NW Corner		NE Corner
9°58' E / 78°46' N	Center	13°10' E / 78°28' N
SW Corner	10°58' E / 78°23' N	SE Corner
8°50' E / 78°17' N		11°56' E / 77°59' N

Satellite	GRS reference		Acquisition date	Instrument	SAT
4	155	136	04/07/2007 12:06:24	1	0

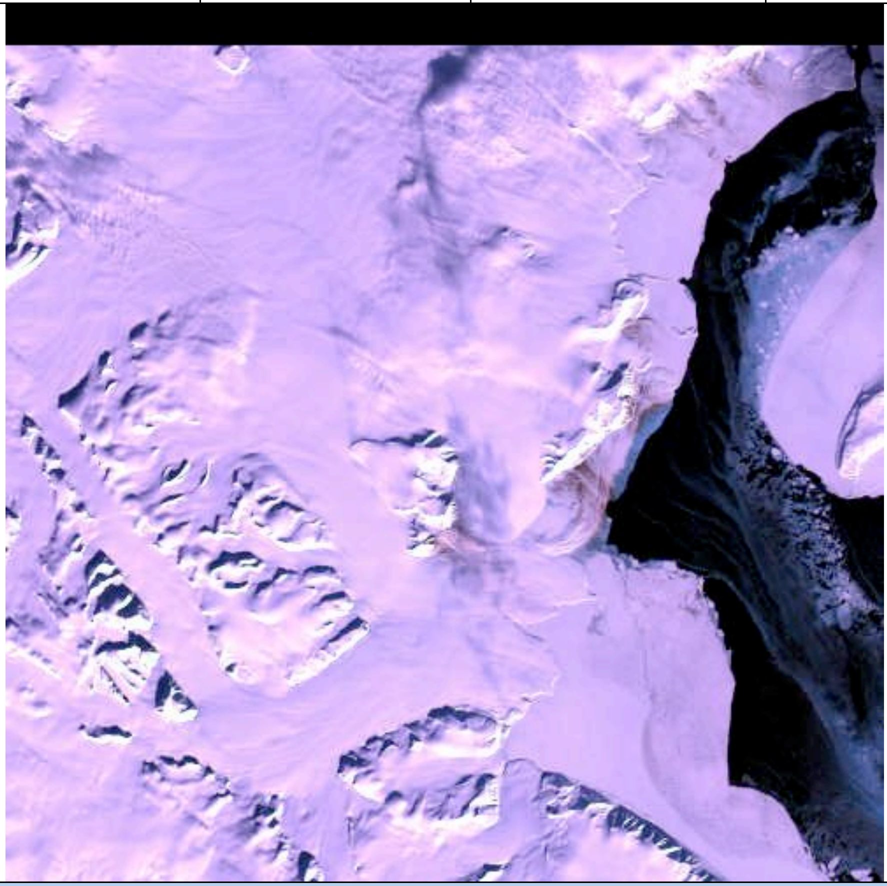

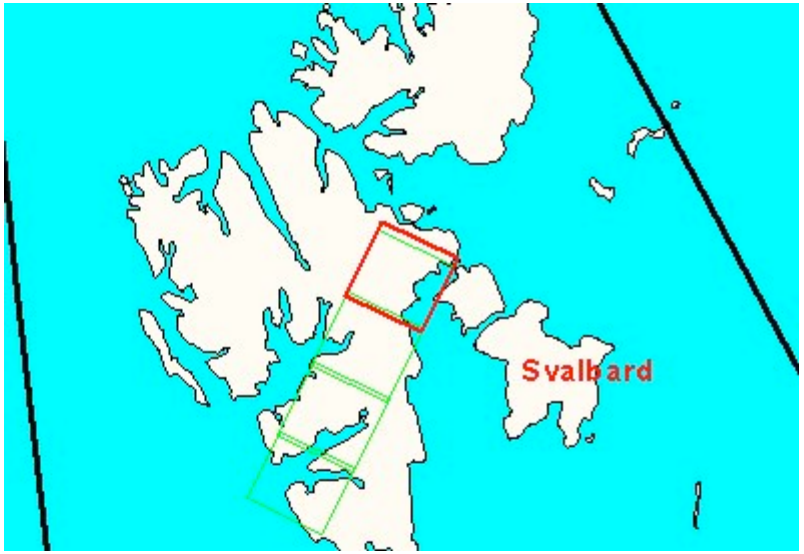

Technical information			
Spectral Mode	[I] 20 m C	Scene Orientation	043.7
Cloud cover (avg.)	AAAAAAAA (A)	Technical quality	Excellent
Snow cover (avg.)	11111111 ()	Incidence angle	-07.0
Sun azimut	201.2	Gains	5256
Sun elevation	+17.0		

Geographic location		
NW Corner		NE Corner
19°19' E / 79°04' N	Center	21°20' E / 78°41' N
SW Corner	19°22' E / 78°41' N	SE Corner
17°24' E / 78°41' N		19°24' E / 78°18' N

Satellite	*GRS reference*		*Acquisition date*	*Instrument*	*SAT*
4	*157*	*139*	*04/07/2007 12:06:32*	*1*	*0*

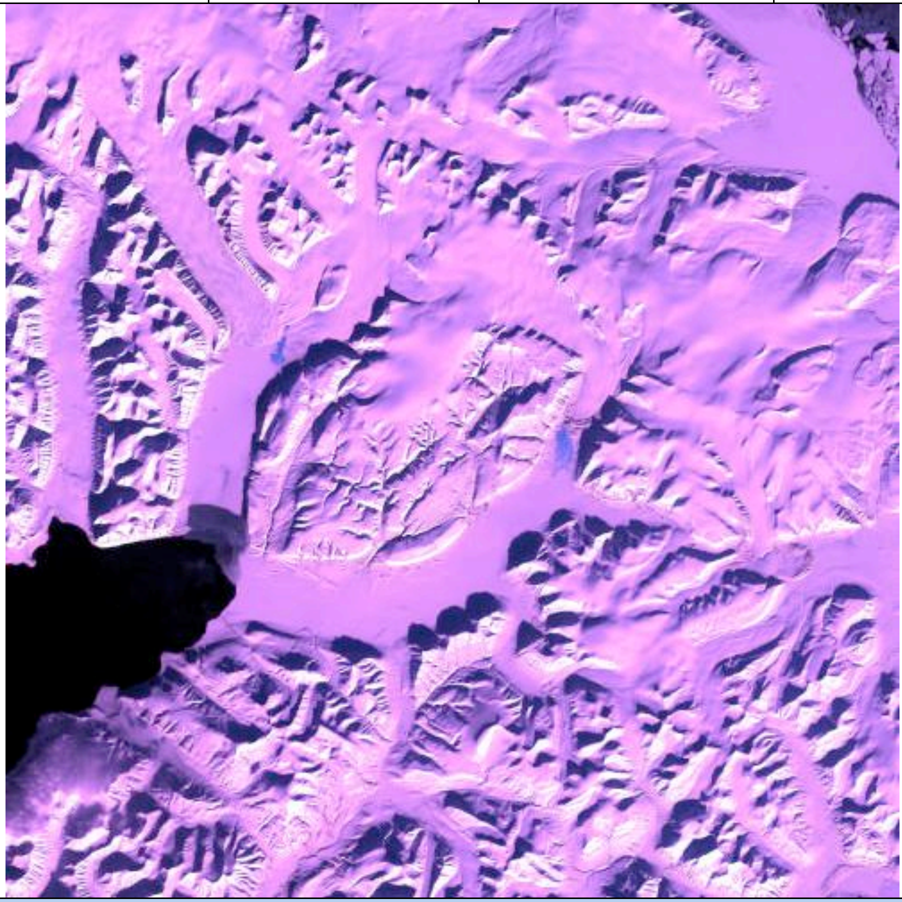

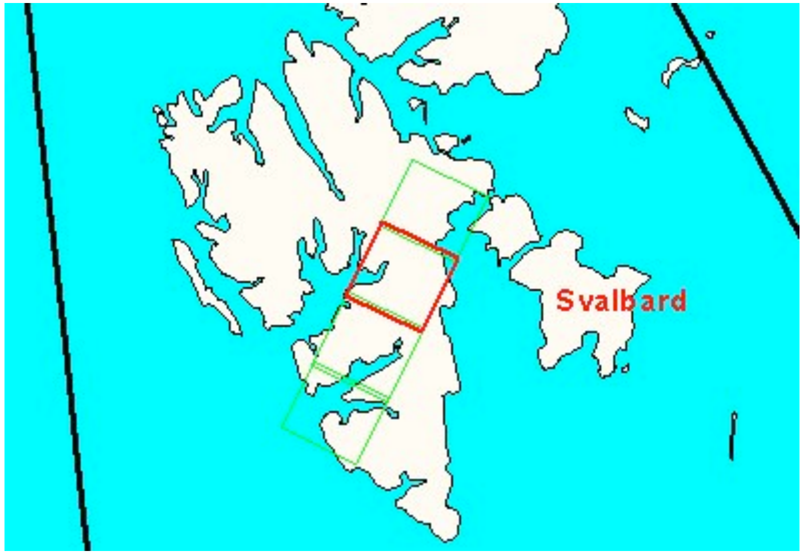

Geographic location		
NW Corner		NE Corner
17°30' E / 78°42' N	Center	19°30' E / 78°19' N
SW Corner	17°36' E / 78°19' N	SE Corner
15°42' E / 78°18' N		17°41' E / 77°56' N

Technical information			
Spectral Mode	[I] 20 m C	Scene Orientation	042.1
Cloud cover (avg.)	AAAAAAAA (A)	Technical quality	Excellent
Snow cover (avg.)	11111111 ()	Incidence angle	-07.0
Sun azimut	199.4	Gains	5256
Sun elevation	+17.5		

Satellite	*GRS reference*		*Acquisition date*	*Instrument*	*SAT*
4	*158*	*142*	*04/07/2007 12:06:41*	*1*	*0*

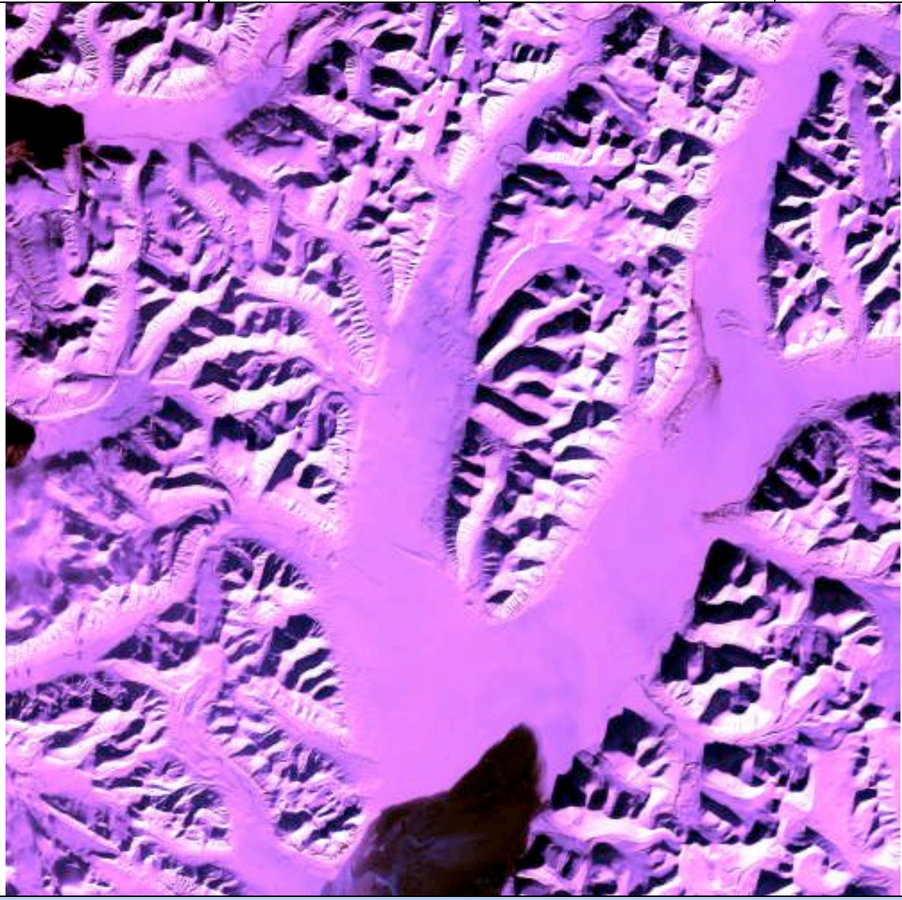

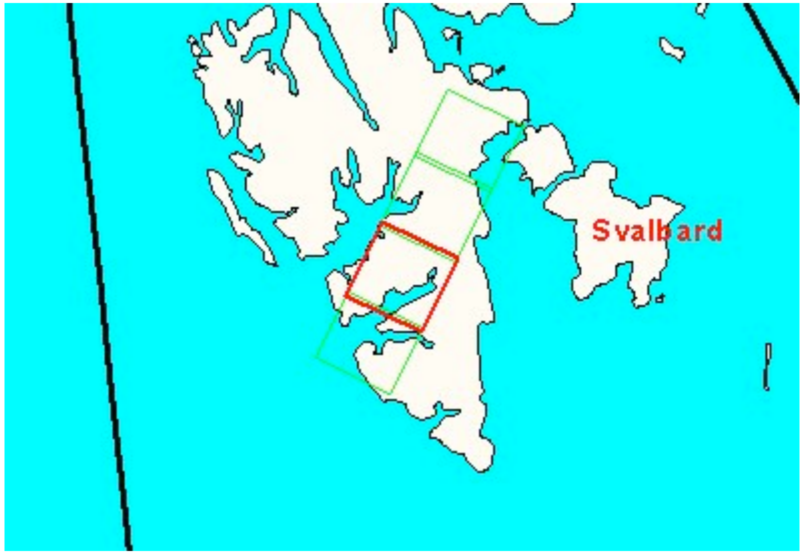

Geographic location		
NW Corner		NE Corner
15°47' E / 78°19' N	Center	17°46' E / 77°57' N
SW Corner	15°56' E / 77°56' N	SE Corner
14°06' E / 77°55' N		16°04' E / 77°33' N

Technical information			
Spectral Mode	[I] 20 m C	Scene Orientation	040.6
Cloud cover (avg.)	AAAAAAAA (A)	Technical quality	Excellent
Snow cover (avg.)	11111111 ()	Incidence angle	-07.0
Sun azimut	197.8	Gains	5256
Sun elevation	+18.0		

Satellite	*GRS reference*		*Acquisition date*	*Instrument*	*SAT*
4	*159*	*144*	*04/07/2007 12:06:50*	*1*	*0*

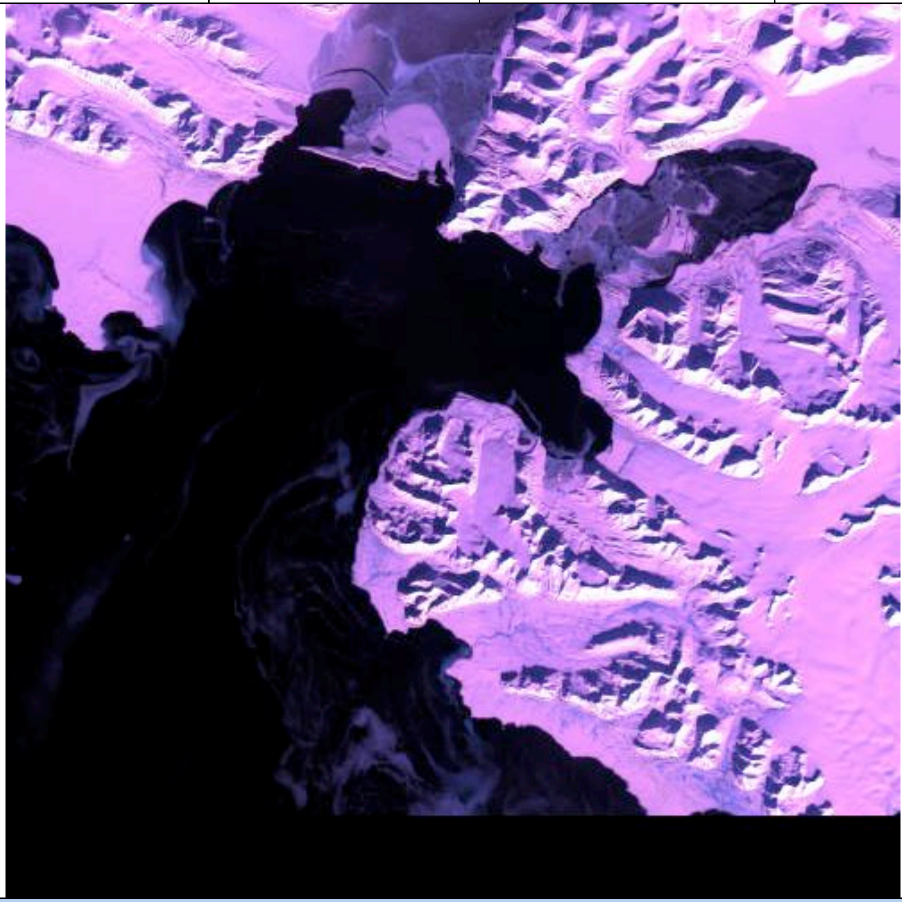

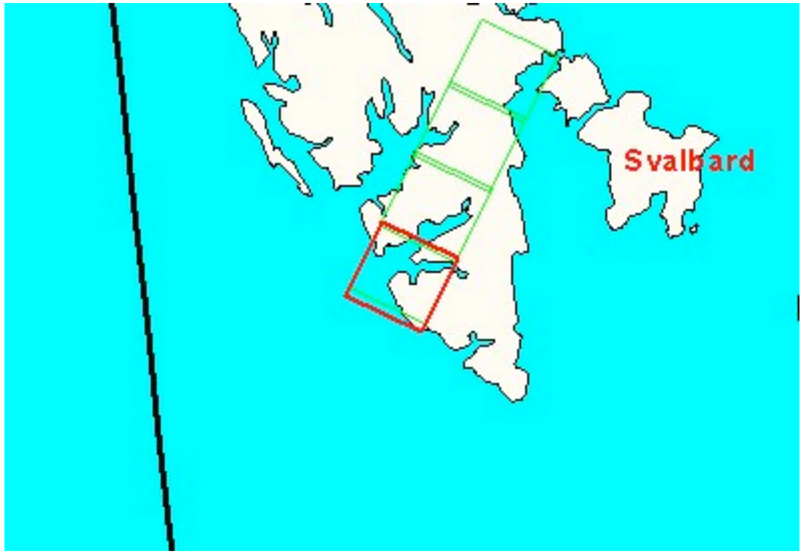

Geographic location		
NW Corner		NE Corner
14°10' E / 77°56' N	Center	16°09' E / 77°35' N
SW Corner	14°22' E / 77°33' N	SE Corner
12°35' E / 77°31' N		14°32' E / 77°10' N

Technical information			
Spectral Mode	[I] 20 m C	Scene Orientation	039.3
Cloud cover (avg.)	AAAAAAAA (A)	Technical quality	Excellent
Snow cover (avg.)	11111111 ()	Incidence angle	-07.0
Sun azimut	196.2	Gains	5256
Sun elevation	+18.4		

Satellite	*GRS reference*		*Acquisition date*	*Instrument*	*SAT*
4	*163*	*146*	*04/07/2007 12:06:58*	*2*	*0*

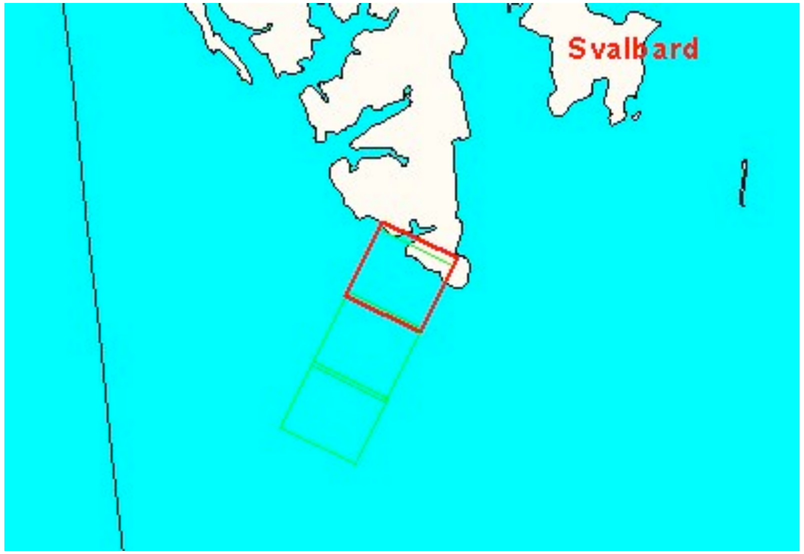

Geographic location		
NW Corner		NE Corner
15°06' E / 77°07' N	Center	16°55' E / 76°46' N
SW Corner	15°14' E / 76°44' N	SE Corner
13°34' E / 76°42' N		15°22' E / 76°22' N

Technical information			
Spectral Mode	[I] 20 m C	Scene Orientation	040.2
Cloud cover (avg.)	AAAAADAB (B)	Technical quality	Excellent
Snow cover (avg.)	11111111 ()	Incidence angle	-01.2
Sun azimut	197.3	Gains	5456
Sun elevation	+19.1		

Satellite	*GRS reference*		*Acquisition date*	*Instrument*	*SAT*
4	*143*	*134*	*04/12/2007 12:10:02*	*1*	*0*

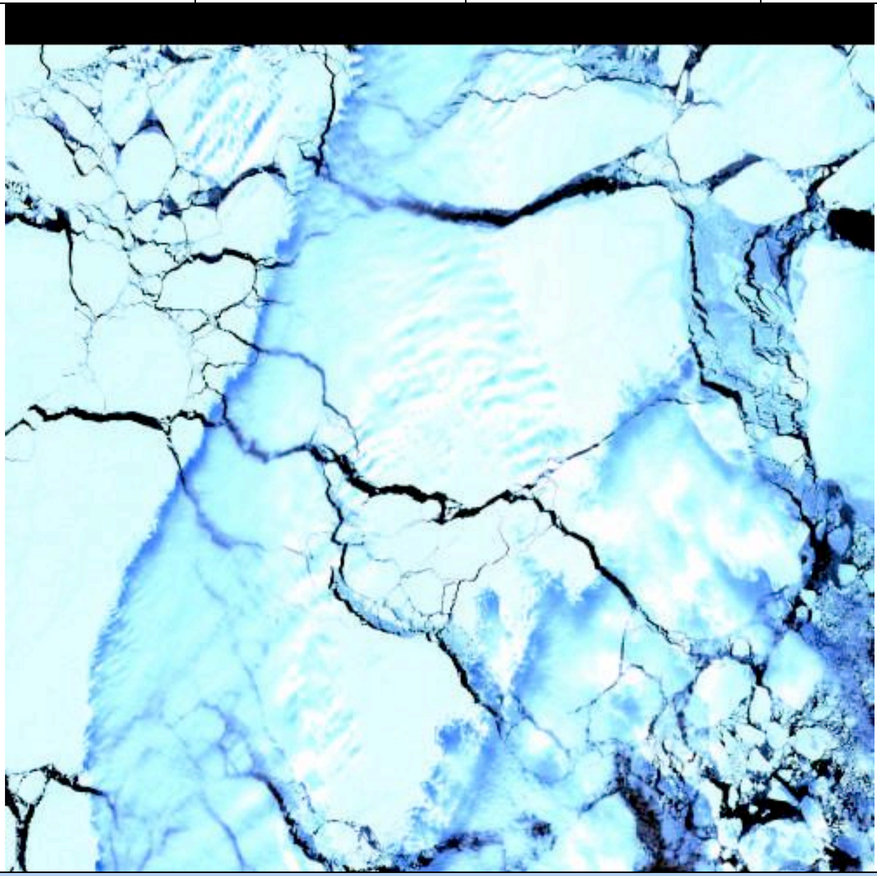

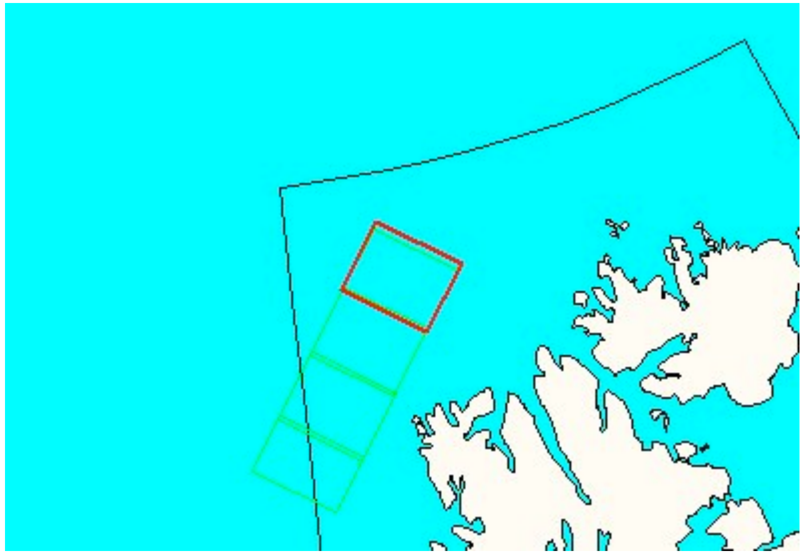

Geographic location		
NW Corner		NE Corner
10°39' E / 81°10' N	Center	13°57' E / 80°46' N
SW Corner	11°17' E / 80°45' N	SE Corner
8°40' E / 80°44' N		11°53' E / 80°21' N

Technical information			
Spectral Mode	[I] 20 m C	Scene Orientation	036.5
Cloud cover (avg.)	AAAAAAAA (A)	Technical quality	Excellent
Snow cover (avg.)	11111111 ()	Incidence angle	-25.5
Sun azimut	194.1	Gains	6556
Sun elevation	+17.3		

Satellite	*GRS reference*		*Acquisition date*	*Instrument*	*SAT*
4	*156*	*143*	*04/12/2007 12:10:35*	*2*	*0*

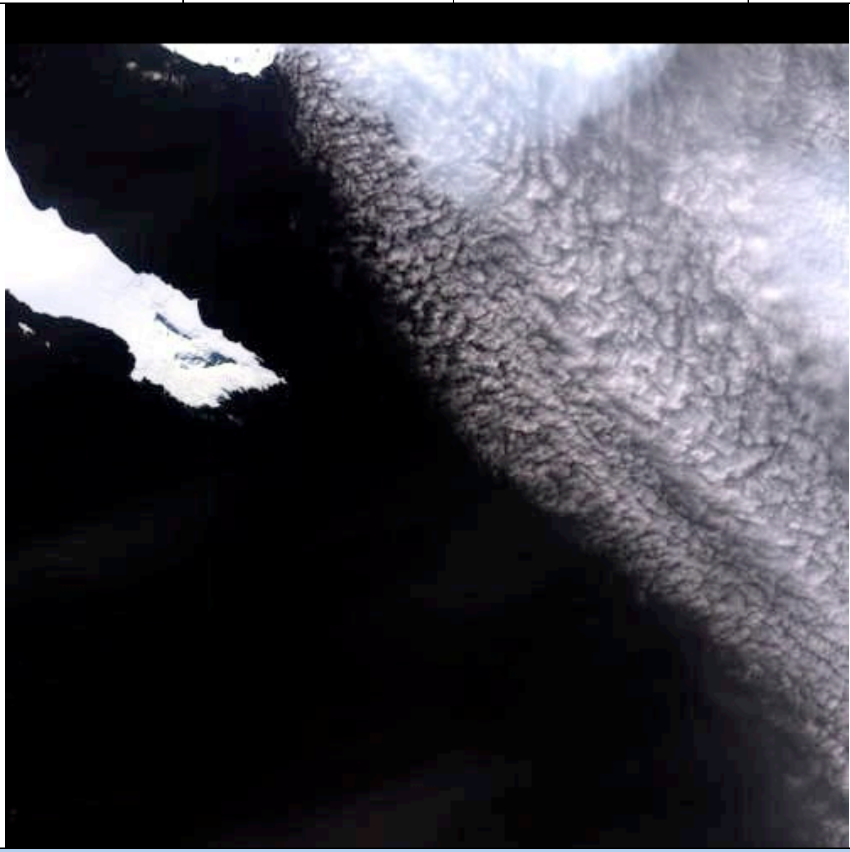

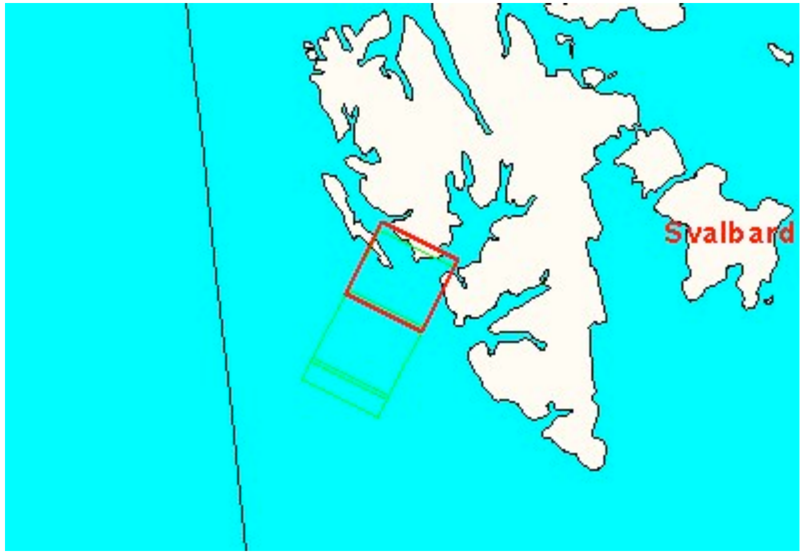

Geographic location		
NW Corner		NE Corner
12°10' E / 78°30' N	Center	14°20' E / 78°09' N
SW Corner	12°26' E / 78°07' N	SE Corner
10°33' E / 78°05' N		12°40' E / 77°45' N

Technical information			
Spectral Mode	[I] 20 m C	Scene Orientation	038.2
Cloud cover (avg.)	CEDEADAB (D)	Technical quality	Excellent
Snow cover (avg.)	11111111 ()	Incidence angle	-11.4
Sun azimut	195.6	Gains	5246
Sun elevation	+19.8		

Satellite	GRS reference		Acquisition date	Instrument	SAT
4	158	146	04/12/2007 12:10:44	2	0

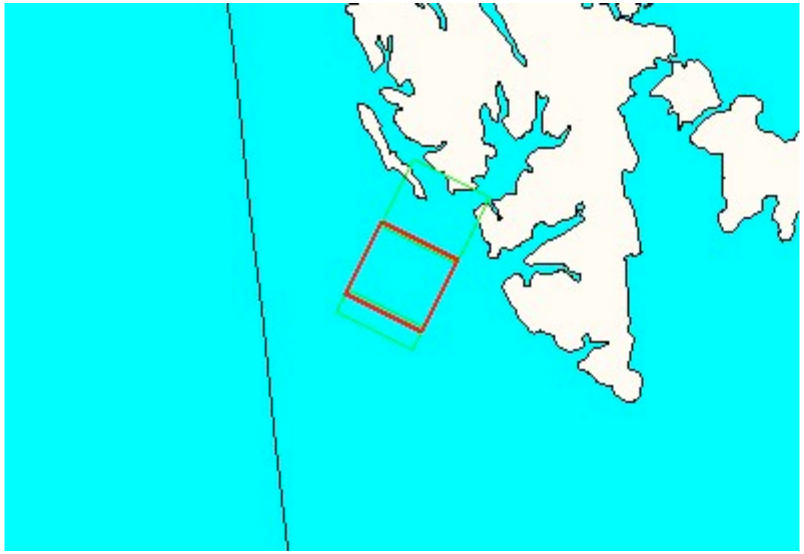

Geographic location		
NW Corner		NE Corner
10°37' E / 78°06' N	Center	12°45' E / 77°46' N
SW Corner	10°56' E / 77°43' N	SE Corner
9°06' E / 77°40' N		11°12' E / 77°21' N

Technical information			
Spectral Mode	[I] 20 m C	Scene Orientation	036.8
Cloud cover (avg.)	AABACADA (B)	Technical quality	Excellent
Snow cover (avg.)	00000000 ()	Incidence angle	-11.4
Sun azimut	194.1	Gains	5246
Sun elevation	+20.3		

Satellite	GRS reference		Acquisition date	Instrument	SAT
4	145	120	04/18/2007 11:53:45	2	0

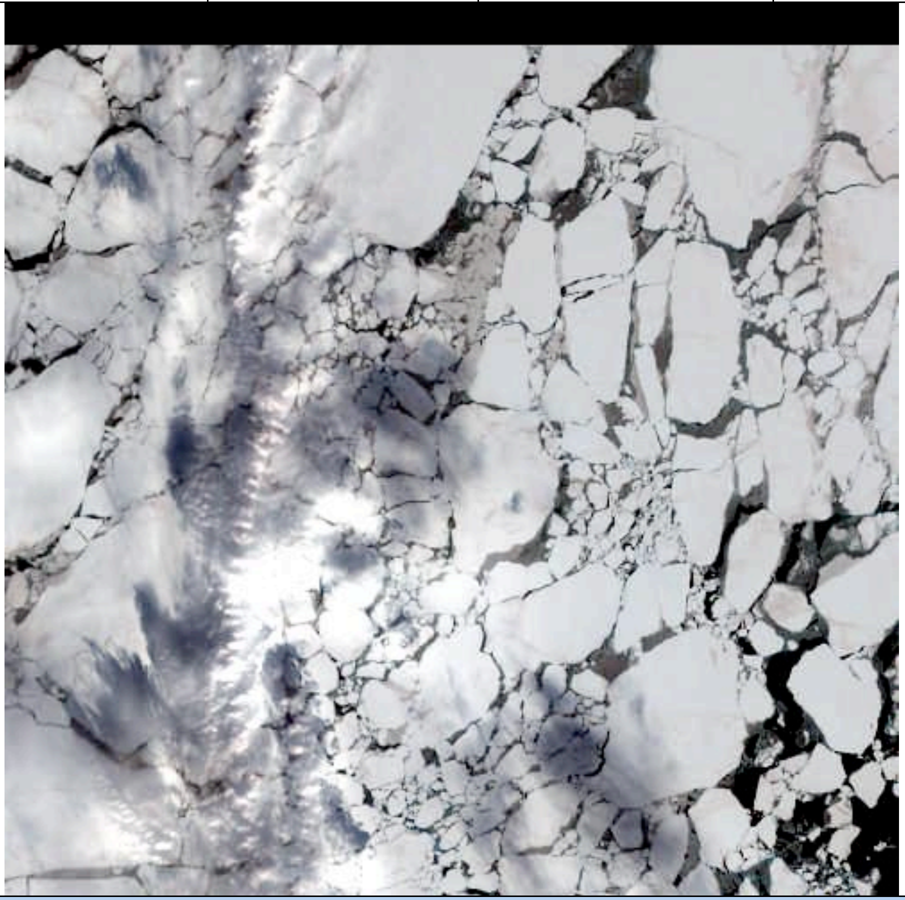

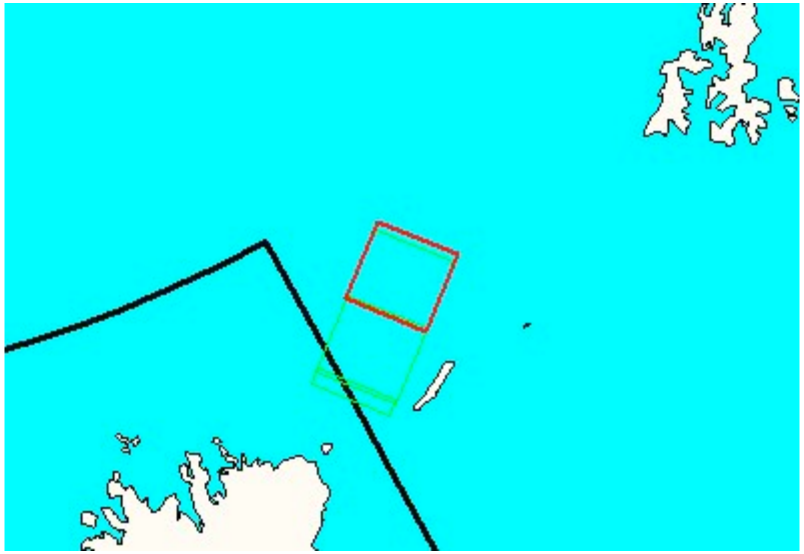

Geographic location

NW Corner		NE Corner
34°09' E / 81°15' N	Center	36°07' E / 80°47' N
SW Corner	33°45' E / 80°51' N	SE Corner
31°20' E / 80°56' N		33°22' E / 80°29' N

Technical information

Spectral Mode	[I] 20 m C	Scene Orientation	054.1
Cloud cover (avg.)	DADADADA (C)	Technical quality	Excellent
Snow cover (avg.)	11111111 ()	Incidence angle	-10.0
Sun azimut	213.6	Gains	3246
Sun elevation	+18.2		

Satellite	GRS reference		Acquisition date	Instrument	SAT
4	147	123	04/18/2007 11:53:54	2	0

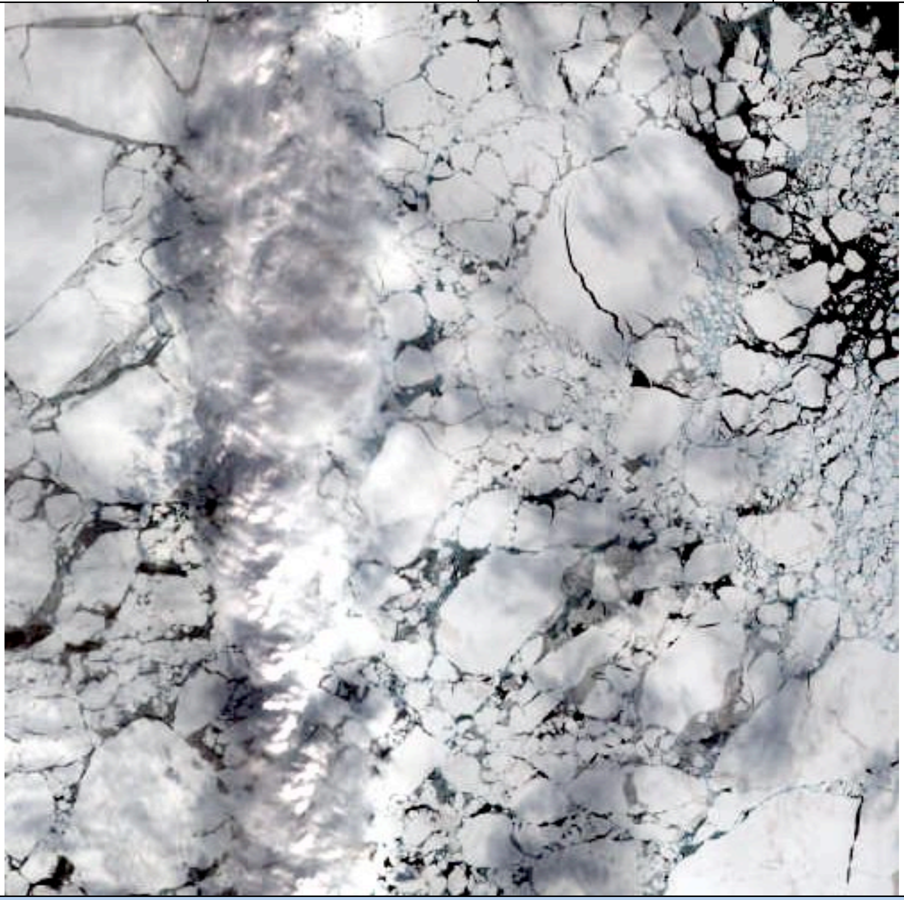

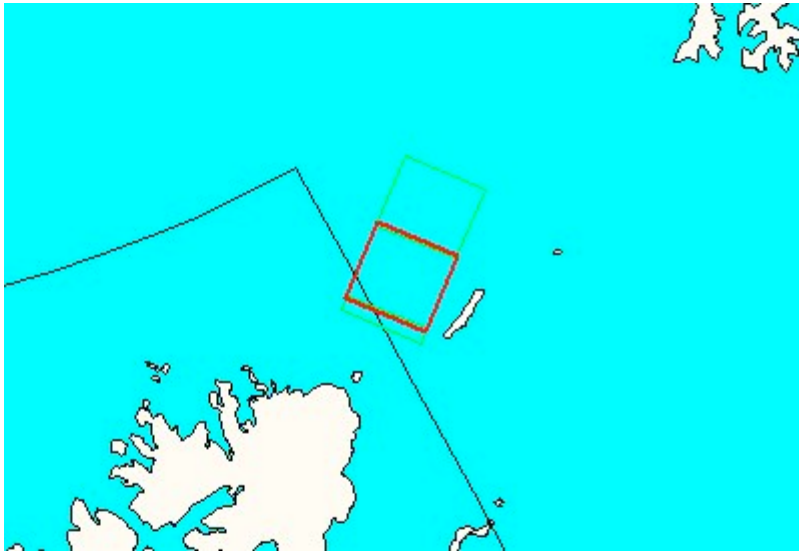

Technical information			
Spectral Mode	[I] 20 m C	Scene Orientation	051.7
Cloud cover (avg.)	DADADADA (C)	Technical quality	Excellent
Snow cover (avg.)	11111111 ()	Incidence angle	-10.0
Sun azimut	211.0	Gains	3246
Sun elevation	+18.6		

Geographic location		
NW Corner		NE Corner
31°28' E / 80°57' N	Center	33°30' E / 80°30' N
SW Corner	31°11' E / 80°34' N	SE Corner
28°50' E / 80°37' N		30°55' E / 80°11' N

Satellite	GRS reference		Acquisition date	Instrument	SAT
4	154	124	04/18/2007 11:54:05	1	0

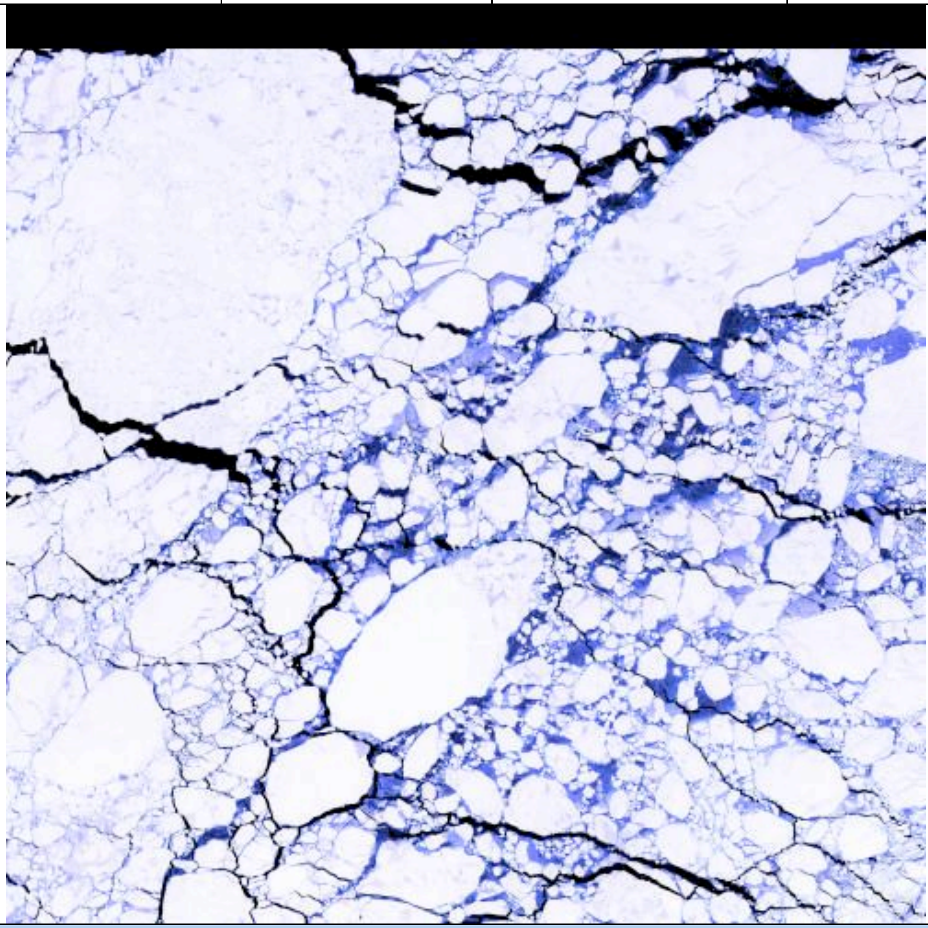

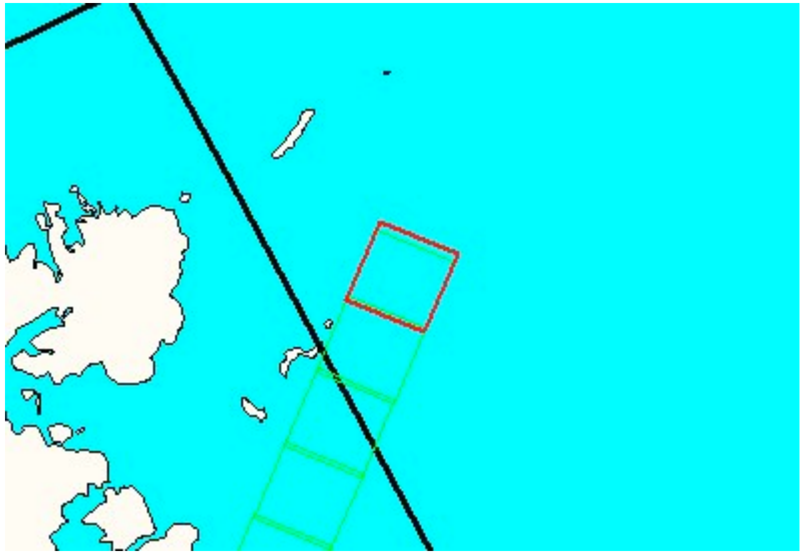

Geographic location

NW Corner		NE Corner
33°30' E / 79°23' N	Center	35°07' E / 78°56' N
SW Corner	33°09' E / 79°00' N	SE Corner
31°10' E / 79°04' N		32°50' E / 78°38' N

Technical information

Spectral Mode	[I] 20 m C	Scene Orientation	053.9
Cloud cover (avg.)	AAAAAAAA (A)	Technical quality	Excellent
Snow cover (avg.)	11111111 ()	Incidence angle	+02.5
Sun azimut	213.4	Gains	6456
Sun elevation	+19.8		

Satellite	*GRS reference*		*Acquisition date*	*Instrument*	*SAT*
4	*156*	*127*	*04/18/2007 11:54:13*	*1*	*0*

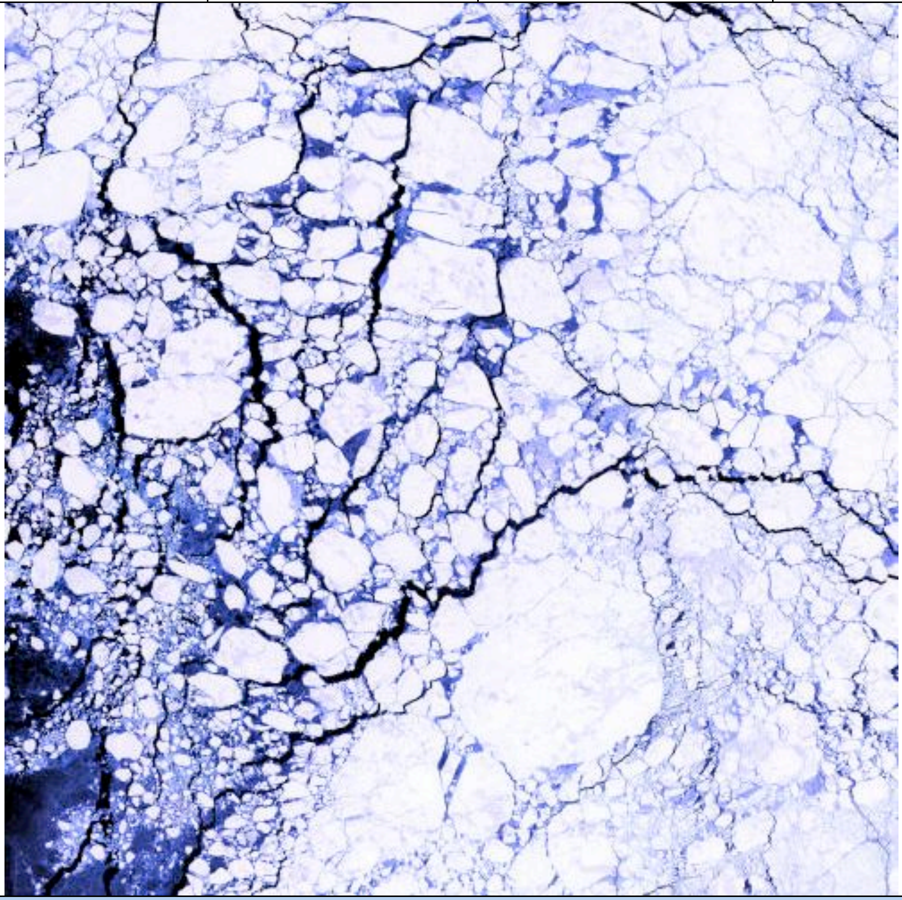

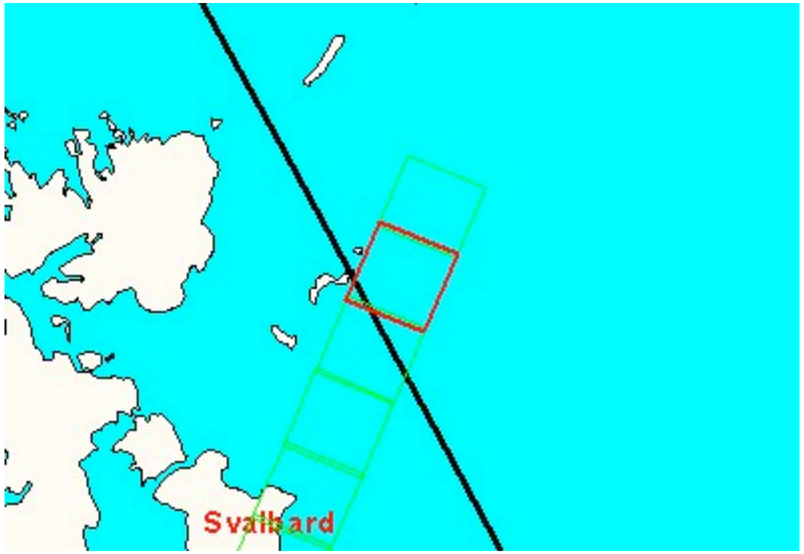

Technical information			
Spectral Mode	[I] 20 m C	Scene Orientation	051.9
Cloud cover (avg.)	AAAAAAAA (A)	Technical quality	Excellent
Snow cover (avg.)	11111111 ()	Incidence angle	+02.5
Sun azimut	211.3	Gains	6456
Sun elevation	+20.2		

Geographic location		
NW Corner		NE Corner
31°16' E / 79°05' N	Center	32°56' E / 78°39' N
SW Corner	31°01' E / 78°42' N	SE Corner
29°04' E / 78°45' N		30°46' E / 78°20' N

Satellite	*GRS reference*		*Acquisition date*	*Instrument*	*SAT*
4	*158*	*130*	*04/18/2007 11:54:22*	*1*	*0*

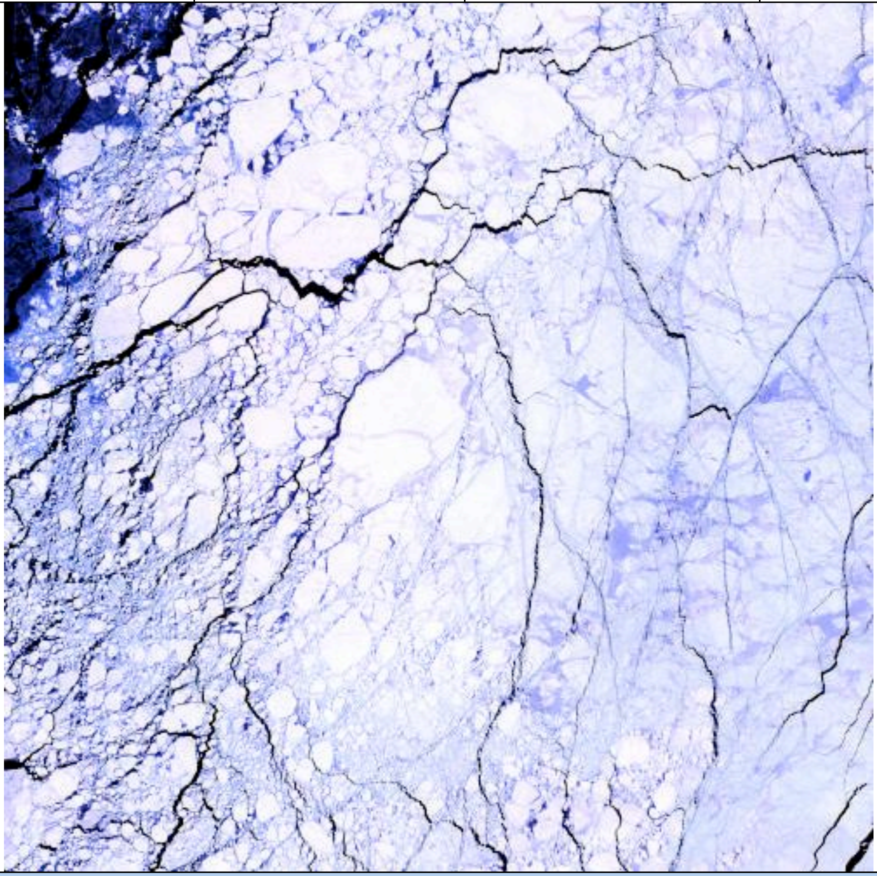

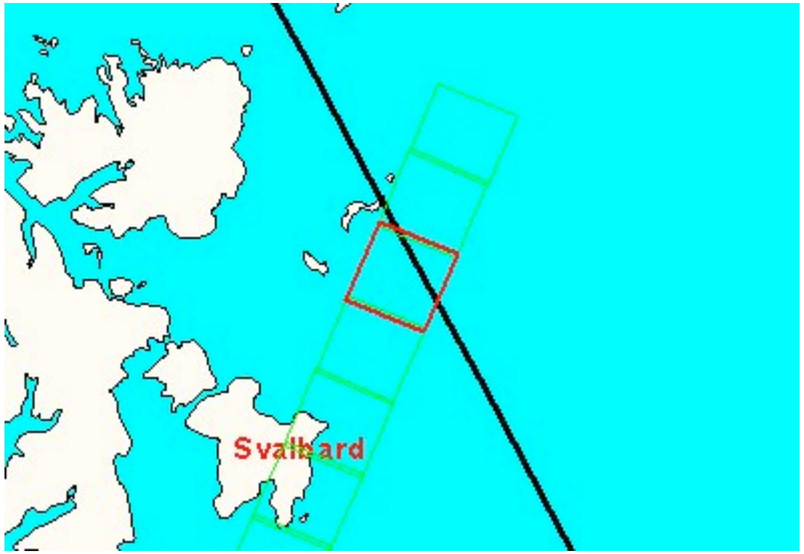

Technical information			
Spectral Mode	[I] 20 m C	Scene Orientation	050.1
Cloud cover (avg.)	AAAAAAAA (A)	Technical quality	Excellent
Snow cover (avg.)	11111111 ()	Incidence angle	+02.5
Sun azimut	209.3	Gains	6456
Sun elevation	+20.7		

Geographic location		
NW Corner		NE Corner
29°10' E / 78°46' N	Center	30°52' E / 78°21' N
SW Corner	28°59' E / 78°24' N	SE Corner
27°05' E / 78°26' N		28°48' E / 78°01' N

Satellite	GRS reference		Acquisition date	Instrument	SAT
4	159	132	04/18/2007 11:54:30	1	0

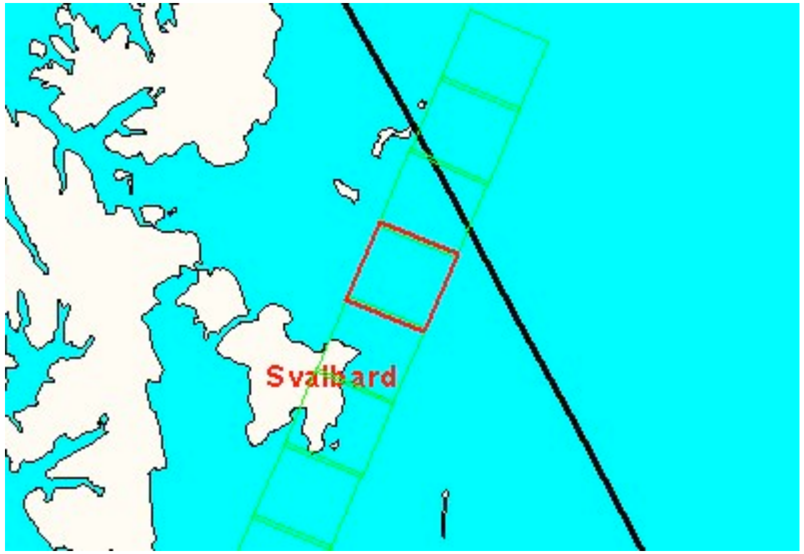

Geographic location		
NW Corner		NE Corner
27°11' E / 78°27' N	Center	28°54' E / 78°02' N
SW Corner	27°04' E / 78°04' N	SE Corner
25°13' E / 78°05' N		26°57' E / 77°41' N

Technical information			
Spectral Mode	[I] 20 m C	Scene Orientation	048.3
Cloud cover (avg.)	AAAAAAAA (A)	Technical quality	Excellent
Snow cover (avg.)	11111111 ()	Incidence angle	+02.5
Sun azimut	207.3	Gains	6456
Sun elevation	+21.2		

Satellite	GRS reference		Acquisition date	Instrument	SAT
4	161	135	04/18/2007 11:54:39	1	0

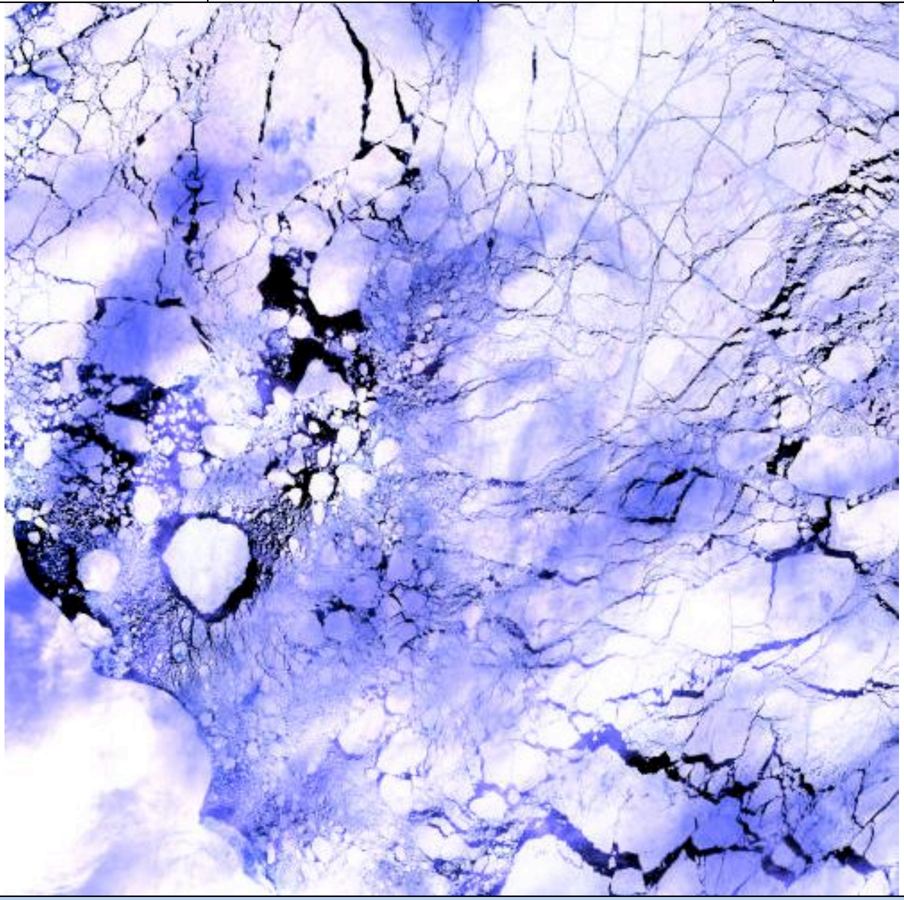

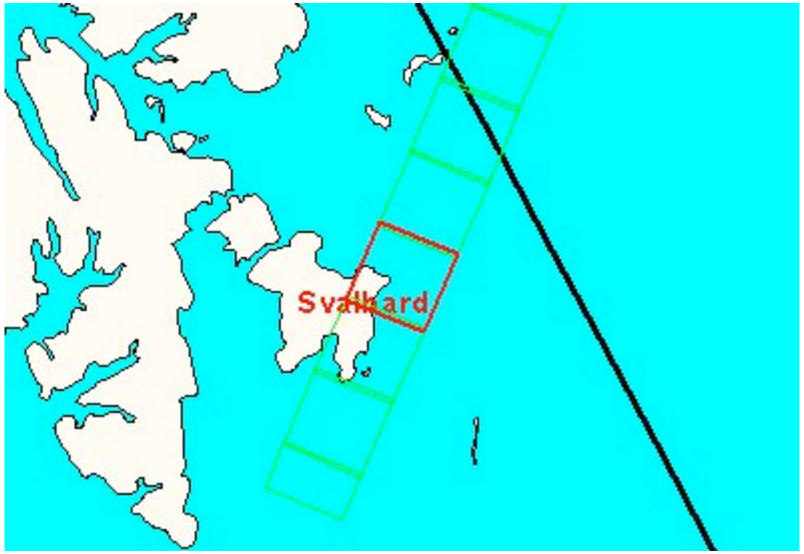

Geographic location		
NW Corner		NE Corner
25°18' E / 78°06' N	Center	27°02' E / 77°42' N
SW Corner	25°14' E / 77°44' N	SE Corner
23°26' E / 77°44' N		25°11' E / 77°21' N

Technical information			
Spectral Mode	[I] 20 m C	Scene Orientation	046.7
Cloud cover (avg.)	AAAAAAAA (A)	Technical quality	Excellent
Snow cover (avg.)	11111111 ()	Incidence angle	+02.5
Sun azimut	205.5	Gains	6456
Sun elevation	+21.7		

Satellite	*GRS reference*		*Acquisition date*	*Instrument*	*SAT*
4	*149*	*126*	*04/21/2007 10:56:01*	*1*	*0*

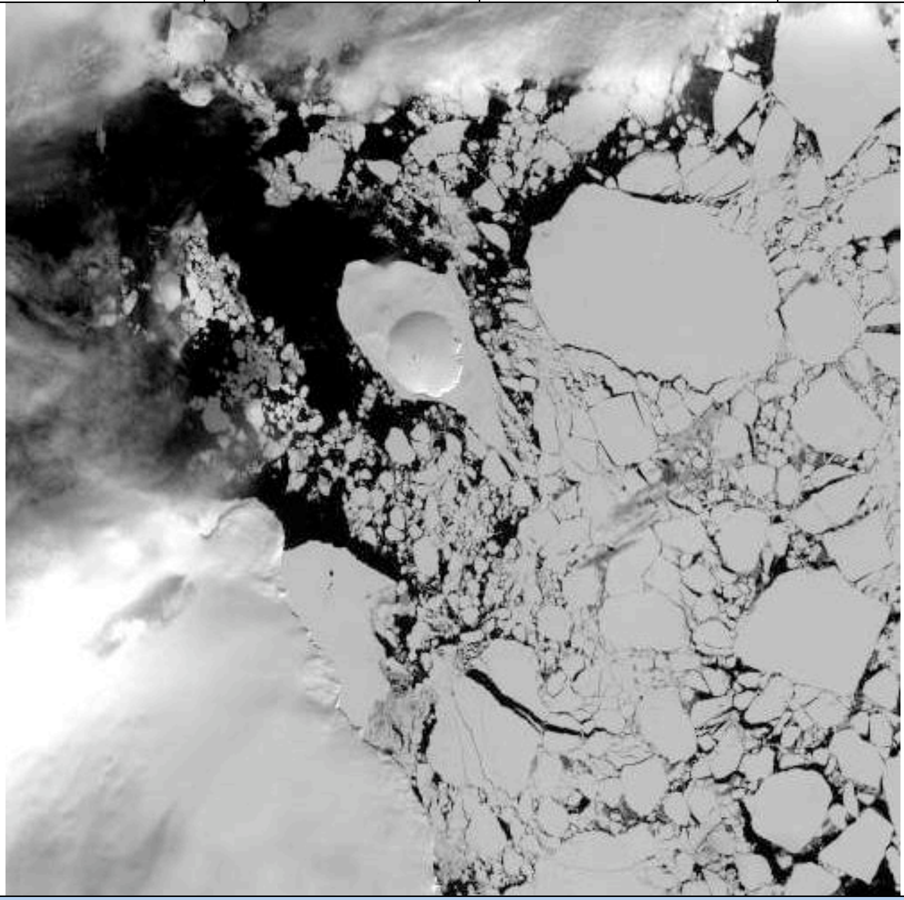

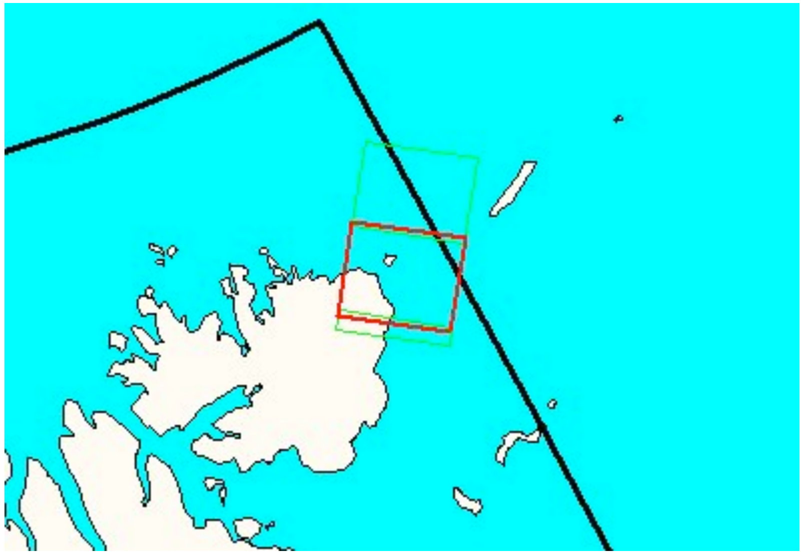

Geographic location		
NW Corner		NE Corner
27°18' E / 80°25' N	Center	30°22' E / 80°03' N
SW Corner	27°58' E / 80°01' N	SE Corner
25°32' E / 79°59' N		28°32' E / 79°37' N

Technical information			
Spectral Mode	[M] 10 m N & B	Scene Orientation	034.9
Cloud cover (avg.)	DDDBDBDB (C)	Technical quality	Excellent
Snow cover (avg.)	11111111 ()	Incidence angle	-24.1
Sun azimut	192.9	Gains	2
Sun elevation	+21.3		

Satellite	*GRS reference*		*Acquisition date*	*Instrument*	*SAT*
4	*157*	*126*	*04/21/2007 10:56:12*	*2*	*0*

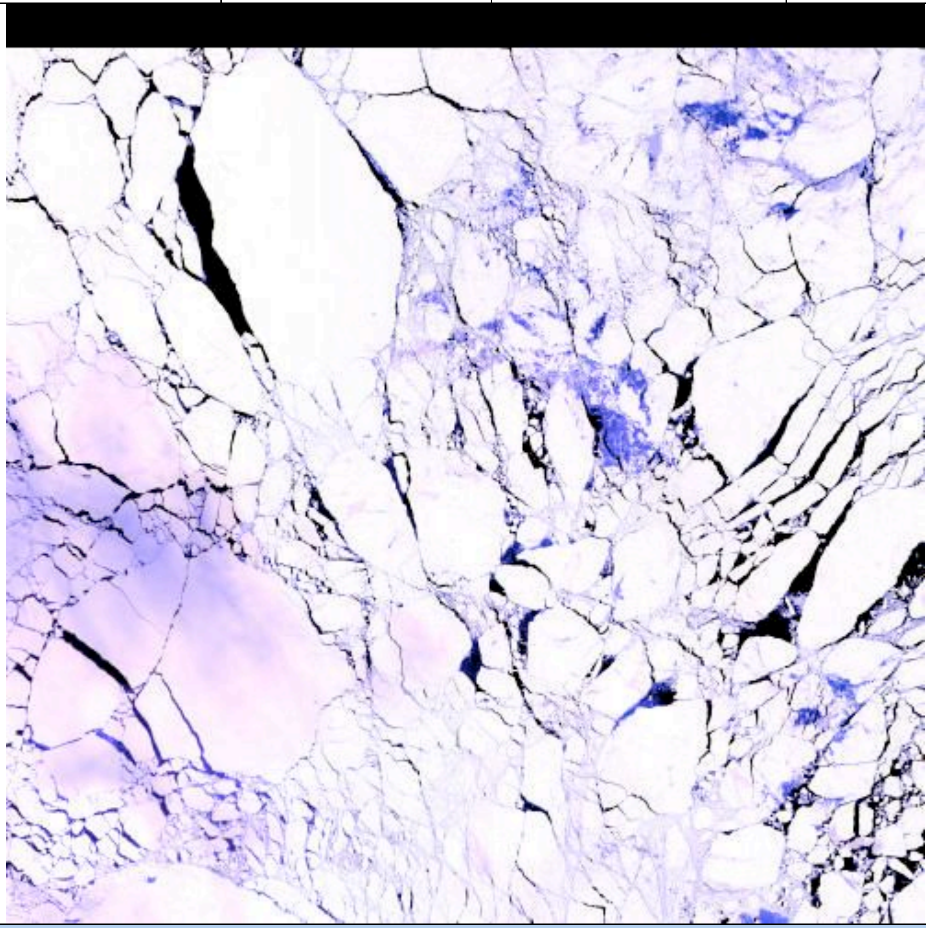

Technical information			
Spectral Mode	[I] 20 m C	Scene Orientation	039.8
Cloud cover (avg.)	AAAAAAAA (A)	Technical quality	Excellent
Snow cover (avg.)	11111111 ()	Incidence angle	-11.4
Sun azimut	198.2	Gains	6456
Sun elevation	+22.5		

Geographic location		
NW Corner		NE Corner
32°33' E / 78°57' N	Center	34°43' E / 78°35' N
SW Corner	32°45' E / 78°33' N	SE Corner
30°47' E / 78°32' N		32°57' E / 78°11' N

Satellite	*GRS reference*		*Acquisition date*	*Instrument*	*SAT*
4	*158*	*128*	*04/21/2007 10:56:20*	*2*	*0*

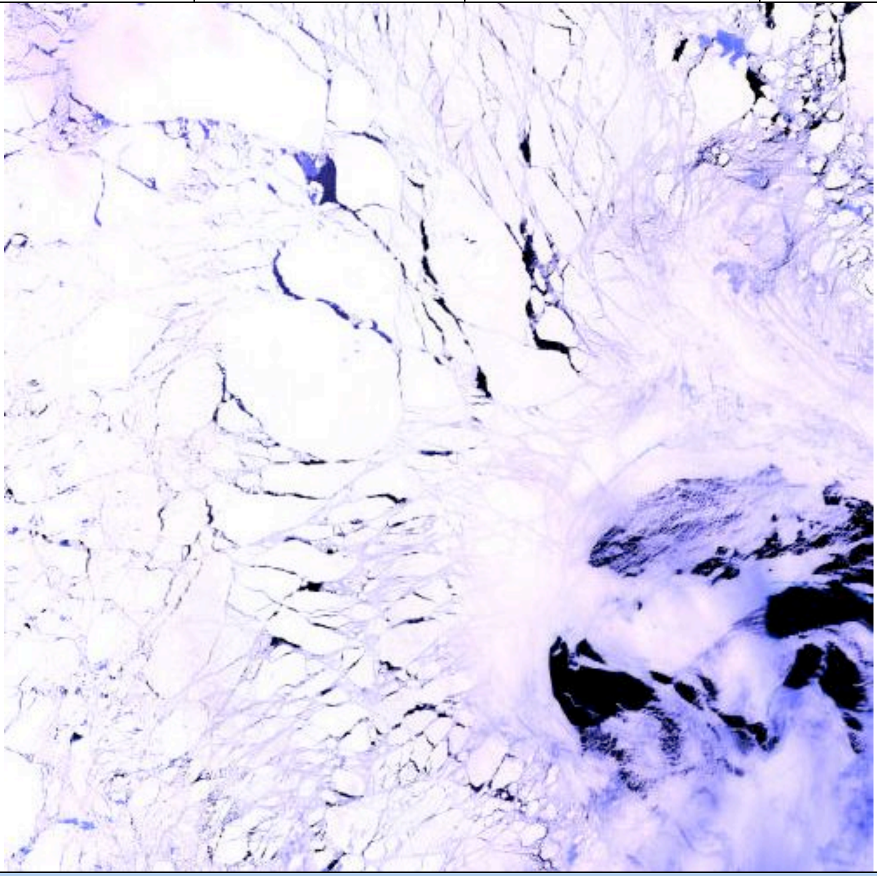

Geographic location		
NW Corner		NE Corner
30°53' E / 78°33' N	Center	33°02' E / 78°12' N
SW Corner	31°08' E / 78°10' N	SE Corner
29°14' E / 78°08' N		31°22' E / 77°47' N

Technical information			
Spectral Mode	[I] 20 m C	Scene Orientation	038.3
Cloud cover (avg.)	AAAAAAAA (A)	Technical quality	Excellent
Snow cover (avg.)	11111111 ()	Incidence angle	-11.4
Sun azimut	196.5	Gains	6456
Sun elevation	+22.9		

Satellite	*GRS reference*		*Acquisition date*	*Instrument*	*SAT*
4	*165*	*137*	*04/21/2007 10:56:50*	*2*	*0*

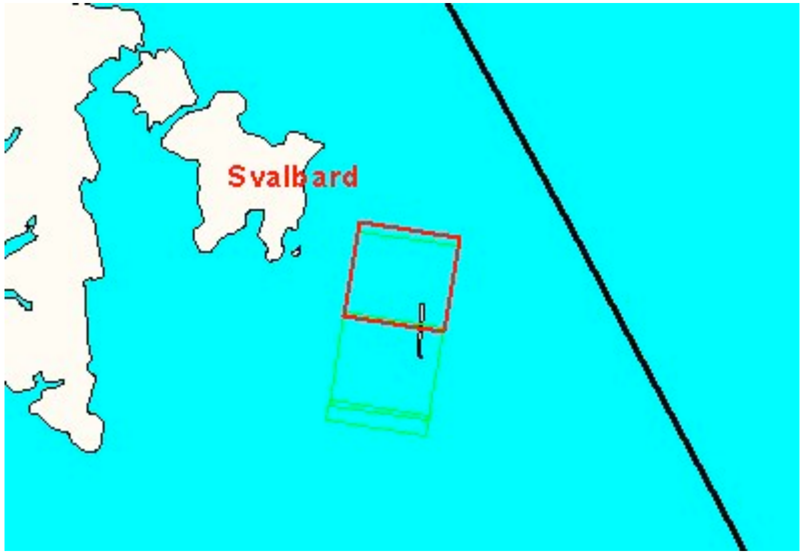

Geographic location		
NW Corner		NE Corner
24°57' E / 77°16' N	Center	27°04' E / 76°57' N
SW Corner	25°21' E / 76°53' N	SE Corner
23°39' E / 76°49' N		25°44' E / 76°31' N

Technical information			
Spectral Mode	[I] 20 m C	Scene Orientation	033.1
Cloud cover (avg.)	AAAAAAAA (A)	Technical quality	Excellent
Snow cover (avg.)	11111111 ()	Incidence angle	-13.4
Sun azimut	190.6	Gains	6456
Sun elevation	+24.5		

Satellite	GRS reference		Acquisition date	Instrument	SAT
4	167	139	04/21/2007 10:56:58	2	0

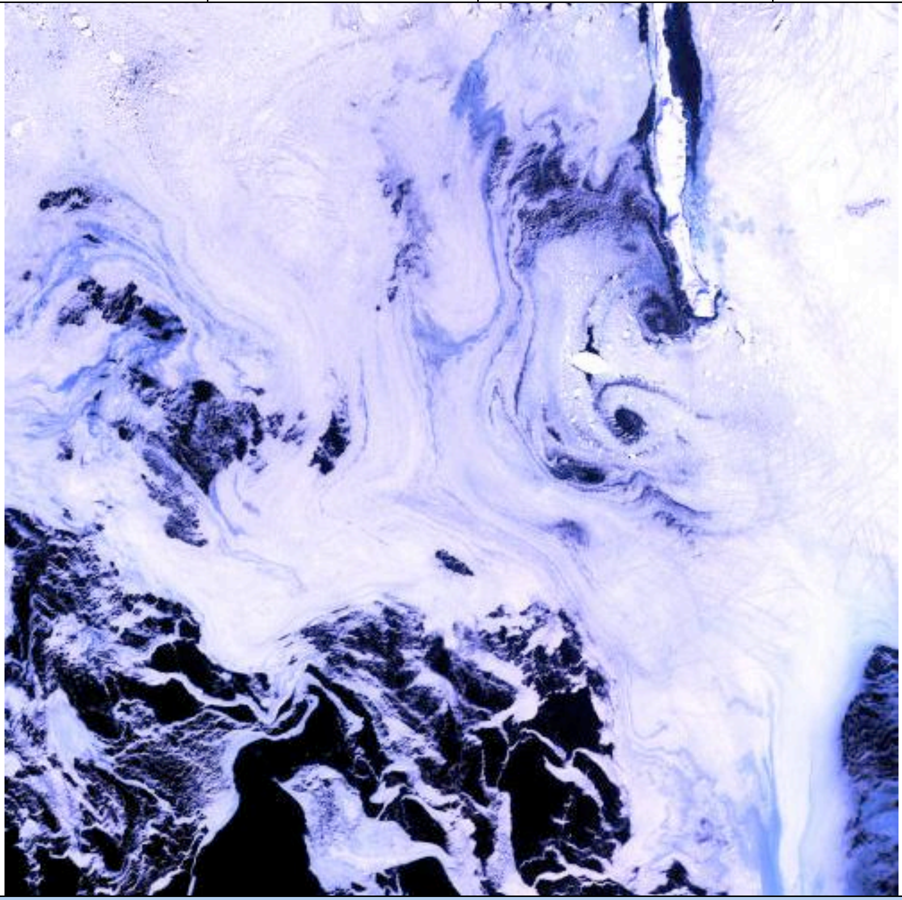

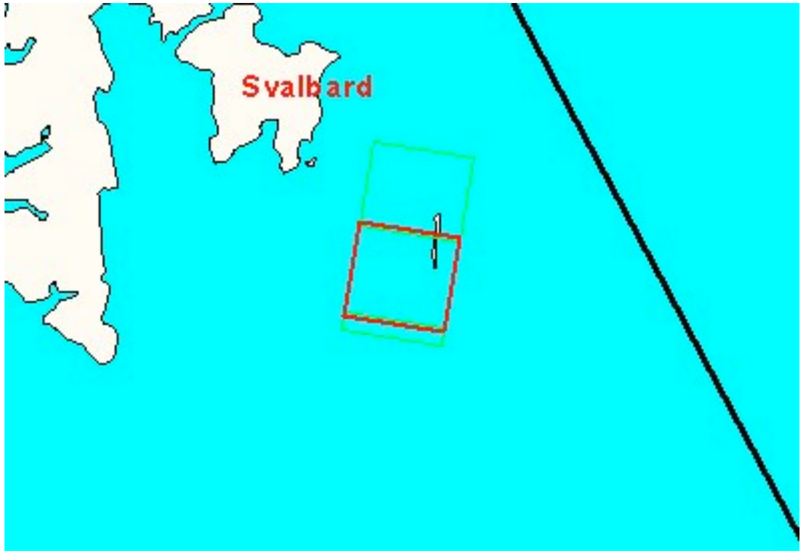

Technical information			
Spectral Mode	[I] 20 m C	Scene Orientation	032.1
Cloud cover (avg.)	AAAAAAAA (A)	Technical quality	Excellent
Snow cover (avg.)	11111111 ()	Incidence angle	-13.4
Sun azimut	189.4	Gains	6456
Sun elevation	+24.9		

Geographic location		
NW Corner		NE Corner
23°43' E / 76°51' N	Center	25°48' E / 76°32' N
SW Corner	24°09' E / 76°28' N	SE Corner
22°30' E / 76°23' N		24°33' E / 76°05' N

Satellite	*GRS reference*		*Acquisition date*	*Instrument*	*SAT*
4	*143*	*126*	*04/22/2007 12:17:15*	*2*	*0*

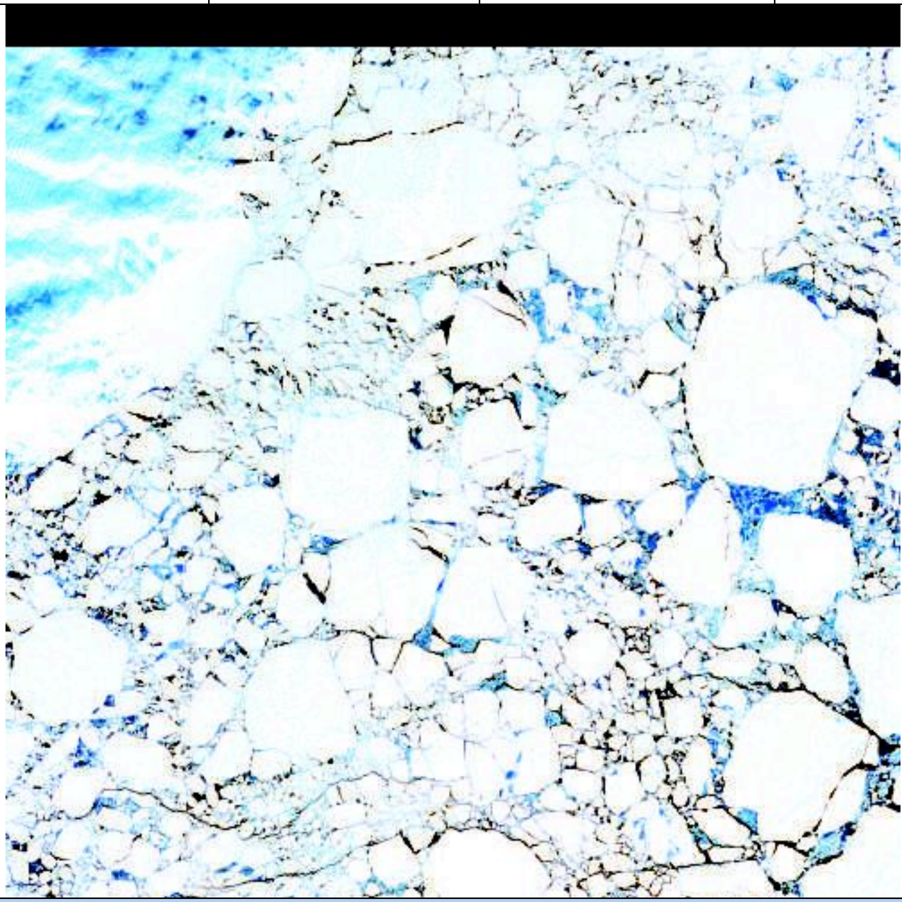

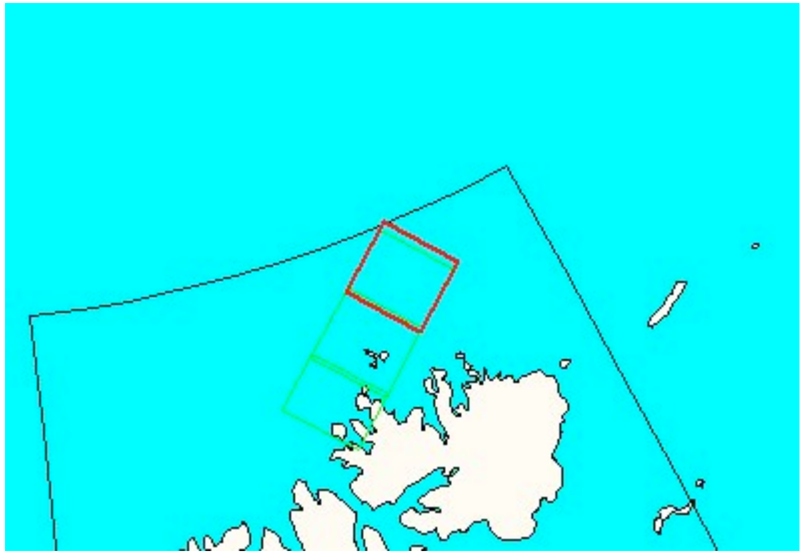

Technical information			
Spectral Mode	[I] 20 m C	Scene Orientation	049.5
Cloud cover (avg.)	DADAAAAA (C)	Technical quality	Excellent
Snow cover (avg.)	11111111 ()	Incidence angle	-15.5
Sun azimut	209.1	Gains	6556
Sun elevation	+19.7		

Geographic location		
NW Corner		NE Corner
23°20' E / 81°32' N	Center	25°43' E / 81°04' N
SW Corner	23°10' E / 81°08' N	SE Corner
20°37' E / 81°11' N		23°02' E / 80°45' N

Satellite	*GRS reference*		*Acquisition date*	*Instrument*	*SAT*
4	*145*	*129*	*04/22/2007 12:17:23*	*2*	*0*

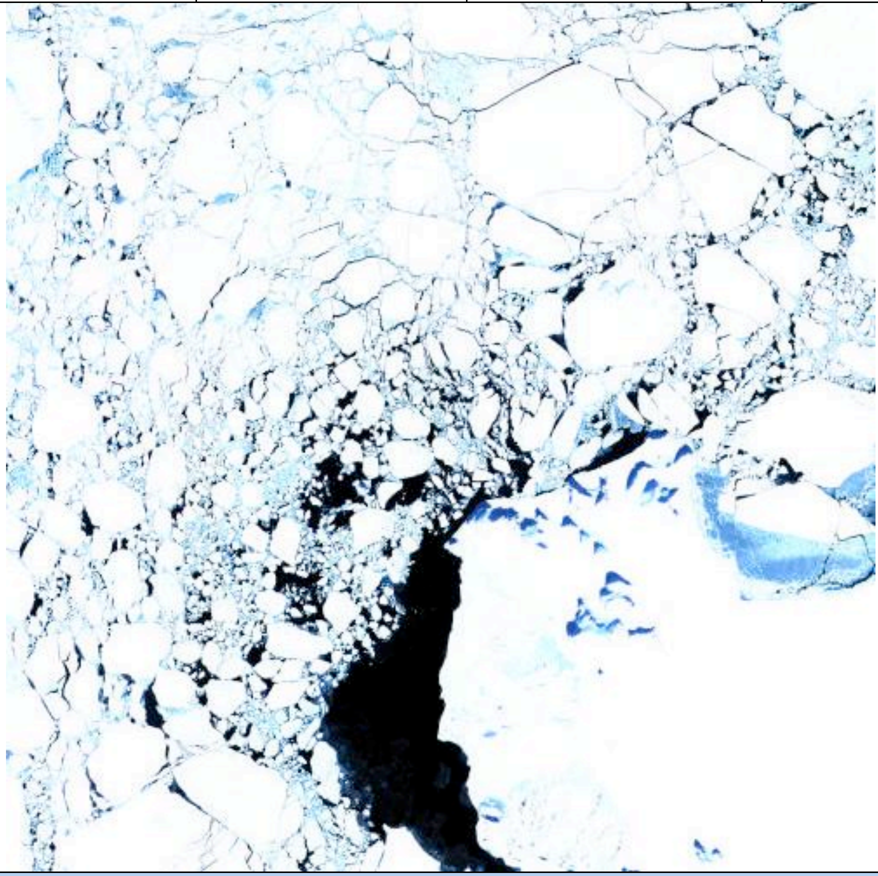

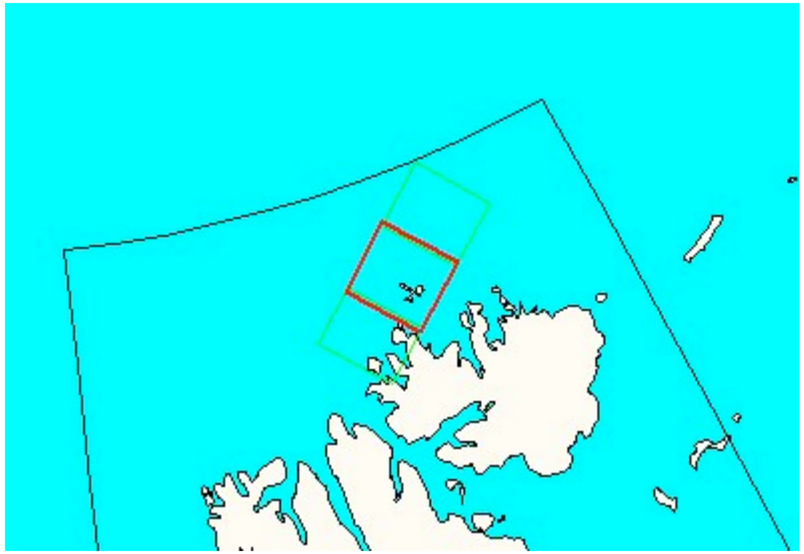

Technical information			
Spectral Mode	[I] 20 m C	Scene Orientation	047.3
Cloud cover (avg.)	AAAAAAAA (A)	Technical quality	Excellent
Snow cover (avg.)	11111111 ()	Incidence angle	-15.5
Sun azimut	206.6	Gains	6556
Sun elevation	+20.2		

Geographic location		
NW Corner		NE Corner
20°45' E / 81°12' N	Center	23°10' E / 80°46' N
SW Corner	20°43' E / 80°48' N	SE Corner
18°14' E / 80°50' N		20°40' E / 80°25' N

Satellite	*GRS reference*		*Acquisition date*	*Instrument*	*SAT*
4	*146*	*131*	*04/22/2007 12:17:32*	*2*	*0*

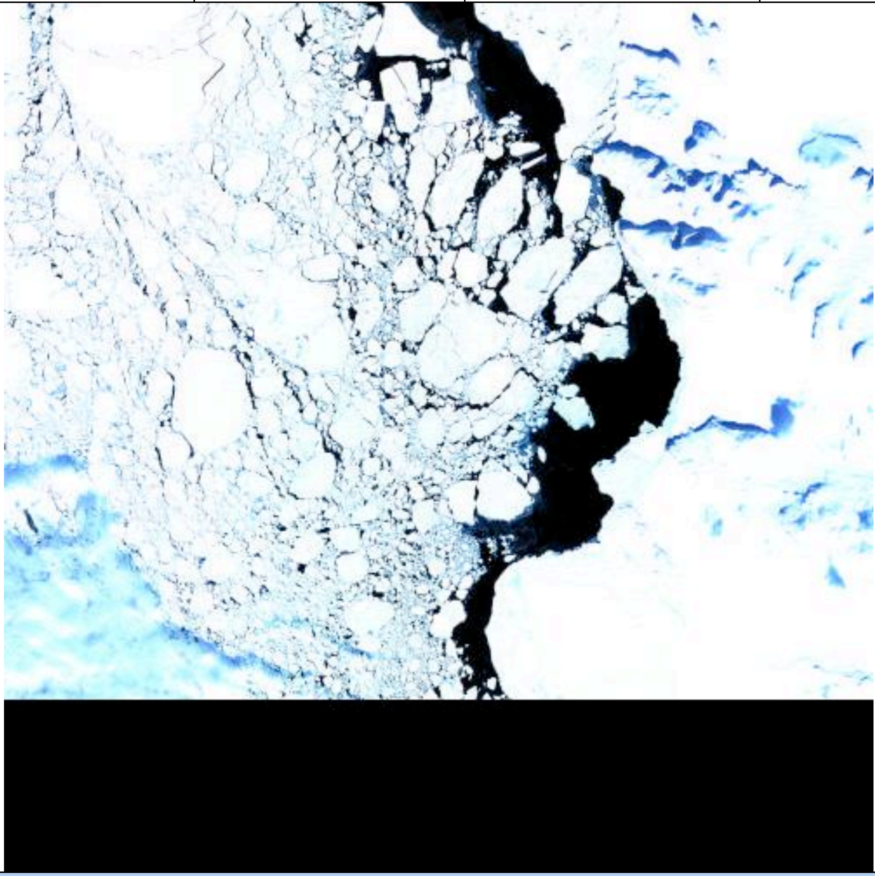

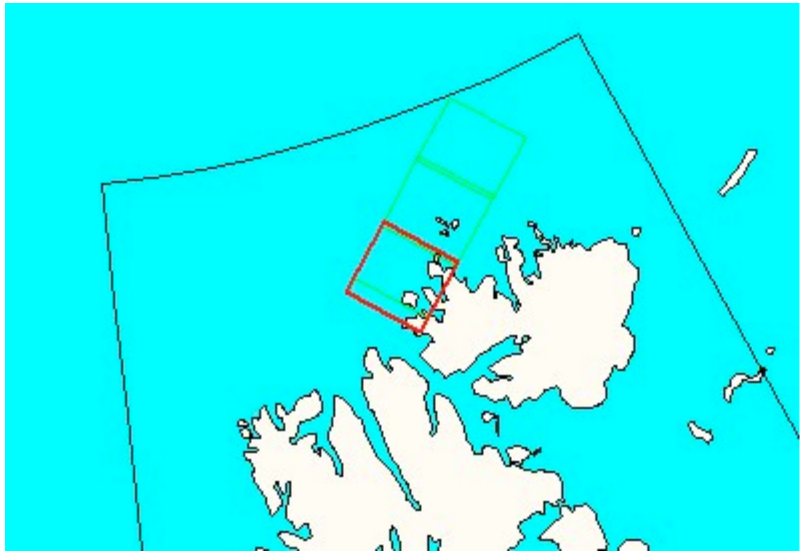

Technical information			
Spectral Mode	[I] 20 m C	Scene Orientation	045.6
Cloud cover (avg.)	AAAADA** (B)	Technical quality	Excellent
Snow cover (avg.)	111111** ()	Incidence angle	-15.5
Sun azimut	204.3	Gains	6556
Sun elevation	+20.6		

Geographic location		
NW Corner		NE Corner
18°21' E / 80°51' N	Center	20°47' E / 80°26' N
SW Corner	18°23' E / 80°27' N	SE Corner
15°60' E / 80°28' N		18°26' E / 80°04' N

Satellite	*GRS reference*		*Acquisition date*	*Instrument*	*SAT*
4	*142*	*135*	*04/22/2007 15:38:43*	*1*	*0*

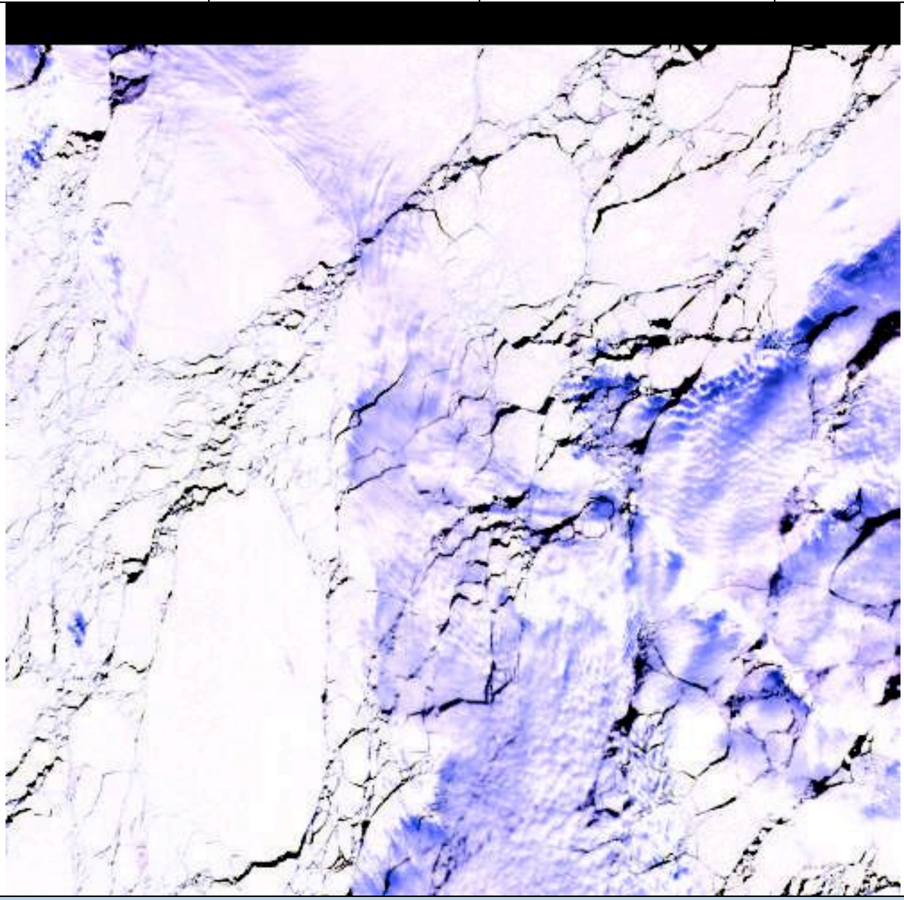

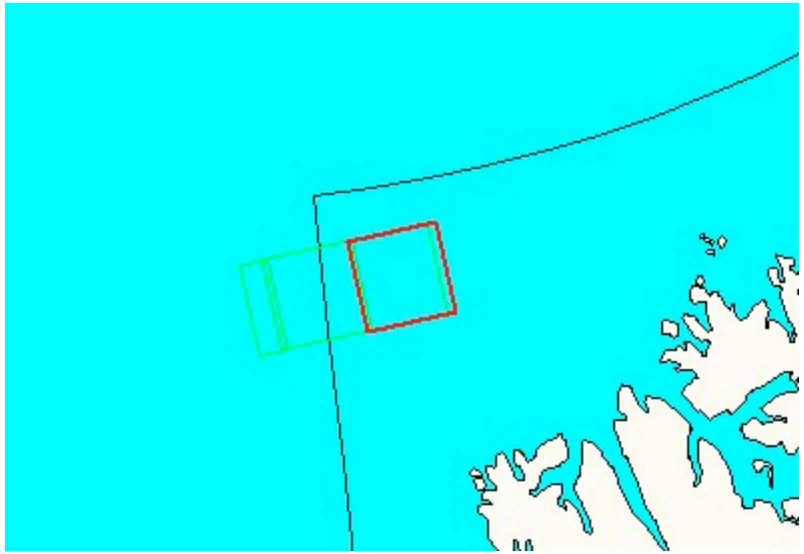

Technical information			
Spectral Mode	[I] 20 m C	Scene Orientation	085.0
Cloud cover (avg.)	AAADBECE (C)	Technical quality	Excellent
Snow cover (avg.)	11111111 ()	Incidence angle	+03.2
Sun azimut	246.5	Gains	6566
Sun elevation	+15.7		

Geographic location		
NW Corner		NE Corner
11°05' E / 81°15' N	Center	11°11' E / 80°42' N
SW Corner	9°26' E / 80°58' N	SE Corner
7°34' E / 81°13' N		7°52' E / 80°41' N

Satellite	GRS reference		Acquisition date	Instrument	SAT
4	144	133	04/23/2007 15:19:12	1	0

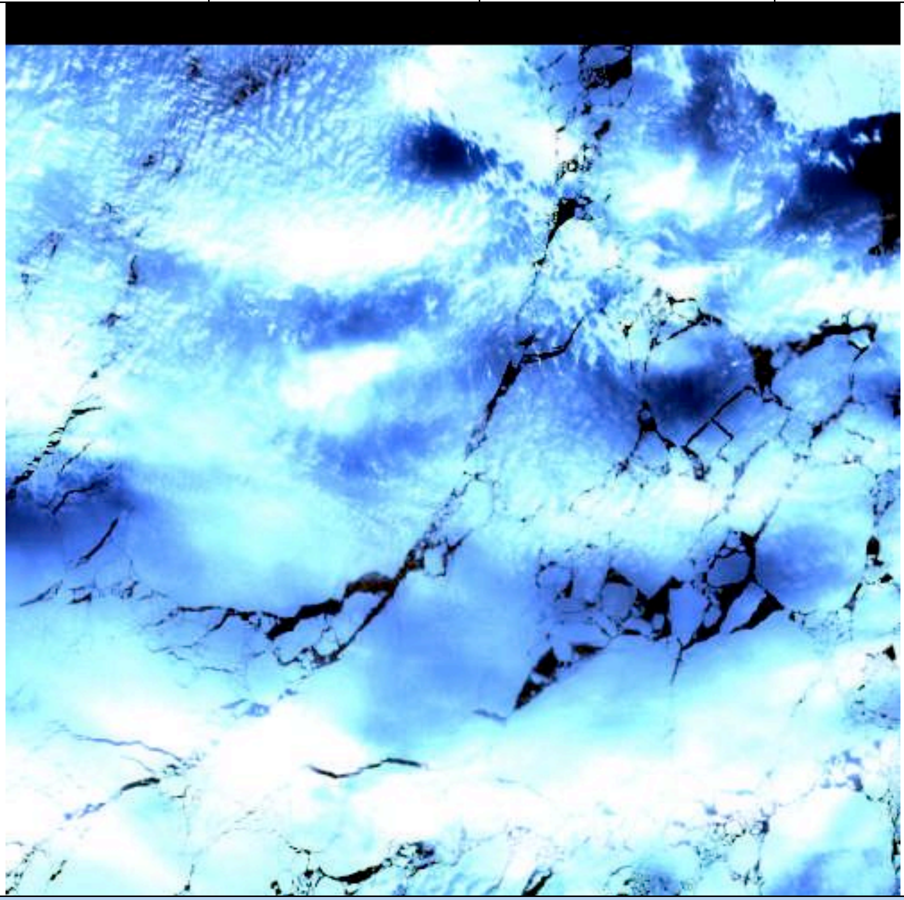

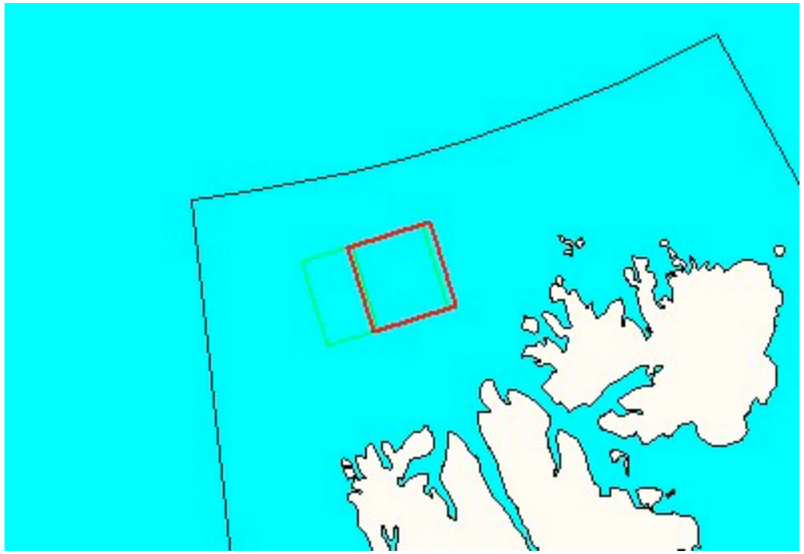

Technical information			
Spectral Mode	[I] 20 m C	Scene Orientation	084.9
Cloud cover (avg.)	EEEEEEEE (E)	Technical quality	Excellent
Snow cover (avg.)	11111111 ()	Incidence angle	+04.6
Sun azimut	246.6	Gains	6556
Sun elevation	+16.1		

Geographic location		
NW Corner		NE Corner
15°53' E / 81°05' N	Center	15°60' E / 80°33' N
SW Corner	14°16' E / 80°48' N	SE Corner
12°26' E / 81°03' N		12°44' E / 80°31' N

Satellite	*GRS reference*		*Acquisition date*	*Instrument*	*SAT*
4	*143*	*134*	*04/23/2007 15:19:20*	*1*	*0*

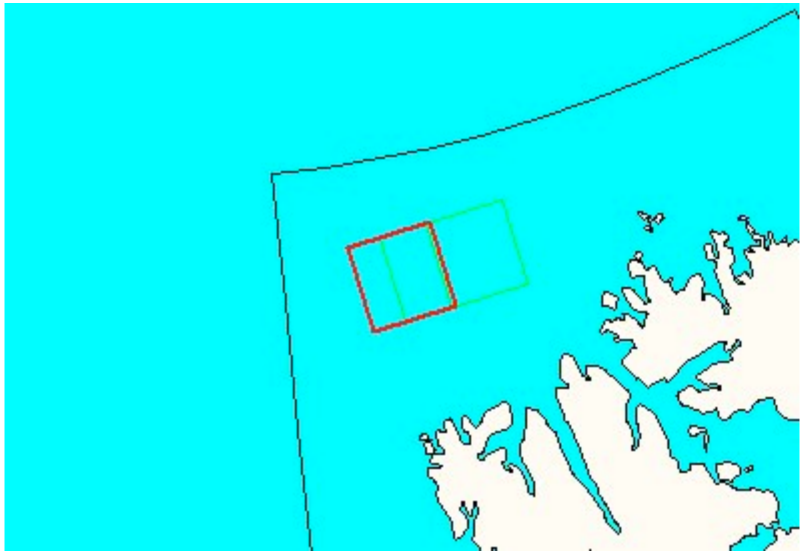

Geographic location		
NW Corner		NE Corner
12°36' E / 81°04' N	Center	12°53' E / 80°31' N
SW Corner	11°04' E / 80°46' N	SE Corner
9°09' E / 80°60' N		9°38' E / 80°28' N

Technical information			
Spectral Mode	[I] 20 m C	Scene Orientation	083.2
Cloud cover (avg.)	AAAA**** (A)	Technical quality	Excellent
Snow cover (avg.)	1111**** ()	Incidence angle	+04.6
Sun azimut	243.4	Gains	6556
Sun elevation	+16.5		

Satellite	GRS reference		Acquisition date	Instrument	SAT
4	154	138	04/27/2007 12:21:43	1	0

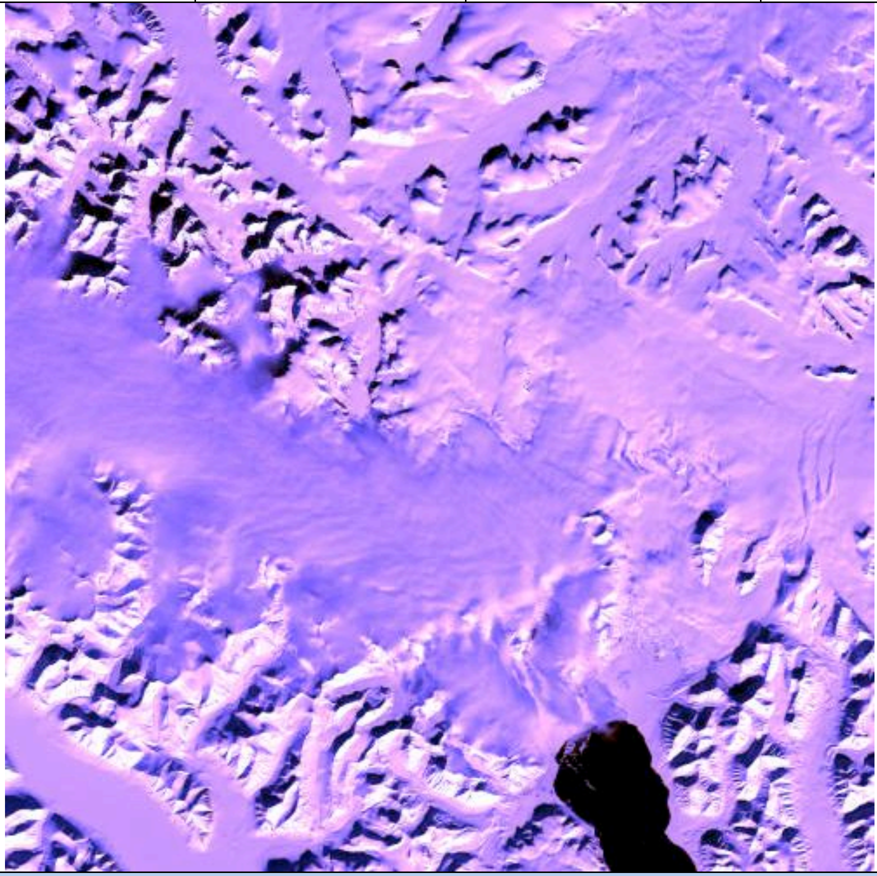

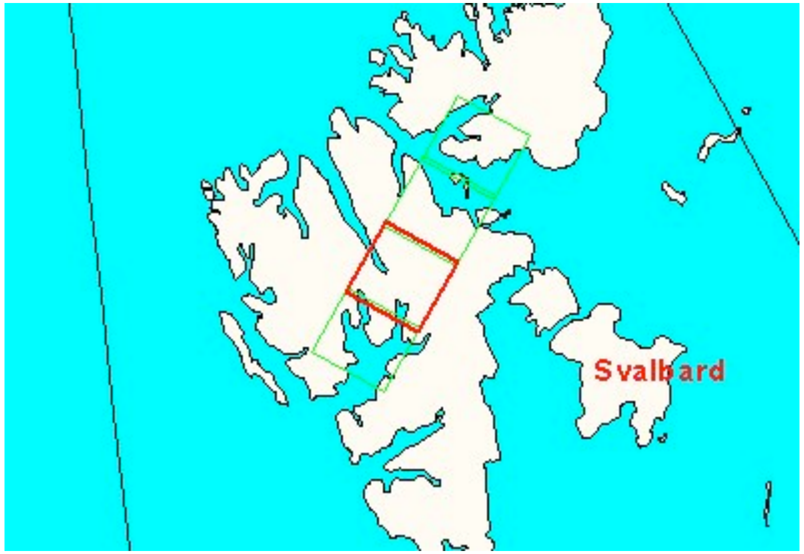

Geographic location		
NW Corner		NE Corner
16°56' E / 79°14' N	Center	18°55' E / 78°50' N
SW Corner	16°56' E / 78°51' N	SE Corner
14°56' E / 78°51' N		16°55' E / 78°28' N

Technical information			
Spectral Mode	[I] 20 m C	Scene Orientation	045.0
Cloud cover (avg.)	BDDBEDCC (D)	Technical quality	Excellent
Snow cover (avg.)	11111111 ()	Incidence angle	-06.3
Sun azimut	204.5	Gains	5246
Sun elevation	+23.8		

Satellite	GRS reference		Acquisition date	Instrument	SAT
4	155	140	04/27/2007 12:21:51	1	0

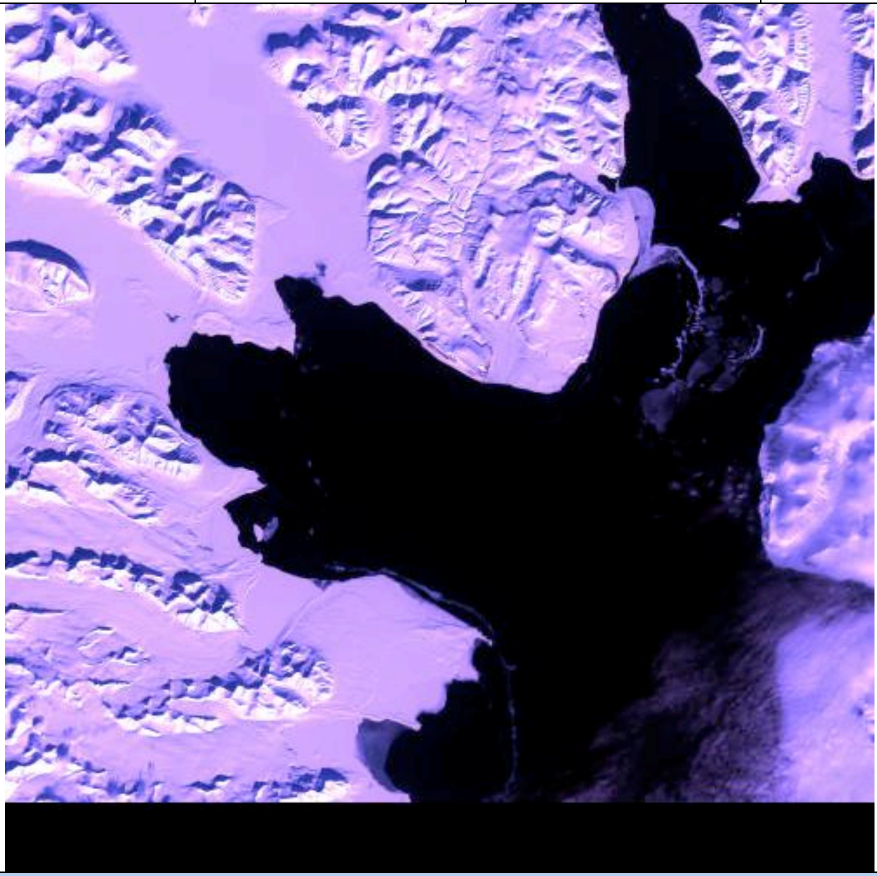

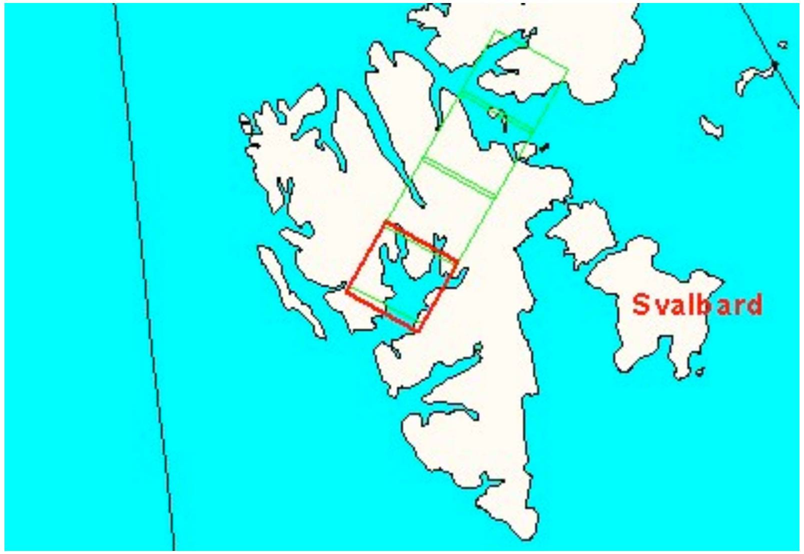

Geographic location		
NW Corner		NE Corner
15°02' E / 78°52' N	Center	17°01' E / 78°29' N
SW Corner	15°05' E / 78°29' N	SE Corner
13°09' E / 78°29' N		15°07' E / 78°06' N

Technical information			
Spectral Mode	[I] 20 m C	Scene Orientation	043.5
Cloud cover (avg.)	AAAAAAAA (A)	Technical quality	Excellent
Snow cover (avg.)	11111111 ()	Incidence angle	-06.3
Sun azimut	202.6	Gains	5246
Sun elevation	+24.3		

Satellite	*GRS reference*		*Acquisition date*	*Instrument*	*SAT*
4	*161*	*143*	*04/27/2007 12:22:00*	*2*	*0*

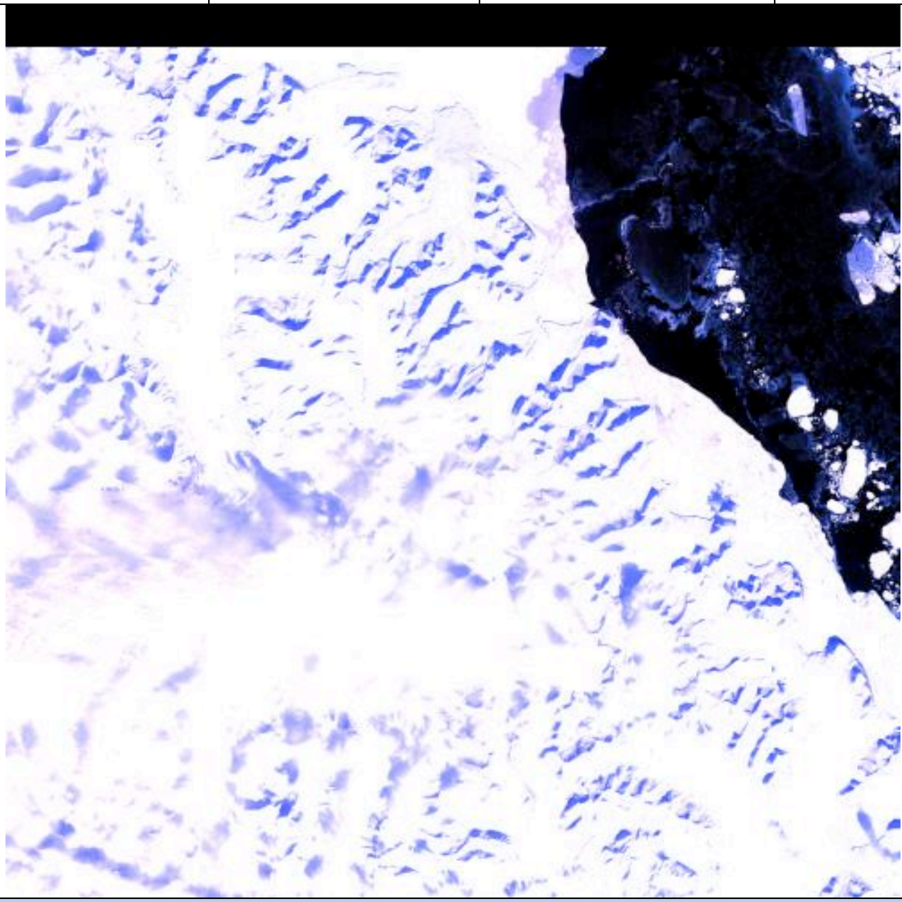

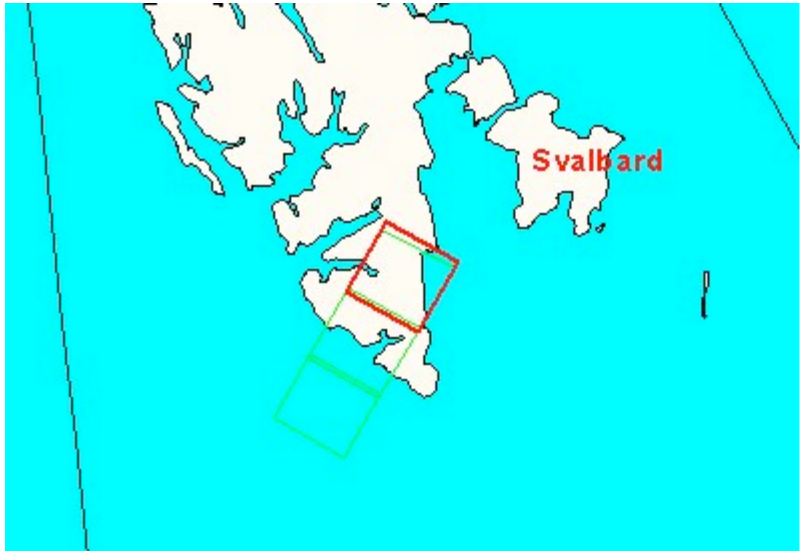

Geographic location		
NW Corner		NE Corner
17°01' E / 77°46' N	Center	18°45' E / 77°22' N
SW Corner	16°59' E / 77°23' N	SE Corner
15°14' E / 77°23' N		16°58' E / 77°00' N

Technical information			
Spectral Mode	[I] 20 m C	Scene Orientation	045.4
Cloud cover (avg.)	AAAAECDB (C)	Technical quality	Excellent
Snow cover (avg.)	11111111 ()	Incidence angle	+02.9
Sun azimut	204.9	Gains	6456
Sun elevation	+25.1		

Satellite	*GRS reference*		*Acquisition date*	*Instrument*	*SAT*
4	*156*	*142*	*04/28/2007 15:23:03*	*2*	*0*

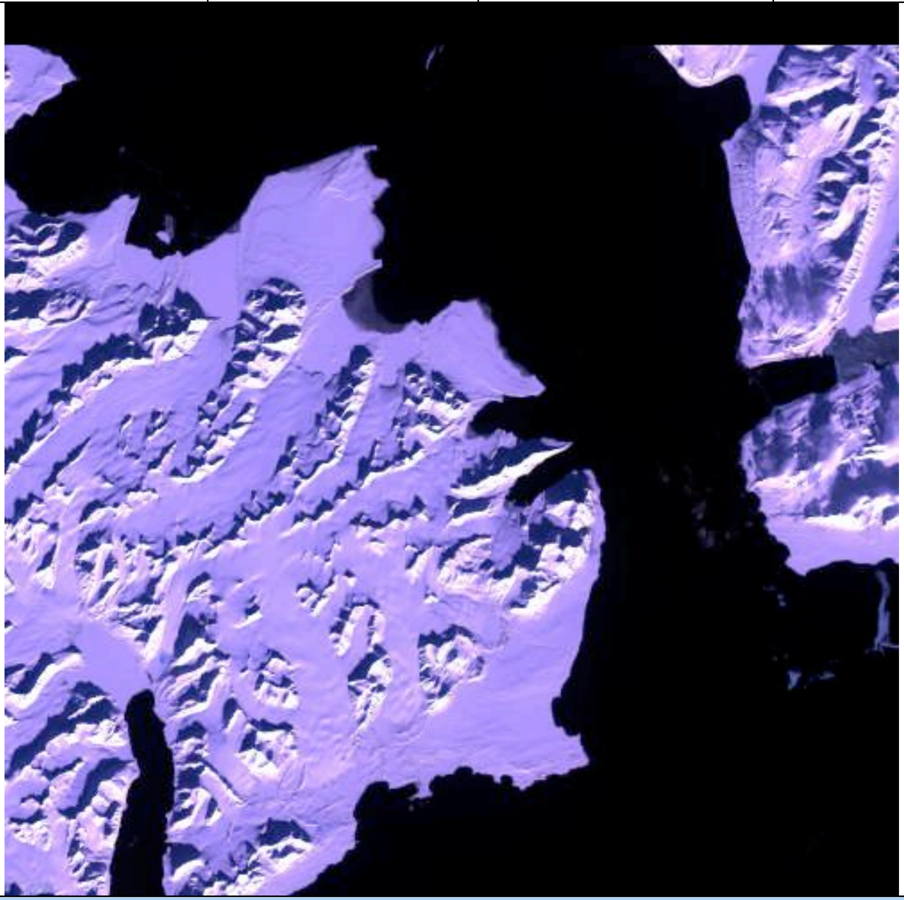

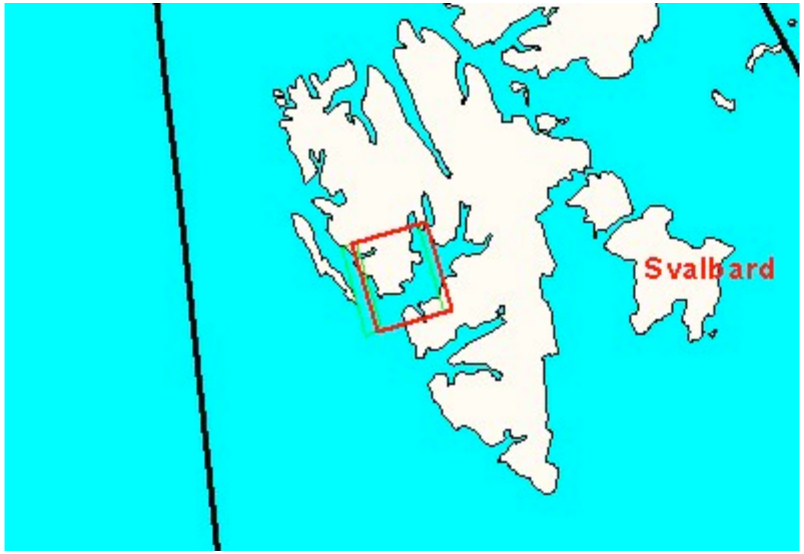

Geographic location		
NW Corner		NE Corner
15°10' E / 78°38' N	Center	15°15' E / 77°60' N
SW Corner	13°53' E / 78°18' N	SE Corner
12°26' E / 78°37' N		12°40' E / 77°58' N

Technical information			
Spectral Mode	[I] 20 m C	Scene Orientation	085.9
Cloud cover (avg.)	AAAAAAAA (A)	Technical quality	Excellent
Snow cover (avg.)	11111111 ()	Incidence angle	+24.8
Sun azimut	248.4	Gains	5246
Sun elevation	+18.5		

Satellite	*GRS reference*		*Acquisition date*	*Instrument*	*SAT*
4	*155*	*144*	*04/28/2007 15:23:11*	*2*	*0*

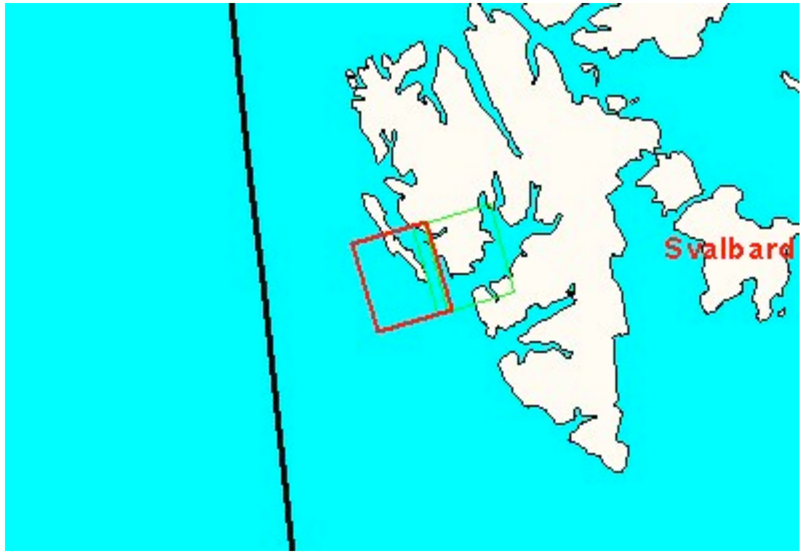

Geographic location		
NW Corner		NE Corner
12°34' E / 78°37' N	Center	12°48' E / 77°58' N
SW Corner	11°20' E / 78°16' N	SE Corner
9°47' E / 78°34' N		10°09' E / 77°55' N

Technical information			
Spectral Mode	[I] 20 m C	Scene Orientation	085.4
Cloud cover (avg.)	AA****** (A)	Technical quality	Excellent
Snow cover (avg.)	11****** ()	Incidence angle	+24.8
Sun azimut	245.9	Gains	5246
Sun elevation	+19.0		

Satellite	*GRS reference*		*Acquisition date*	*Instrument*	*SAT*
4	*153*	*143*	*04/28/2007 15:23:14*	*1*	*0*

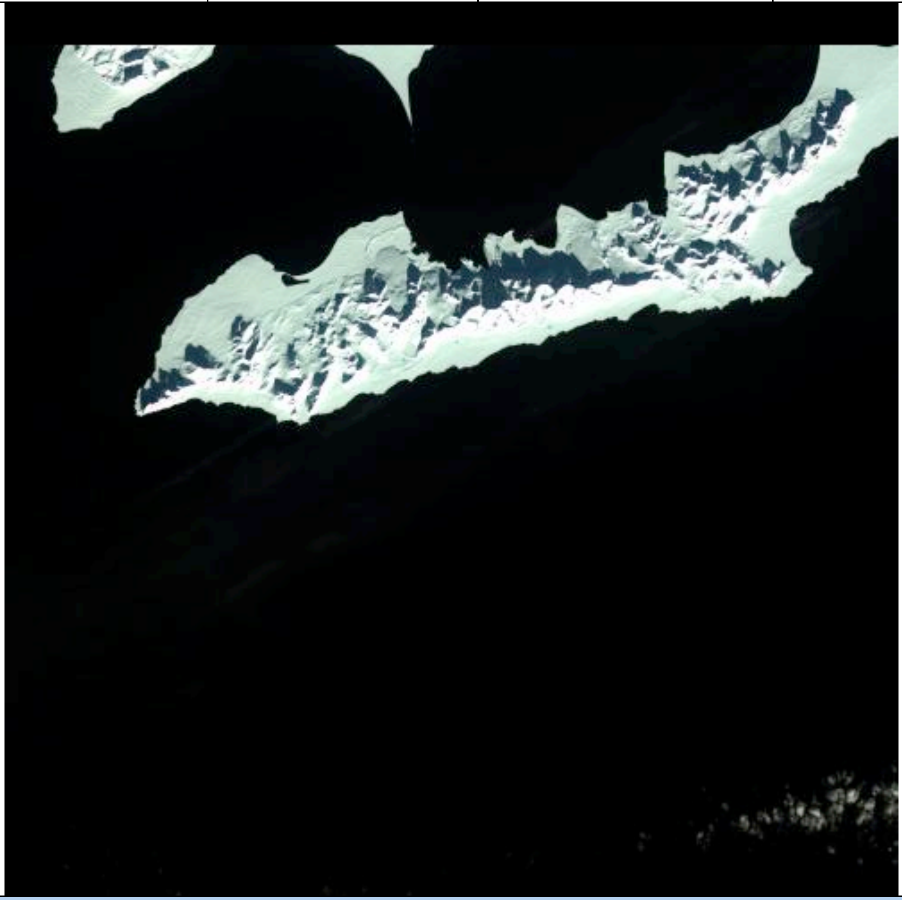

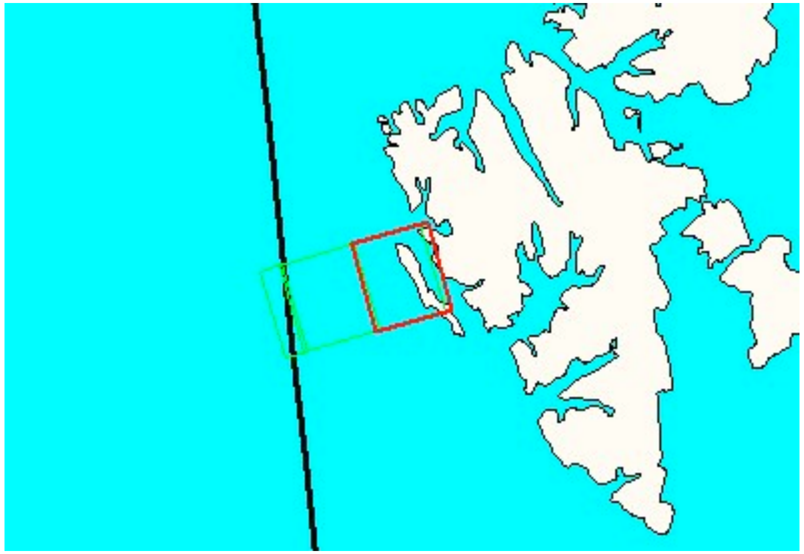

Geographic location		
NW Corner		NE Corner
11°43' E / 79°01' N	Center	11°59' E / 78°23' N
SW Corner	10°29' E / 78°40' N	SE Corner
8°55' E / 78°57' N		9°19' E / 78°20' N

Technical information			
Spectral Mode	[I] 20 m C	Scene Orientation	082.6
Cloud cover (avg.)	ABAAAAAB (A)	Technical quality	Excellent
Snow cover (avg.)	00000000 ()	Incidence angle	+21.6
Sun azimut	244.9	Gains	4446
Sun elevation	+19.0		

Appendix B. Terra ASTER quicklook images

<table>
<tr><td>

28 April 2007 North of Svalbard

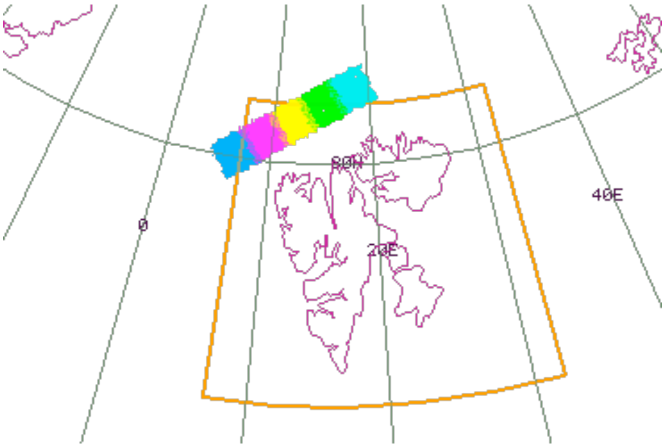

Location of the ASTER quicklook images. The stripe of the four northeasterly images is shown to the right. The westernmost image is shown below.

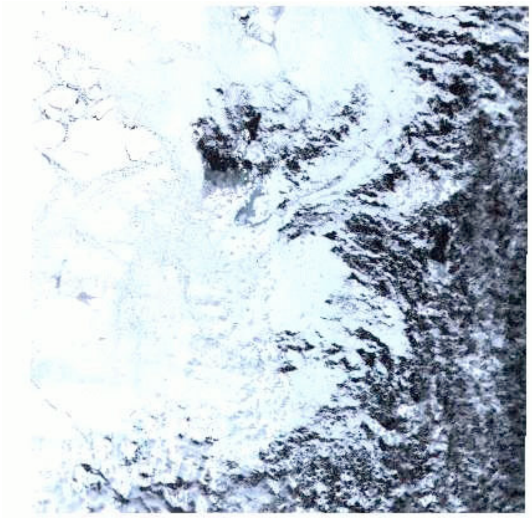

</td><td>

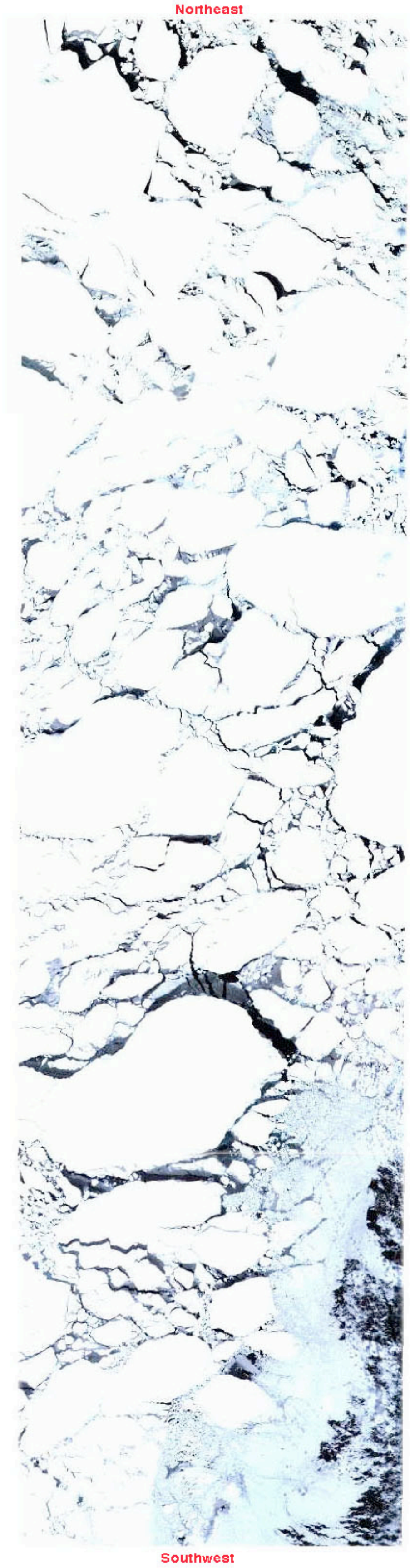

</td></tr>
<tr><td>

28 April 2007 South of Nordaustlandet

</td><td>northeast</td></tr>
</table>

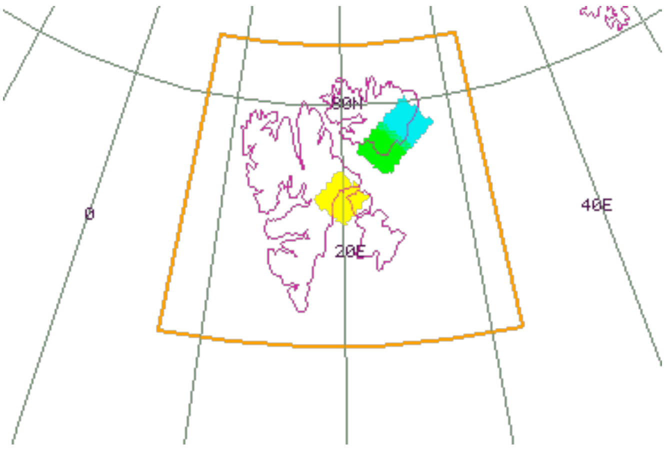

ASTER provided three images in the area, as shown to the right. LANDSAT provided an image on 29 April, covering a much larger area, including overlap with the ASTER, as shown below.

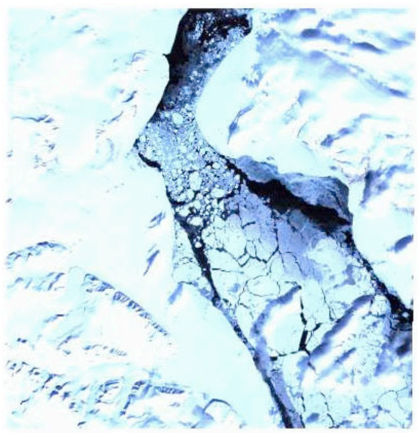

Storfjorden

10 May 2007 North of Svalbard

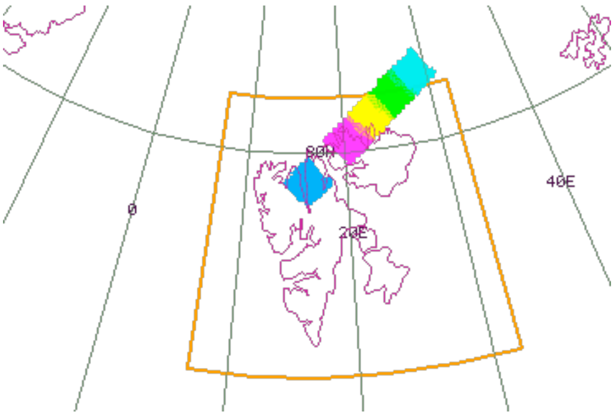

Location of the ASTER quicklook images. The stripe of the four northeasterly images is shown to the right. The westernmost image is shown below.

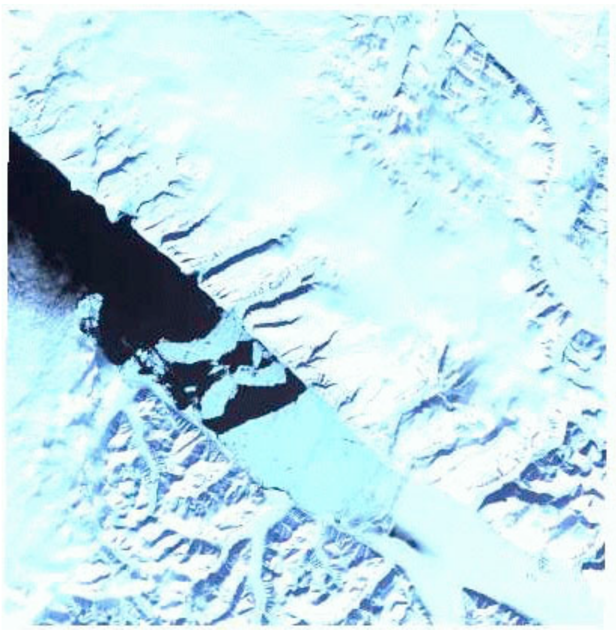

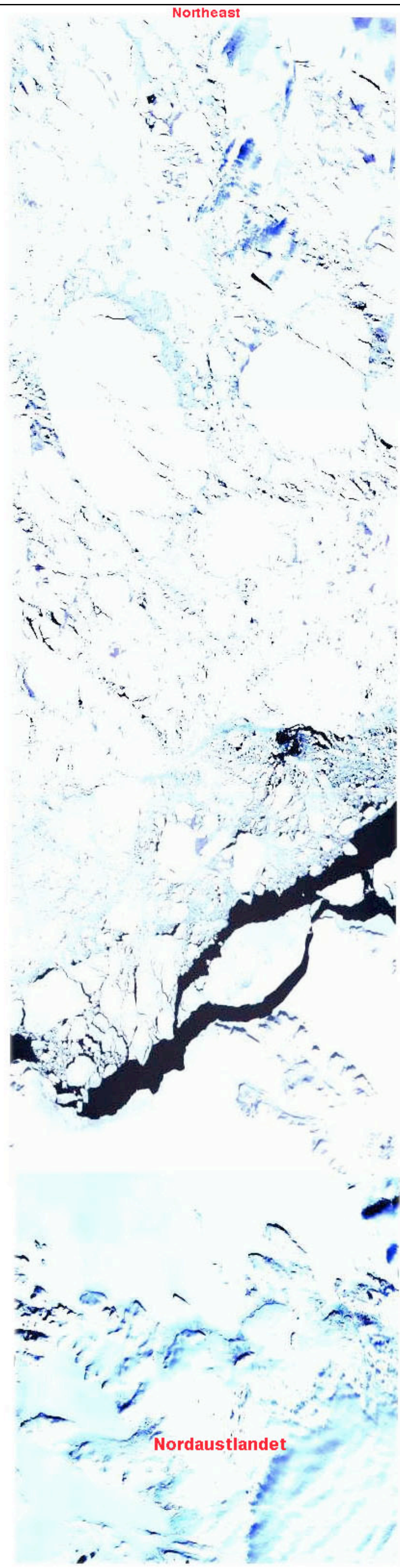

Appendix C. Landsat quicklook images

29 April 2007

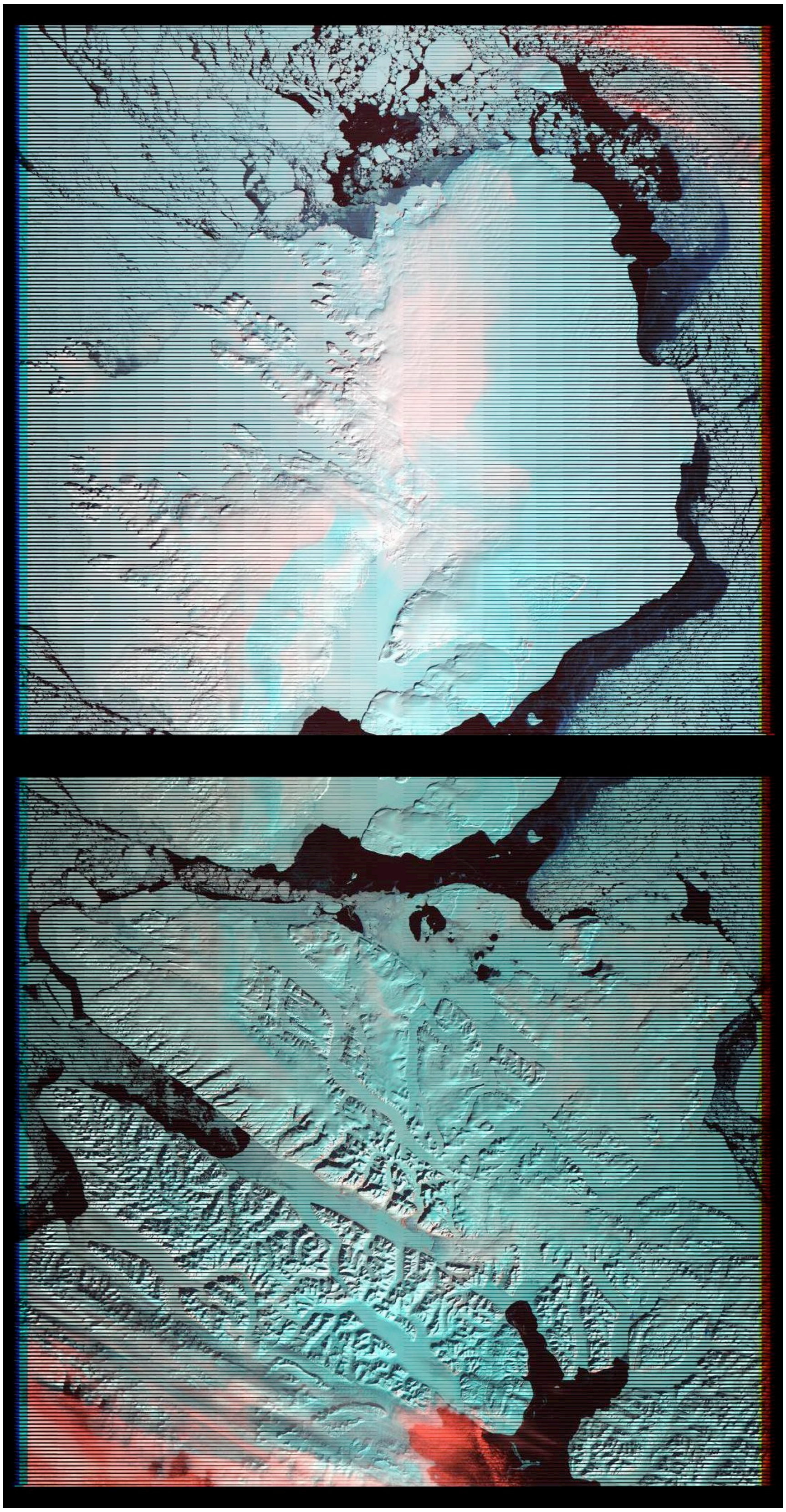

27 June 2007